# SECONDARY CELLS WITH LITHIUM ANODES AND IMMOBILIZED FUSED-SALT ELECTROLYTES

H. Shimotake, G. L. Rogers, and E. J. Cairns

Argonne National Laboratory
9700 South Cass Avenue
Argonne, Illinois
60439

## Introduction

Today's rapidly-advancing technology requires a wide spectrum of power sources and energy-storage devices. In many applications, the power sources are required to have a minimum size or weight per unit of power or energy. These requirements have motivated a great deal of the recent work on high-specific-energy (watt-hr/lb) and high-specific-power (watt/lb) secondary cells. The maximization of the specific energy requires that reactants of low equivalent weight and high free energy of reaction be used. For high specific energy (> 50 watt-hr/lb) cells with aqueous electrolytes, zinc and cadmium have served as anode materials while nickel oxide, silver oxide, and oxygen (or air) have served as cathode materials.[1,2,3] The elimination of water from the electrolyte permits more reactive metals such as calcium and the alkali metals to be considered as anode materials. Lithium has a very low equivalent weight and low electronegativity, making it particularly attractive as an anode material for high specific energy cells. A number of cathode materials have been used in combination with nonaqueous electrolytes and lithium anodes, depending on the operating temperature and the electrolyte.

Lithium-anode cells designed for operation at room temperature use nonaqueous electrolytes comprised of solutions of inorganic salts such as $Li_3PF_4$ or $LiClO_4$ dissolved in organic solvents such as propylene carbonate or dimethyl sulfoxide; the cathodes are usually metal halides such as $NiF_4$, $CuF_2$ or CuCl.[1,3] Although these cells have the potentiality of supplying over 100 watt-hr/lb at low discharge rates, their specific power is low (2-20 watt/lb),[1,3] limiting their range of applicability. The specific power for cells with organic-solvent electrolytes is low because of the low conductivity of the electrolyte ($\sim 10^{-2}$ ohm$^{-1}$ cm$^{-1}$).

The use of fused-salts as electrolytes provides very high conductivities (1-4 ohm$^{-1}$ cm$^{-1}$) thus allowing specific powers in excess of 100 watt/lb to be achieved.[4-8] Because of their relatively high melting points, fused-salt electrolytes require elevated operating temperatures (260-650°C). A number of secondary cells with fused-salt electrolytes have been investigated, including sodium/bismuth,[9] lithium/chlorine,[7,8] lithium/tellurium,[4-6] and lithium/selenium,[10] all using free liquid electrolytes.

A general indication of the theoretical maximum specific energies of some couples suitable for use with fused-salt electrolytes is given in Figure 1, where the specific energy (as calculated from the equivalent weight of the cell products indicated and the average emf of the couple) is plotted against the equivalent weight of the active material. Usually, the higher specific energy materials are more difficult to handle from a corrosion viewpoint.

A great deal of design flexibility and compactness can be gained by immobilizing the fused-salt electrolyte either in an absorbent matrix or in the form of a rigid paste.[11-13] This work deals with secondary cells having liquid lithium anodes, liquid bismuth or tellurium cathodes and fused-lithium-halide electrolytes immobilized as a rigid paste, operating at temperatures in the range 380 to 485°C.

## Experimental

Typical lithium/bismuth and lithium/tellurium cells are shown in Figures 2 and 3. The cell housing in Figure 2 was made from Type 316 stainless steel; the electrode compartments were 3.2 mm deep, and had 4 concentric fins which

served as current collectors. The exposed electrolyte area was 1.98 $cm^2$, and the paste electrolyte thickness was 0.34 cm. Prior to assembly, the anode compartment was loaded with 0.064 gm of lithium (Foote Mineral Co., 0.003 % Na, 0.003% K, 0.003% $N_2$, 0.003% $Cl_2$, surface oxide removed), heated to 530°C to ensure good wetting of the current collector. The cathode compartment contained 2.764 gm of bismuth (United Mineral and Chemical Corp., 99.999% minimum purity). These amounts of reactants correspond to a cathode-alloy composition of 41 a/o Li in Bi at complete discharge, and a cell capacity of 0.25 amp-hr. The cell was prepared and assembled under a high-purity helium atmosphere.[14] No gaskets were used; the smooth-surfaced electrolyte disc provided a leak-tight seal against the cell housing.

The lithium/tellurium cell, made of pure iron, had current collectors consisting of sheets of sintered porous stainless steel in the anode compartment, and a network of pure-iron wires in the cathode compartment in place of the meshes shown in Figure 3. The exposed electrolyte area was 3.25 $cm^2$; the electrolyte thickness was 0.32 cm. The cell compartments were loaded with 0.75 gm of lithium and 5.45 gm of tellurium, (American Smelting and Refining Co., 99.999% minimum purity) corresponding to 71.6 a/o Li in Te at complete discharge.

The electrolyte was the ternary eutectic composed of 11.7 m/o LiF - 29.1 m/o LiCl - 59.2 m/o LiI, which melts at 340.9°C and has a specific conductance of 2.3 $ohm^{-1}$ $cm^{-1}$ at 375°C and 3.0 $ohm^{-1}$ $cm^{-1}$ at 475°C.[15] The eutectic was prepared from weighed amounts of the pure salts: LiF, LiCl, and LiI all supplied by Anderson Physics Laboratories, Inc. After the components were melted together to form the eutectic, the electrolyte was solidified, pulverized to -300 mesh, and mixed (50 w/o) with an inert filler material. The electrolyte-filler powder mixture was then molded into discs. For the Li/Bi cell, discs 1.85 cm in dia. were prepared by pressing the electrolyte-filler powder first at room temperature to form "cold-pressed" discs, and then at 400°C for final densification. All operations except for the hot-pressing were carried out in a pure helium atmosphere. For the Li/Te cell, discs 2.5 cm in dia. were pressed at room temperature and sintered at 400°C without pressing, eliminating all exposure to air.

The paste electrolyte has a continuous phase of fused-lithium-halide eutectic at the cell operating temperature. The relative amounts of finely-divided inert filler and lithium halide are chosen such that the electrolyte fills the interstitial spaces among the very small filler particles, and holds the paste firmly by means of its high surface tension, low contact angle with the filler, and the small pore size of the compact. Similar paste electrolytes have been used with success in molten-carbonate fuel cells.[11-13]

The measurements of cell performance were carried out with the aid of a constant-current DC power supply, precision voltmeters and ammeters (1/4 percent), and a strip-chart recorder. The voltage-current density curves for the discharge mode of operation were measured starting with the cell in the fully-charged condition; the curves for the charge mode of operation were usually measured from the fully-discharged condition. All results are reported on a resistance-included basis. The cells were held at operating temperature in an electrically-heated tube furnace.

## Results and Discussion

The voltage-current density curves for the Li/Bi cell operating at 380°, 453°, and 485°C are shown in Figure 4. As might be expected, the highest performance in both charge and discharge modes was obtained at the highest temperature. Current densities up to 2.2 amp/$cm^2$ were obtained, based on the effective electrode area of 1 $cm^2$ (the electrode compartments were only about half-filled with active materials during these experiments). Since the cathode composition during the discharge experiments averaged about 5 a/o Li,[16] these performances are typical of those obtainable near the beginning of the plateau of the corresponding voltage-

time curves at constant current discharge. The maximum power density at 485°C was 0.57 watt/cm$^2$ at 0.6 volt.

The slopes of the charge and discharge curves in Figure 4 are different because of the difference in state of charge for the two modes of operation. The internal resistance of the cell is expected to be lower for the discharge curves because most of the original amount of lithium was still in the anode compartment when the discharge data were taken. During the charging experiments, however, almost no lithium was present in the lithium compartment, resulting in a relatively high internal resistance. When charge and discharge curves are taken under identical conditions, the curves have the same slope. The internal resistance of the cell at high current densities was 0.45 ohm at 485°C, compared to a value of 0.23 ohm calculated from the specific conductance of the electrolyte and a paste-to-pure electrolyte resistivity ratio of 2.[11,13] This discrepancy could be caused by the presence of some $Li_2O$ resulting from hydrolysis of the lithium halides during hot-pressing or incomplete wetting of the paste by Li.

From the reasonably high current density capabilities of the Li/Bi cell of Figure 4, it is clear that the cell can be fully charged from complete discharge in about 15 minutes.

The performance characteristics of the (larger) Li/Te cell operating at 475°C are shown in Figure 5. As expected on the basis of the emf measurements of Foster and Liu[17] and earlier experience with Li/Te cells,[4-6] the open circuit voltage was 1.7 to 1.8 volts, and the voltage-current density curves were straight lines, indicating the absence of any significant concentration or activation overvoltages. The short-circuit current density was 2.2 amp/cm$^2$, and the maximum power density was 1 watt/cm$^2$ at 0.9 volt, a considerable improvement in power density over the Li/Bi cell.

The internal resistance of the Li/Te cell during discharge was 0.24 ohm, compared to 0.065 ohm calculated from the electrolyte conductivity and a paste-to-pure electrolyte resistivity ratio of 2. The ratio of observed-to-calculated cell resistances is higher for the Li/Te cell than for the Li/Bi cell, possibly because of the fact that the paste electrolyte disc for the Li/Te cell was not hot-pressed, and therefore probably contained voids which increased the resistivity of the paste.

The Li/Te cell, with a capacity of 2.91 amp-hr could be fully charged from complete discharge in less than half an hour. This is a much higher charge rate than can be used with secondary cells having aqueous electrolytes or cells with nonaqueous organic solvent electrolytes.

Extensive investigations of constant-current charge and discharge characteristics, charge retention, and cycle life still remain to be done. The data presented above were interesting enough, however, that some preliminary design calculations have been performed, based upon the voltage-current density curves of Figures 4 and 5.

The principles, equations, and sample calculations involved in the design of secondary batteries have already been discussed elsewhere[4], therefore, no detailed explanations will be given here. The most important parameter in many applications is battery weight; therefore, the energy and power values are expressed per unit weight as specific energy (watt-hr/lb) and specific power (watt/lb). The calculation of battery weight involves the selection of the ratio of reactant weights, and the calculation of the weights of reactants, electrolyte, cell housing, terminals, etc. required, per unit of active cell area. The specific power available is calculated from the current density-voltage curve and the battery weight per unit active area. The specific energy is calculated from the average cell operating voltage, the amount of lithium per unit of active cell area and the battery weight per unit of active area.[4] The values used in these calculations are summarized in Table I.

The results of the design calculations for Li/Bi and Li/Te secondary batteries are shown in Figure 6. Because of the lower equivalent weight and higher electronegativity, the Li/Te cell has higher specific energy and specific power capabilities than the Li/Bi cell. As an example, Figure 6 shows that for the 30-minute-discharge rate, a Li/Bi cell having 3 cells per inch and an electrolyte thickness of 0.32 cm has a specific power of 43 watt/lb and a specific energy of 21 watt-hr/lb, whereas the Li/Te cell of similar dimensions can attain 110 watt/lb and 55 watt-hr/lb. The design analysis results presented in Figure 6 also indicate that if the electrolyte thickness is decreased to 0.1 cm, it is possible to achieve 90 watt/lb and 45 watt-hr/lb for the Li/Bi cell and 200 watt/lb and 110 watt-hr/lb for the Li/Te cell. The performances of some other types of secondary batteries including lead-acid, nickel/cadmium, sodium/sulfur, and lithium/chlorine are presented in Figure 6 for comparison.

Possible applications for secondary cells with the characteristics of the Li/Te cell include space power sources, military communications power sources, military vehicle propulsion, and perhaps special commercial vehicle propulsion.[5]

The areas which deserve further attention in the development of Li/Bi and Li/Te cells include the optimization of paste electrolyte properties (particularly the resistivity), current collection, corrosion, cycle life, and thermal cycling.

## Conclusions

1. It is possible to form acceptable paste electrolytes from fused-lithium halides and inert filler materials. The paste electrolytes presently show two to three times the expected electrolytic resistivities.

2. Lithium/bismuth and lithium/tellurium cells operating with lithium halide paste electrolytes can operate at power densities of 0.57 and 1.0 watt/cm$^2$, respectively at about 480°C.

3. These cells can be charged at very high rates (less than 30 minutes), making them possible candidates for many applications where fast recharge is important.

4. Design calculations indicate that the Li/Te cell with paste electrolyte can be expected to show a specific power in excess of 360 watt/lb and a specific energy of 80 watt-hr/lb, suggesting many possible applications, including special vehicle propulsion and energy storage.

## Acknowledgment

It is a pleasure to thank Mr. J. Gerard for help with some of the experiments, and Drs. A. D. Tevebaugh, C. E. Johnson, and M. S. Foster for helpful discussions during the course of this work. Mr. B. S. Baker of the Institute of Gas Technology generously provided advice and materials on the preparation of paste electrolytes.

## References


1. R. Jasinski, "High-Energy Batteries", Plenum Press, New York (1967).

2. A. M. Moos and N. I. Palmer, in *Proc. 21st Ann. Power Sources Conf.*, PSC Publications Committee, Red Bank, New Jersey (1967).

3. H. N. Seiger, S. Charlip, A. E. Lyall and R. C. Shair, in *Proc. 21st Ann. Power Sources Conf.*, PSC Publications Committee, Red Bank, New Jersey (1967).

4. H. Shimotake and E. J. Cairns, Presented at the Intersociety Energy Conversion Engineering Conf., Miami Beach, August, 1967, in *Advances in Energy Conversion Engineering*, Amer. Soc. Mech. Eng., New York (1967), p. 951.

5. E. J. Cairns and H. Shimotake, Presented at Amer. Chem. Soc. Meeting, Chicago, September 1967, Abstr. No. L-70; See also *Preprints of Papers Presented to the Division of Fuel Chemistry 11*, No. 3, 321 (1967).

6. H. Shimotake, G. L. Rogers, and E. J. Cairns, Presented at Electrochem. Soc. Meeting, Chicago, October, 1967, Abstr. No. 18; See also *Extended Abstracts J-1 of the Battery Div., 12*, 42 (1967).

7. R. A. Rightmire and A. L. Jones, in *Proc. 21st Ann. Power Sources Conf.*, PSC Publications Committee, Red Bank, New Jersey (1967).

8. H. A. Wilcox, in *Proc. 21st Ann. Power Sources Conf.*, PSC Publications Committee, Red Bank, New Jersey (1967).

9. H. Shimotake and E. J. Cairns, Presented at Electrochem. Soc. Meeting, Dallas, May, 1967, Abstr. No. 143; See also *Extended Abstrs. of the Industrial Electrolytic Div., 3*, 4 (1967).

10. H. Shimotake and E. J. Cairns, Submitted for Presentation at the International Power Sources Symposium, Brighton, September, 1968.

11. G. H. J. Broers and M. Schenke, in "Fuel Cells", Vol. 2, G. J. Young, Ed., Reinhold, New York (1963).

12. B. S. Baker, L. G. Marianowski, J. Zimmer and G. Price, in "Hydrocarbon Fuel Cell Technology", B. S. Baker, Ed., Academic Press, New York (1965).

13. A. D. S. Tantram, A. C. C. Tseung, and B. S. Harris, in "Hydrocarbon Fuel Cell Technology", B. S. Baker, Ed., Academic Press, New York (1965).

14. C. E. Johnson, M. S. Foster, and M. L. Kyle, *Nuclear Appl., 3*, 563 (1967).

15. C. E. Johnson, Submitted for Presentation at the San Francisco Meeting of The Amer. Chem. Soc., Apr., 1968.

16. M. S. Foster, S. E. Wood, and C. E. Crouthamel, *Inorg. Chem., 3*, 1428 (1964).

17. M. S. Foster and C. C. Liu, *J. Phys. Chem., 70*, 950 (1966).

Table I

Data for Battery Design Calculations

| | Li/Bi | Li/Te |
|---|---|---|
| Open-circuit voltage, volts | 0.8 | 1.7 |
| Short-circuit current density, amp/cm$^2$ | | |
| for electrolyte thickness 0.3 cm | 1.8 | 2.2 |
| for electrolyte thickness 0.1 cm | 6.1 | 7.0 |
| Cathode alloy, fully discharged | | |
| composition, a/o Li | 70 | 60 |
| density, g/cm$^3$ | 4.4 | 3.3 |
| Anode metal density, g/cm$^3$ | 0.53 | 0.53 |
| Current efficiency, % | 100 | 100 |
| Cell partition thickness, cm/cell | 0.1 | 0.1 |
| Density of housing material, g/cm$^3$ | 7.8 | 7.8 |
| Density of paste electrolyte, g/cm$^3$ | 3.0 | 3.0 |
| Weight allowance for framing, terminals, etc. % (electrolyte + partition weight) | 50 | 50 |

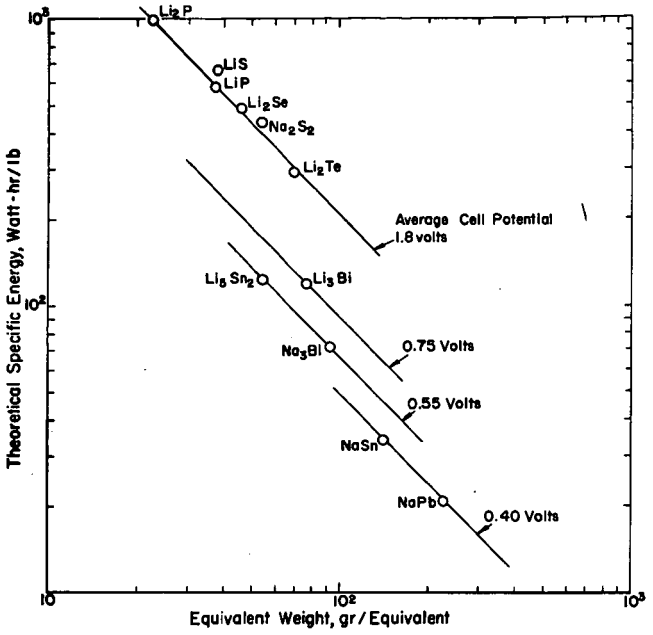


Fig. 1. Relationship between theoretical specific energy and equivalent weight

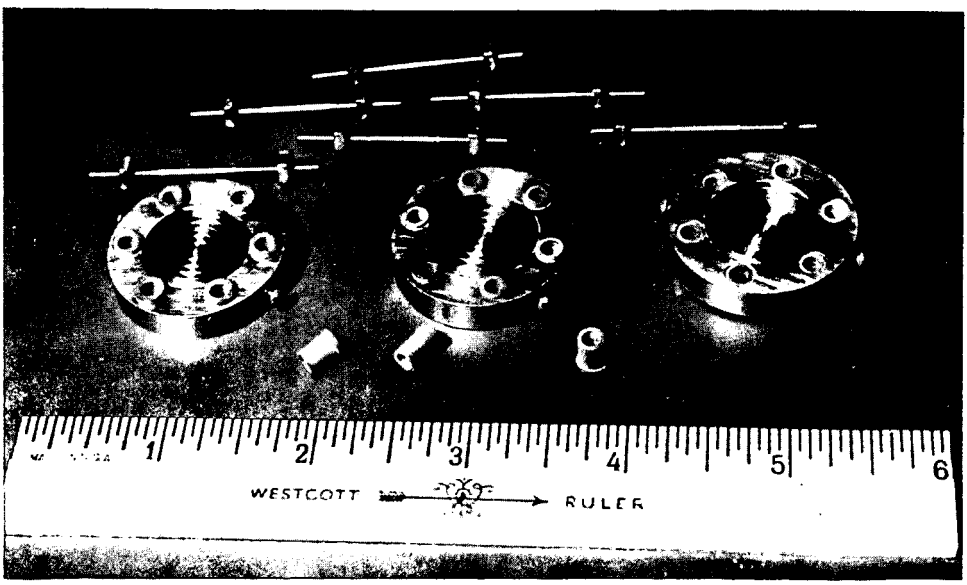


Fig. 2. View of lithium-bismuth-cell parts. Enough cell parts to make a two-cell battery are shown.

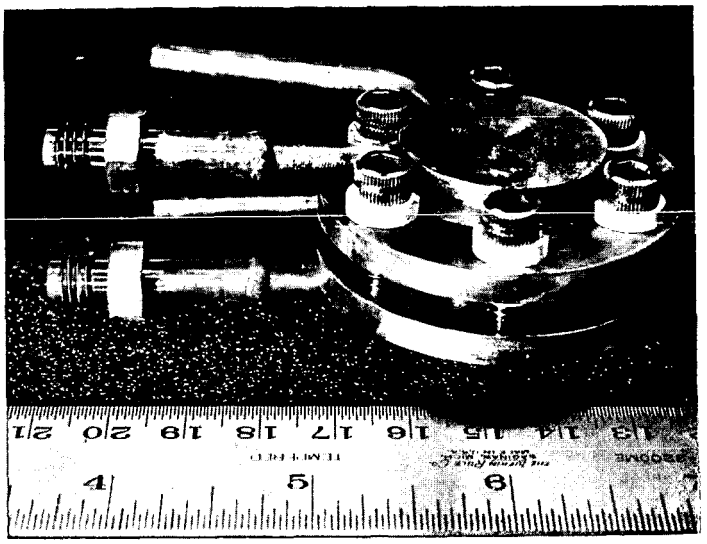

Fig. 3a. View of assembled lithium-tellurium cell

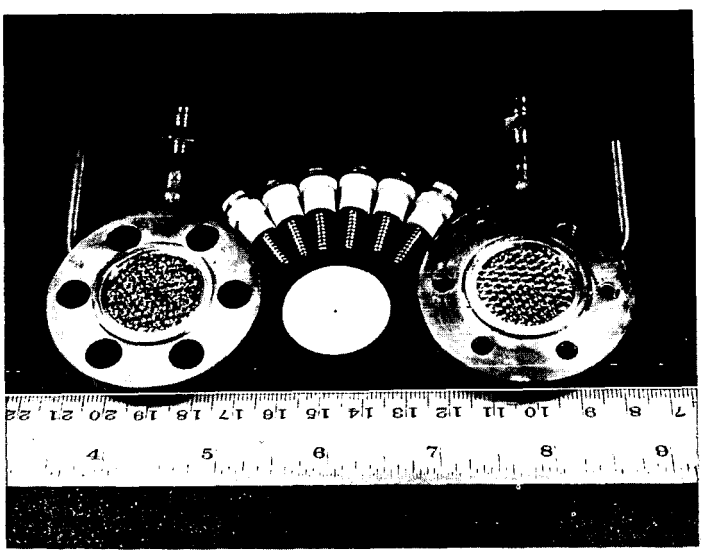

Fig. 3b. View of lithium-tellurium-cell parts

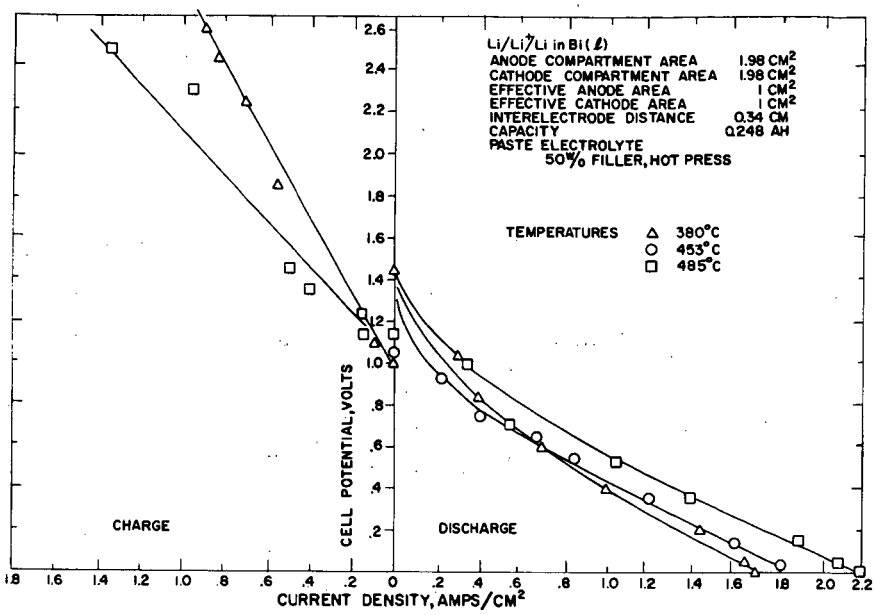


Fig. 4. Voltage-current density curves for a lithium-bismuth cell

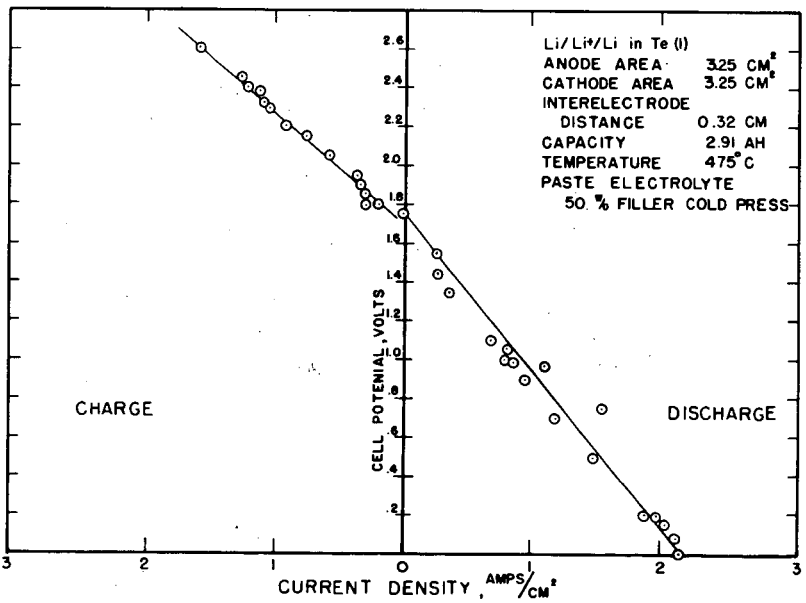


Fig. 5. Voltage-current density curves for a lithium-tellurium cell

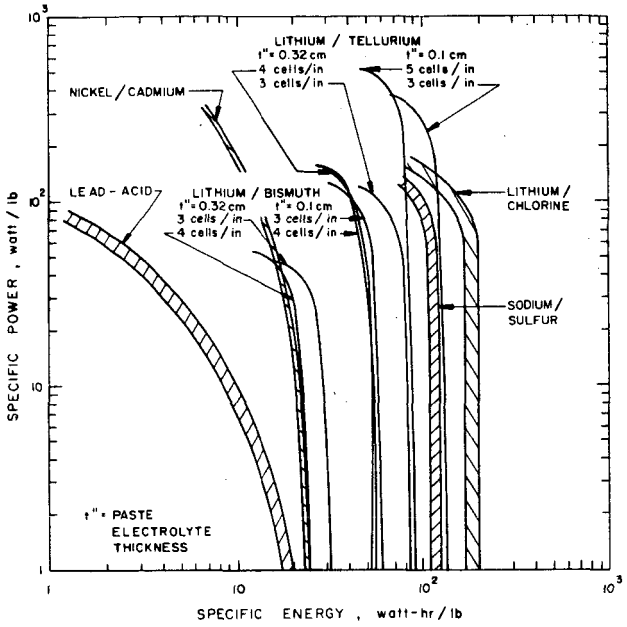


Fig. 6. Specific power-specific energy curves for some secondary batteries

# COAL PYROLYSIS USING LASER IRRADIATION

F. S. Karn, R. A. Friedel, and A. G. Sharkey, Jr.

U.S. Department of the Interior, Bureau of Mines
Pittsburgh Coal Research Center, Pittsburgh, Pa. 15213

## INTRODUCTION

The purpose of this investigation is to observe the effect of laser irradiation on the pyrolysis of coal. Coal irradiated with laser light can decompose into gases rich in acetylene. Coal pyrolysis at the usual coking temperatures yields gases high in methane but very low in acetylene. The acetylene/methane ratio and the probable commercial value of the product gas should be related directly to the temperature of the decomposing coal.

Conventional coal pyrolysis varies in temperature from 450° to 1,400°C and includes hundreds of different processes and coals. A typical high-temperature pyrolysis gas was obtained from a Pittsburgh seam (hvab) coal carbonized at 900° C.[5] Fifteen percent of the coal (40.7 percent volatile matter) was collected as gas (table 1). Laser irradiation can bring about significant changes in the $C_2H_2/CH_4$ ratio by increasing pyrolysis temperature. The equilibrium constant for the reaction

$$2CH_4 \rightleftharpoons C_2H_2 + 3H_2$$

increases from $10^{-7}$ at 1,000° K to $10^{+9}$ at 4,000° K. Temperatures resulting from laser irradiation could be very high. The energy concentration due to a 6-joule focused beam from a ruby laser is sufficient to raise the temperature of a perfect absorber by 14,000° C. This estimate is based on the laser energy and on the heat capacity of the target. However, much of the laser energy is dissipated by reflection, conduction, and vaporization. In these experiments with coal the maximum target temperature was estimated to be less than 1,300° K--largely due to coal volatility. Interesting observations of target temperatures of laser-irradiated solids have been reported. Berkowitz and Chupka[1] analyzed the vapor ejected from graphite and found it compatible with an assumption of thermodynamic equilibrium and a temperature of 4,000° K. Verber and Adelman,[7] using tantalum as a target, measured thermionic emission due to a surface temperature increase which was calculated from classical heat transfer theory. In the following experiments temperatures have not been measured directly due to the small size of the coal crater and to the rapid heating and cooling of the sample.

## EXPERIMENTAL

A variety of coals and coal macerals have been exposed to laser irradiation. Using a focused beam, energy concentrations as high as 100 megawatts per square centimeter can be reached. The general procedure has been to seal the coal sample in a glass vessel through which the laser beam can be fired. The vessel was evacuated or evacuated and partially refilled with a specific gas before irradiation. Samples, usually about 8 mm cubes, were sealed in glass tubes 10 mm i.d. and 90 mm long.[6] Samples were dried under vacuum at 100° C for 20 hours, then sealed and irradiated. The usual irradiation was 1 pulse of a 6-joule ruby laser beam which was focused by a convex lens. Gaseous products were analyzed by the mass spectrometer in two or more fractions distilling from liquid nitrogen, dry ice, ice water, room temperature, and 60° C baths. Both total volume and gas distribution were determined for each fraction. Solid products were obtained from the glass walls for ultimate analysis or for inspection by infrared spectrometry.

Table 1.- Product gas

| | 900°C carbonization | Laser irradiation |
|---|---|---|
| | Mole percent | |
| $H_2$ | 55.6 | 52.2 |
| CO | 7.4 | 22.5 |
| $CO_2$ | 0.4 | 8.7 |
| $CH_4$ | 31.5 | 5.1 |
| $C_2H_2$ | 0.05 | 10.6 |
| $C_2H_4$ | 3.4 | 0.0 |
| $C_2H_6$ | 1.2 | 0.0 |
| $> C_2$ | 0.5 | 0.0 |
| HCN | 0.0 | 0.9 |
| | Weight percent of coal | |
| | 15 | 52 |
| | $C_2H_2/CH_4$ | |
| | < 0.002 | 2.1 |

In studying any new process for coal pyrolysis, there are several useful variables to be considered. Among these are coal rank, maceral, particle size, and atmosphere. There are also several variables which are characteristic of the processing unit. For the laser they are quantity of energy discharged, rate of discharge, area of target, and wavelength of radiant energy.

Coals have been treated with the same total light energy from 3 different lasers. Lasers used in these experiments were as follows: The ruby laser delivers 6 joules of 6,943 A light in about 1 millisecond. Source of the light is a cylindrical ruby 76 mm long by 6.3 mm in diameter. It is activated by a xenon flash lamp and a capacitor capable of delivering a 2,000-volt pulse. The neodymium laser is a glass rod 152 mm long and capable of a 28-joule pulsed discharge. The third laser type is a continuous $CO_2$ laser. Its total power output is only 10 watts (10 joules/sec) but since it operates continuously the total energy and the quantity of product gas can be made to equal that of the pulsed lasers. Irradiation from the $CO_2$ laser has a wavelength of 106,000 A.

## RESULTS

A comparison of product gases from a 900° C carbonization and from irradiation by a ruby laser verified the prediction of higher $C_2H_2$ to $CH_4$ ratio for the laser (table 1).

Rank. Coal composition and coal utilization vary widely with rank. Irradiation products as a function of rank were studied earlier and the results are summarized in table 2.[3/] As rank decreases the yield of gaseous product increases. Yields of acetylene, hydrogen, and HCN reach a maximum for a high-volatile bituminous coal.

Macerals. Macerals from a single coal seam can be separated visually or by specific gravity. They provide information about the origin of a coal and about its coking properties. Maceral separation is a tedious job and well separated samples are usually small.[2/] Macerals of Hernshaw (hvab) coal in sufficient quantity for laser pyrolysis were irradiated (table 3). As hydrogen and volatile matter in the maceral increased the product gas increased, and the quality of the product gas (based on $C_2H_2/CH_4$ ratio) decreased.

Table 2.- Product gases from laser irradiation of coals

| | Anthracite | Pocahontas lvb | Pittsburgh hvab | Lignite |
|---|---|---|---|---|
| | Moles x $10^7$ | | | |
| $H_2$ | 13 | 23 | 30 | 21 |
| CO | 8 | 5 | 12 | 24 |
| $CO_2$ | 4 | 1 | 3 | 10 |
| $CH_4$ | 1 | 1 | 3 | 1 |
| $C_2H_2$ | 3 | 4 | 9 | 6 |
| HCN | 0.3 | 0.3 | 1.2 | 0.7 |
| Total[a/] | 31 | 35 | 60 | 63 |

a/ $H_2O$, $N_2$, $O_2$ free.

Table 3.- Gas from laser irradiation of macerals of Hernshaw (hvab) coal

| Maceral | $H_2$, percent[a/] | Volatile matter, percent[a/] | Product gas Moles x $10^7$ | Product gas $C_2H_2/CH_4$ |
|---|---|---|---|---|
| Fusinite | 3.2 | 13.4 | 43 | 59 |
| Micrinite | 4.8 | 31.4 | 52 | 34 |
| Vitrinite | 5.4 | 33.7 | 90 | 12 |
| Exinite | 6.4 | 55.4 | 103 | 8 |

a/ See reference 2.

Particle Size. Variation of gas yield with particle size was studied. Samples of Pittsburgh seam coal with particle diameters from 240 μ down to 10 μ (figure 1) were irradiated. For the smaller particles there was a modest decrease in methane and an increase in acetylene. This may indicate less cooling by conduction and higher temperatures.

Types of Lasers. Although laser activity has been produced in many different materials, this study has been carried out using only three--ruby, neodymium, and carbon dioxide. The ruby is a pink crystal of $Al_2O_3$ with 0.05 weight percent of $Cr_2O_3$. The chromium ions, excited by the xenon flash lamp, emit a pulse of 6,943 A laser light. The intensity of this pulse can be varied by changing the input to the lamp, by focusing the laser beam, and by Q-switching to shorten the discharge time. The standard irradiation for these experiments was a 6-joule pulse discharged in about 1 millisecond. Without optical alteration this produces a crater 6 mm in diameter (equal to the ruby rod) and an energy concentration at the target of 14 kw $cm^{-2}$. With a focusing lens this is increased to over 40 kw $cm^{-2}$ and, using an electro-optical Q-switch, to 40 Mw $cm^{-2}$.

The neodymium laser can deliver a 28-joule pulse of 10,600 A light. Using precise focusing but no Q-switching the light intensity at the target is about 400 kw $cm^{-2}$.

The $CO_2$ laser has a continuous output of 10 watts at a wavelength of 106,000 A. Using a focused beam it can produce a flux of 0.2 kw $cm^{-2}$.

Data from these three lasers, including several variations in the energy intensities of the ruby have been compared at approximately the same total energy output to determine if there are differences in product-gas quantity and distribution.

The $CO_2$ laser emits the least intense light beam because of its slow rate of emission. The ruby pulses were progressively increased in concentration due to focal variations. This can readily be measured on the coal targets. Craters in the coal irradiated by the defocused ruby laser beam had an average area of 1.3 $cm^2$. All irradiations with neodymium were focused and the craters averaged 0.02 $cm^2$. The best focused $CO_2$-laser beam produced a crater with an area of 0.03 $cm^2$. The product-gas data are shown as functions of crater area (figure 2). Only the data from irradiations with the $CO_2$ laser were not consistent with the other data due to its slow heating and cooling rates. The more intense laser beams produced greater quantities of product gas and higher acetylene to methane ratios. In figure 3 crater area was replaced by light flux (kilowatts $cm^{-2}$) and the $CO_2$-laser data could be included.

Temperature. Since the same amount of energy was available in each of these tests the temperatures of the craters or of the gas generating sites should be related to energy concentration. An attempt was made to estimate these temperatures from the composition of the gas using gas equilibria data. The chief interest is in the relationship between methane, acetylene, and hydrogen. Equilibrium data to 4,000 K are shown in figure 4.[4]

Gas analyses from various laser irradiations were introduced as shown in the sample calculation using data from irradiation with a neodymium laser.

$$K = \frac{(pC_2H_2)(pH_2)^3}{(pCH_4)^2} = \frac{(.00277)(.00987)^3}{(.000774)^2} = .00444$$

$$\log K = 2.351$$

Assuming the gases to be in equilibrium during their generation, figure 4 gives a temperature of 1,250° K. Temperatures were estimated for other laser irradiations where gas analyses were available (figure 5). Temperatures increase consistently with increase in energy concentration. Since acetylene was not detected in the gases from the $CO_2$ laser a temperature estimate could not be made. However, a gas analysis was available for product from a 900° C carbonization of coal and a comparison with equilibrium data indicated a temperature of 827° C, in reasonable agreement with the measured temperature.

Variations in types of irradiation cause great changes in gas yield and selectivity. However, most of these changes in the product can be explained on the basis of heat concentration at the target. A greater heat concentration increases gas yield, increases the probable crater temperature, and increases the acetylene to methane ratio. Even data from the $CO_2$ laser fits into this pattern although the heat concentration is achieved by additional radiation time instead of laser power.

Photochemistry. A fundamental question in the laser irradiation of coal is the possible importance of the wavelength of the energy. Is the laser simply a thermal energy source capable of raising coal to high temperatures or can the monochromatic energy stimulate specific chemical reactions in coal? The usual photochemical reactions take place with wavelengths of 2,000 A to 8,000 A.

The lasers available for this coal study were:

| | | |
|---|---|---|
| Ruby | 6,943 A | - visible spectrum |
| Neodymium | 10,600 A | - infrared |
| Carbon dioxide | 106,000 A | - infrared |

At this time it is impossible to measure the photochemical influence of the laser energy because duplicate craters have not been produced by different lasers and the temperature effect is much stronger than the photochemical effect. A first estimate is that the influence is small (compare ruby-focus and neodymium, figure 3) but perhaps using lower energy pulses differences can be detected.

Another conclusion to be drawn from these data is the effectiveness of a concentrated beam of laser light in promoting acetylene production in coal pyrolysis. This has been shown for both ruby and neodymium lasers and for coals of varying rank, maceral, and particle size. Due to coal volatility temperatures have been lower than expected. Higher coal temperatures could be predicted by irradiating pretreated coal in a pressurized system and should lead to gas compositions even richer in acetylene.

## References

1. Berkowitz, J., and Chupka, W. A., J. Chem. Phys., 40, 2735 (1964).

2. Ergun, S., McCartney, J. T., Mentser, M., Econ. Geology, 54, 1068 (1959).

3. Karn, F. S., Friedel, R. A., and Sharkey, A. G. Jr., Carbon, 5, 25 (1967).

4. McBride, B. J., Heimel, S., Ehlers, J. G., and Gordon, S., NASA SP-3001, Office of Sci. and Tech. Information, Nat'l Aeronautics and Space Admin., Washington, D. C., 1963, 328 pp.

5. Sharkey, A. G., Jr., Shultz, J. L., and Friedel, R. A., Bureau of Mines Report of Investigations 6868, 1966, 9 pp.

6. Shultz, J. L., and Sharkey, A. G. Jr., Carbon, 5, 57 (1967).

7. Verber, C. M., and Adelman, A. H., J. Applied Physics, 36, No. 5, 1522 (1965).

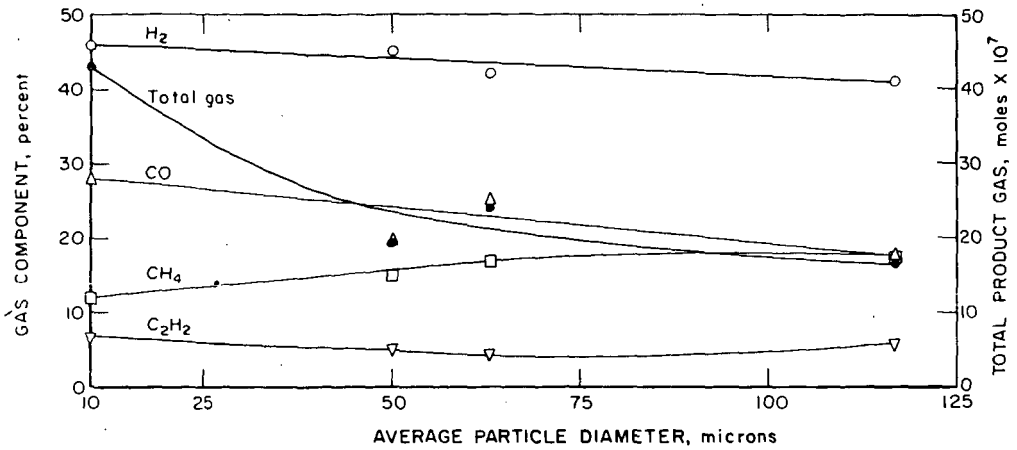


Figure 1. — Laser irradiation of Pittsburgh coal. Product gas as a function of coal particle diameter.

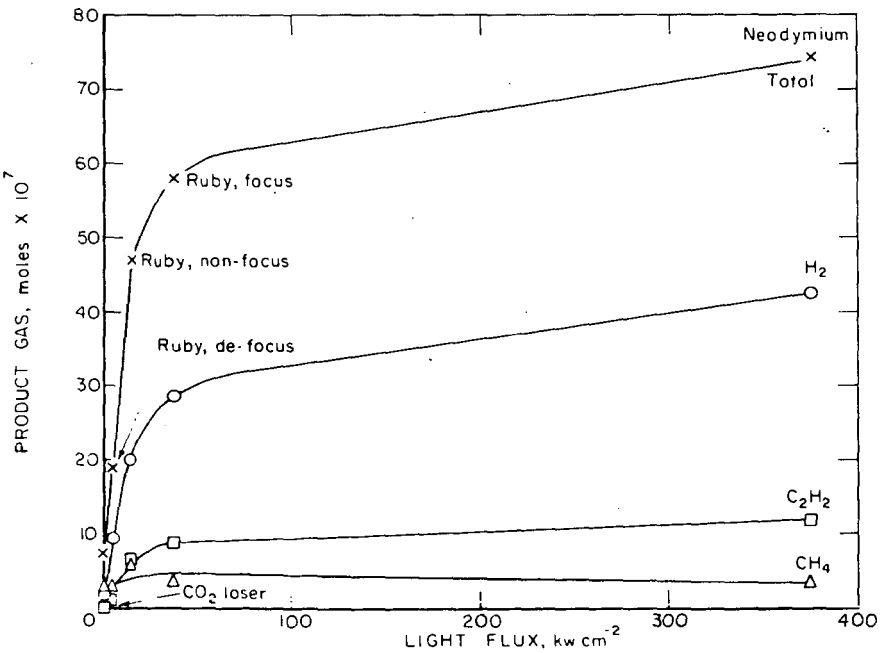


Figure 3 — Gas composition as a function of light flux. Laser irradiation of Pittsburgh seam coal.

L-10293

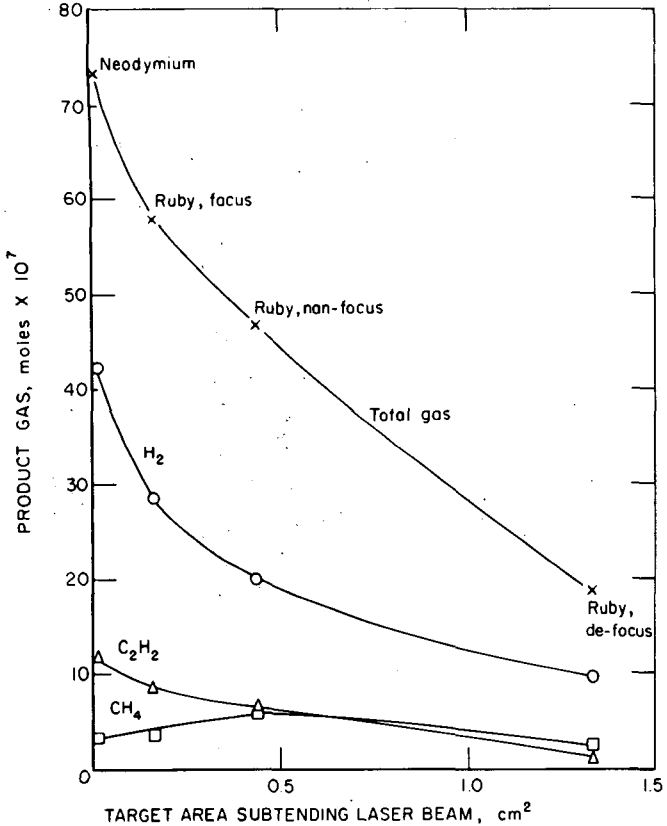


Figure 2.- Pittsburgh seam (hvab) coal irradiated with ruby and neodymium lasers. Gas in moles x $10^7$ per 6 joule pulse.

12-6-67 L-10292

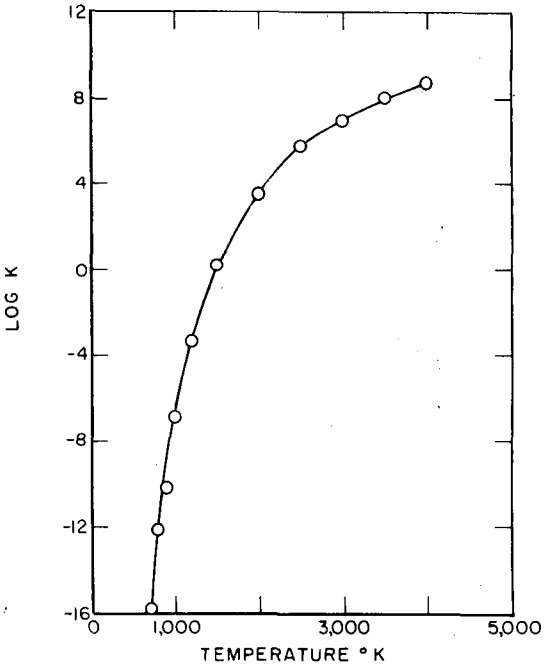


Figure 4.—Equilibrium for $2CH_4 \rightleftharpoons C_2H_2 + 3H_2$ calculated from NASA SP—3001. (ref 4)

L-10294

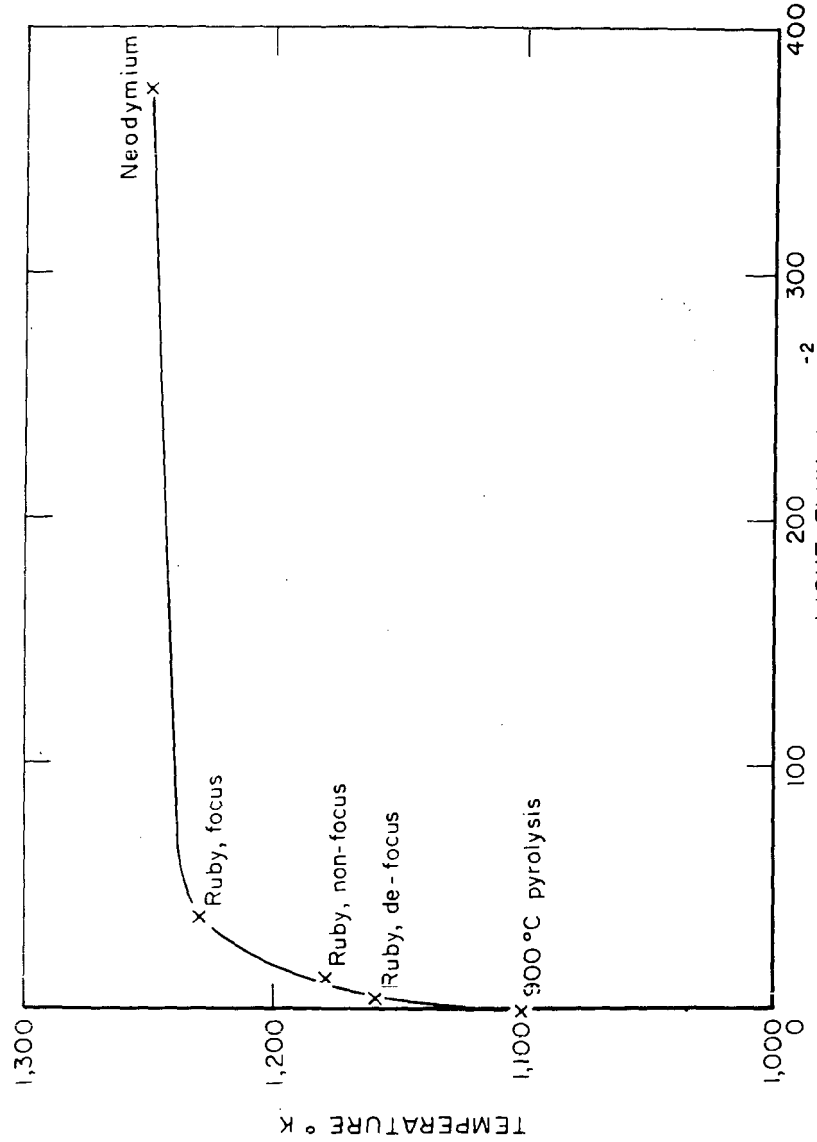


Figure 5.— Temperatures of laser irradiated coal as estimated from gas analyses.

# PYROLYSIS OF COAL IN A MICROWAVE DISCHARGE*

Yuan C. Fu and Bernard D. Blaustein

Pittsburgh Coal Research Center, Bureau of Mines,
U. S. Department of the Interior
4800 Forbes Avenue, Pittsburgh, Pennsylvania 15213

## INTRODUCTION

The nature of the thermal decomposition of coal differs greatly depending on the reaction temperature and the rate of heating. Recent investigations using various energy sources, e.g., plasma jets,[1-3] laser beam,[4,5] flash heating,[6] arc-image reactors,[7] etc., have shown that extremely rapid pyrolysis of coal produces high yields of acetylene. It has also been shown that high-volatile bituminous coal, when reacted in a microwave discharge in argon,[8] is readily gasified to produce a significant yield of acetylene.

The present study deals with the pyrolyses of coals of various ranks under the influence of a microwave discharge. The readiness of coal to give up a small part of its volatiles under the microwave irradiation permits the discharge to be sustained even when starting initially under a high vacuum. The relationship between the pressure increase during the discharge pyrolysis of coal and time shows that the principal reaction is a rapid gasification, which is induced by the active bombardment of the coal by energetic species present in the discharge. Studies of the gas composition at various stages of the discharge pyrolysis; of the effect of initial presence of Ar; and of the effect of cooling the gaseous products (as they are being formed); have all given further insight into the nature of the decomposition of coal which takes place in the microwave discharge.

## EXPERIMENTAL

Experiments were carried out in a Vycor tube reactor attached to a vacuum system provided with a Pace Engineering pressure transducer. The transducer was connected to a Fisher recorder, so that the pressure increase due to the devolatilization of coal in a known volume could be recorded during its discharge pyrolysis. The discharge was produced by a Raytheon microwave generator (2450 $MH_z$) coupled to an air-cooled Opthos coaxial cavity. The discharge was initiated by a Tesla coil either in a vacuum ( $\sim 10^{-4}$ mm Hg) or in the initial presence of argon (5-10 mm Hg), and the power level was maintained at 50 watts. The coal was located in the discharge zone.

All pressure-time data were obtained from experiments using 10 mg of vitrain of coal in a 163 ml reactor. Chemical analyses and origins of the vitrains of different coals used are given in Table 1. All the vitrains were -200 mesh, and were degassed in a high vacuum at 100° C prior to the experiment. The gaseous products were analyzed by mass spectrometry.

Tars and chars were pressed into KBr pellets for infrared analysis. Tars were also dissolved in benzene or ethanol for ultraviolet analysis.

---

* Vitrains of coals were used throughout this paper.

Table 1. Analyses of vitrains (moisture free basis, percent)

| | C | H | N | S | O (by diff.) | Ash | Volatile matter |
|---|---|---|---|---|---|---|---|
| Anthracite[1/] | 91.06 | 2.49 | 0.96 | 0.83 | 2.98 | 1.77 | 6.1 |
| Low volatile bituminous[2/] | 89.57 | 4.67 | 1.25 | .81 | 2.17 | 1.53 | 20.2 |
| High-volatile bituminous[3/] | 81.77 | 5.56 | 1.71 | .97 | 7.93 | 2.06 | 39.2 |
| Lignite[4/] | 66.45 | 5.40 | .31 | 1.40 | 22.84 | 3.60 | 44.0 |

1/ Dorrance Mine, Lehigh Valley Coal Co., Luzerne County, Pennsylvania.
2/ Pocahontas No. 3 Bed, Buckeye No. 3 Mine, Page Coal and Coke Co., Stephenson, Wyoming County, West Virginia.
3/ Bruceton, Pennsylvania Bed, Allegheny County, Pennsylvania.
4/ Beulah-Zap Bed, North Unit, Beulah Mine, Knife River Coal Mining Co., Beulah, Mercer County, North Dakota.

## RESULTS AND DISCUSSION

### Gas Evolution During the Discharge Pyrolysis

Coal, on being subjected to microwave radiation and excitation by a Tesla coil, readily gives up enough of its volatiles to sustain the discharge initially. Figure 1 shows the pressure-time relationships during the discharge pyrolyses for a lignite, a high-volatile bituminous coal, a low-volatile bituminous coal, and an anthracite. The zero time is the time the plasma appeared, and there is usually some sort of "induction period" before an extensive build-up of the pressure takes place, except for the lignite where the pressure rise is spontaneous. For each vitrain, the pressure reaches a plateau after some time. Substantial amounts of tars were produced from the hvab and the lvb coals, and it was noticed that the tars deposited on the reactor wall immediately after the discharge was initiated.

The results and the pressure-time relationships show that the discharge pyrolysis of coal (except for lignite) may be divided into three stages:

(1) Partial carbonization to produce tar. This proceeds at a relatively low rate without significant gas evolution -- an "induction period" for gas evolution.

(2) The principal reaction -- pyrolysis with accompanying gasification. This proceeds at a relatively high rate.

(3) Degassing of residual char. This rate is very slow.

The high evolution of gases in the second stage takes place only after the pressure in the system has gradually built up to a point (0.5 to 1 mm), where there are sufficient concentrations of electrons, atoms, and ions present in the discharge so that these energetic species can actively bombard the coal to accelerate the decomposition of the coal. For the lignite the rapid gas evolution takes place spontaneously, presumably owing to its readiness to release sufficient amounts of volatile matter which is converted to the energetic species. As shown in Figure 1, the rate of gas evolution at this stage increases with volatile matter content of the coal.

In the third stage, the gas evolution reaches a limit. Table 2 shows the typical product analyses obtained at the end of the reaction time indicated in Figure 1. The extent of devolatilization or gasification increases with volatile matter content of the coal. In general, the amounts of gases evolved are comparable to those evolved from thermal decompositions of the coals at about 1000° C, but the products are richer in $H_2$ and $C_2H_2$.

Table 2. Discharge pyrolysis of coal

| | Lignite | hvab | lvb | Anthracite |
|---|---|---|---|---|
| Volatile matter, percent | 44.0 | 39.2 | 20.2 | 6.1 |
| Reaction time, min | 10 | 20 | 20 | 20 |
| Product, $10^{-1}$ mmoles/g. coal | | | | |
| $H_2$ | 86.5 | 103 | 120 | 60.2 |
| $CH_4$ | 2.7 | 3.5 | 1.4 | 5.0 |
| $C_2H_2$ | 7.8 | 15.0 | 7.9 | 1.8 |
| $C_2H_6$ | 0.7 | 0.9 | 0.2 | trace |
| CO | 83.5 | 35.7 | 11.3 | 3.9 |
| $CO_2$ | 8.7 | 0.8 | 0.1 | trace |
| $H_2O$ | 5.5 | 2.0 | 3.5 | 1.9 |
| Total gases, wt pct | 32.6 | 17.5 | 8.6 | 3.3 |
| C gasified, percent | 20.6 | 11.1 | 4.2 | 1.2 |
| C converted to gaseous hydrocarbons, percent | 3.9 | 5.7 | 2.7 | 0.6 |

## Effect of Initial Presence of Argon

The pressure-time relationship during the discharge pyrolysis in the presence of added argon (Figure 2) shows that the rapid gas evolution takes place as soon as the discharge is initiated and proceeds at a higher rate. Here, the gas evolution also quickly reaches a limit, but the initial "induction period" for the gas evolution does not exist. Evidently, the added argon immediately forms sufficient concentrations of energetic species upon initiation of the discharge, thus allowing stages 1 and 2 to proceed concurrently. The gas evolution reaches a limit sooner, but the extent of devolatilization of the coal and the gaseous product type do not differ significantly. The results are shown in Table 3.

## Gas Composition at Various Stages of Discharge Pyrolysis

In order to investigate the composition of the gases evolved at various stages of the devolatilization, the pyrolysis was interrupted at several stages by discontinuing the discharge. At each stage, the evolved gases were measured and collected for mass spectrometric analysis. The discharge -- and the pyrolysis -- were then continued for the remaining coal until no more noticeable devolatilization could be observed.

Figures 3 and 4 show the results obtained for the lignite and the hvab coal, respectively. The gas composition at various stages of the thermal pyrolysis (the gases were collected at 200° C interval) of the hvab coal is also shown in Figure 5 for comparison. Acetylene in addition to methane are the major constituents of the hydrocarbons produced from the discharge pyrolysis, and their concentrations are nearly constant at each stage, except that they decrease at the later stages, possibly because of less evolution of hydrogenated carbon-species from the coal.

Table 3. Discharge pyrolysis of coal in the presence of Ar

| | Lignite | hvab | lvb | Anthracite |
|---|---|---|---|---|
| Volatile matter, percent | 44.0 | 39.2 | 20.2 | 6.1 |
| Initial pressure of Ar, mm | 5.1 | 5.1 | 5.1 | 5.1 |
| Reaction time, min | 5 | 20 | 20 | 20 |
| Product, $10^{-1}$ mmoles/g. coal | | | | |
| $H_2$ | 86.8 | 98.5 | 113 | 64.5 |
| $CH_4$ | 2.1 | 2.5 | 4.0 | 0.4 |
| $C_2H_2$ | 10.4 | 15.8 | 8.8 | 2.0 |
| $C_2H_4$ | 0.6 | 0.7 | 0.8 | trace |
| CO | 79.5 | 31.9 | 10.8 | 4.2 |
| $CO_2$ | 8.6 | 0.7 | 0.2 | trace |
| $H_2O$ | 7.5 | 3.4 | 4.9 | 1.6 |
| Total gases, wt pct | 33.5 | 16.5 | 9.4 | 3.4 |
| C gasified, percent | 19.4 | 11.4 | 4.9 | 1.2 |
| C converted to gaseous hydrocarbons, percent | 4.5 | 6.6 | 3.5 | 0.7 |

Tar -- Substantial amounts of tars were obtained from the hvab and the lvb coals in the discharge pyrolyses. The tars were compared by IR and UV analyses with the tar obtained from the thermal pyrolysis (at 700° C) of the hvab coal. All the IR spectra showed the presence of usual aliphatic C-H bands (2860-2940 $cm^{-1}$) and aromatic bands (740-860 $cm^{-1}$) which are typical of pitch and coal. The tars obtained from the discharge pyrolyses, however, exhibited weaker aromatic bands and a stronger carbonyl band (1710 $cm^{-1}$) than the tar obtained from thermal pyrolysis. The UV spectra (of the tars extracted by benzene or ethanol) exhibited no distinct absorption band for the tar obtained from the thermal pyrolysis, but exhibited bands at 3140, 3300, and 3470 Å (which could be attributed to derivatives of pyrene) for those obtained from the discharge pyrolyses.

All the residual chars exhibited no distinct band over the entire IR spectrum.

Effect of Cooling by Liquid Nitrogen

A. Hvab Coal -- When one end of an h-shaped reactor (vol. = 41 ml) was cooled with liquid $N_2$ while the other leg containing the hvab coal was subjected to the discharge pyrolysis, it was observed that the pressure reading of the reactor never exceeded 0.5 mm during the course of the decomposition. The end products consisted mainly of hydrocarbons and water, without significant amounts of $H_2$ and CO. Acetylene was the main hydrocarbon, but substantial amounts of other $C_2$, $C_3$, $C_4$, $C_5$ and $C_6$ hydrocarbons were also formed. Without liquid $N_2$ cooling, the other $C_2$ and $C_3$ hydrocarbons were insignificant and the $C_4$, $C_5$ and $C_6$ hydrocarbons were not measurable. The product analyses, except that for $C_4$, $C_5$ and $C_6$ hydrocarbons which constitute less than 2 percent of the gases, are shown in Table 4. The extent of devolatilization and the hydrocarbon yield are significantly increased.

Table 4. Effect of liquid nitrogen cooling on discharge pyrolysis of coal

| | $P_{Ar}$ mm | Time, min. | Product, $10^{-1}$ mmole/g. coal | | | | | | | | | Total gases, wt percent | Percentage of C present as | |
|---|---|---|---|---|---|---|---|---|---|---|---|---|---|---|
| | | | $H_2$ | $CH_4$ | $C_2H_2$ | $C_2H_4$ | $C_2H_6$ | $C_3H_6$ | $C_3H_8$ | CO | $CO_2$ | $H_2O$[2] | | Gaseous products | Gaseous hydrocarbons |
| hvab [1] | - | 15 | 1.2 | 0.4 | 40.4 | 3.4 | 5.6 | 2.9 | 1.7 | 2.7 | 0.8 | 23 | 20.4 | 17.2 | 16.7 |
| [1] | - | 30 | 3.2 | 0.5 | 48.4 | 3.6 | 9.4 | 3.8 | 2.7 | 3.6 | 0.7 | 30 | 26.2 | 21.7 | 21.1 |
| [1] | - | 45 | 1.1 | 0.4 | 48.8 | 2.6 | 7.5 | 4.5 | 3.0 | 4.5 | 0.7 | 26 | 25.3 | 21.6 | 20.8 |
| | 10 | 30 | 17.6 | 0.4 | 85.2 | 6.1 | 5.4 | 0.9 | 0.7 | 6.7 | 1.3 | 14 | 31.7 | 30.4 | 29.3 |
| Lignite | - | 7 | 0.6 | 0.5 | 47.0 | 1.9 | 3.7 | 0.7 | 0.9 | 0.8 | 13.8 | 74 | 34.3 | 22.7 | 20.1 |
| | - | 10 | 0.9 | 0.3 | 50.2 | 1.0 | 3.2 | 0.6 | 1.0 | 0.6 | 11.9 | 75 | 34.0 | 22.8 | 20.6 |
| | 10 | 20 | 12.9 | 0.2 | 38.2 | 0.8 | 1.3 | 0.3 | 0.3 | 9.8 | 14.2 | 43 | 27.8 | 19.3 | 14.9 |

[1] $C_4$, $C_5$, and $C_6$ hydrocarbons were also formed.

[2] $H_2O$ content as obtained from mass spectrometric analyses are only approximate, and data are reported only to show trends.

With Ar initially present and with cooling, however, the pressure reading increased rather rapidly to a maximum within a few minutes, and then decreased gradually. Presumably, large amounts of $H_2$, CO (noncondensable at -196° C) and hydrocarbons were rapidly formed due to the high rate of gasification of the coal in the Ar discharge. The pressure decrease in the later stage is attributed to the continuous reaction of $H_2$ and CO to form condensable hydrocarbons. As seen in Table 4, however, appreciable $H_2$ and CO still remained after 30 minutes of reaction. The yield of acetylene is very high, but that of other $C_2$ and $C_3$ hydrocarbons is low. No measurable amounts of $C_4$, $C_5$ and $C_6$ hydrocarbons were found

These results may be interpreted as follows. In the absence of added Ar, small reactive species (H, O, C, CH, etc.) and perhaps some larger fragments (radicals) are slowly detached from coal molecules, but are rapidly converted to stable products such as acetylene, higher hydrocarbons, and water, which are finally condensed at the liquid $N_2$ temperature. In the presence of Ar, however, the detachment of these fragments proceeds at such a high rate that all the products formed cannot be immediately condensed by the liquid $N_2$. As a result, the larger molecules further decompose or react with O-species to form large amounts of $H_2$ and CO. It is also quite possible that different types of species (or smaller fragments) are released in the presence of Ar, resulting in rapid formation of noncondensable $H_2$ and CO. With prolonged reaction time, the $H_2$ and the CO would then continue to react to form relatively lower hydrocarbons and water.

Increases in the extent of devolatilization and in the hydrocarbon yield under these conditions are due primarily to the removal of hydrocarbons (therefore no further decomposition or polymerization), and of water[9] (therefore no reaction of water with hydrocarbons to form $H_2$ and CO).

B. Lignite -- As seen in Figure 1, lignite releases gases spontaneously at a higher rate than the hvab coal. Thus, when the discharge pyrolysis of the lignite was subjected to liquid $N_2$ cooling, it was observed that the pressure reading increased rapidly to a maximum within 1 to 2 minutes, and then decreased gradually to practically zero after several minutes. At this point, the major part of the pyrolysis of the coal seemed to be completed and the discharge could not be maintained.

The reasons for this different behavior (from that of the hvab coal) may be (i) the spontaneous gas evolution at a higher rate and (ii) the release of more numerous smaller fragments from lignite, resulting in rapid formation of noncondensable $H_2$ and CO. All the $H_2$ and the CO are eventually converted to hydrocarbons and water in the later stage. The results in Table 4 also show that the hydrocarbon yield is very significantly increased under these conditions.

Similar behavior was observed with added Ar except that some part of the $H_2$ and CO remain unreacted, owing perhaps to the slowness with which the product species diffusing into the cold trap in the presence of high concentration of Ar.

It was also noticed that the lignite yielded a significant amount of $CO_2$, while the hvab coal yielded very small amounts of $CO_2$ under all conditions. This suggests that $CO_2$ molecules are released from the lignite structure rather than formed from interactions of CO and active O-species in the discharge.

## CONCLUSIONS

The principal reaction in the discharge pyrolysis of coal is rupture of the bonds in the coal structure by bombardment of energetic species (whether released from the coal or formed from argon in the discharge) on the coal surface. Numerous species such as H-species, O-species, gaseous C, and hydrogenated carbon fragments (CH, $C_2H$ or $C_xH_y$) are produced from coal in the discharge, these in turn decompose or combine with each other to form hydrogen, water, carbon oxides, and hydrocarbons. After extensive decomposition of the coal structure, all the species present in the discharge reach a steady state, where the formation of hydrocarbons is limited by back reactions with water to form $H_2$ + CO and gasification of solid is somewhat compensated by polymerization of hydrocarbons.

Thus, if the decomposition products are rapidly removed by a liquid nitrogen trap as they are formed, high yield of hydrocarbons consisting mainly of acetylene can be obtained. The process for the discharge pyrolysis of high-volatile bituminous coal under these conditions is unique in that it converts more than 21 percent of carbon in coal to higher hydrocarbons (up to $C_6$) without the accompanying formation of $H_2$ and CO. With argon initially present under similar conditions, however, the pyrolysis products are lower hydrocarbons (below $C_4$) and substantial amounts of $H_2$ and CO, owing to the increased rate of gasification. Hence, the product type and distribution can be influenced by the rate of formation or removal of the products.

## ACKNOWLEDGEMENTS

The authors wish to thank Dr. Irving Wender for his valuable discussions, Gus Pantages and George Kambic for their technical assistance, A. G. Sharkey, Jr. and Janet L. Shultz for their mass spectrometric analyses, and John Queiser for his infrared analysis.

## REFERENCES

1. Bond, R. L., Ladner, W. R., and McConnell, G. I. T. Fuel, Lond. 1966, 45, 381
2. Graves, R. D., Kawa, W., and Hiteshue, R. W. Ind. Eng. Chem. Proc. Design and Develop., 1966, 5, 59
3. Kawana, Y., Makino, M., and Kimura, T. Kogyo Kagaku Zasshi, 1966, 69, 1144
4. Shultz, J. L. and Sharkey, A. G. Jr. Carbon, 1967, 5, 57
5. Karn, F. S., Friedel, R. A., and Sharkey, A. G. Jr. Carbon, 1967, 5, 25
6. Rau, E. and Seglin, L. Fuel, Lond. 1964, 43, 147
7. Rau, E. and Eddinger, R. T. Fuel, Lond. 1964, 43, 246
8. Fu, Y. C. and Blaustein, B. D. Chem. and Ind., Lond. 1967, 1257.
9. Blaustein, B. D. and Fu, Y. C. In "Chemical Reactions in Electrical Discharges," Adv. Chem. Series, R. F. Gould, Editor, Amer. Chem. Soc., Washington, D. C., Volume in press, 1968

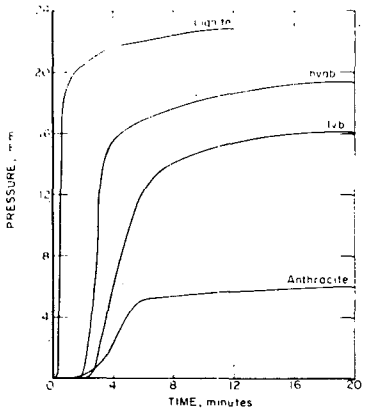


Figure 1 — Pressure as a function of time during the discharge pyrolysis of coal (10 mg coal in 163 ml reactor)

12-12-67 L-10305

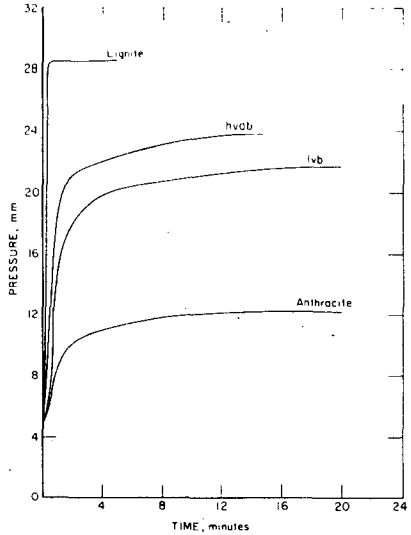


*Figure 2 - Pressure as a function of time during the discharge pyrolysis of coal in the presence of Ar ($P_{Ar}$ = 51 mm, 10 mg coal in 163 ml reactor)*

12-5-67 L-10288

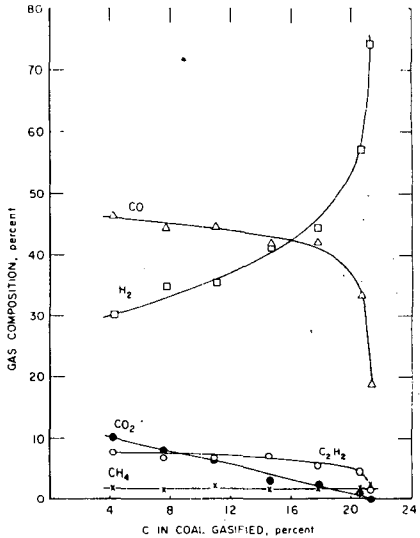


Figure 3 - Gas composition at various stages of discharge pyrolysis of lignite.

12-5-67 L-10289

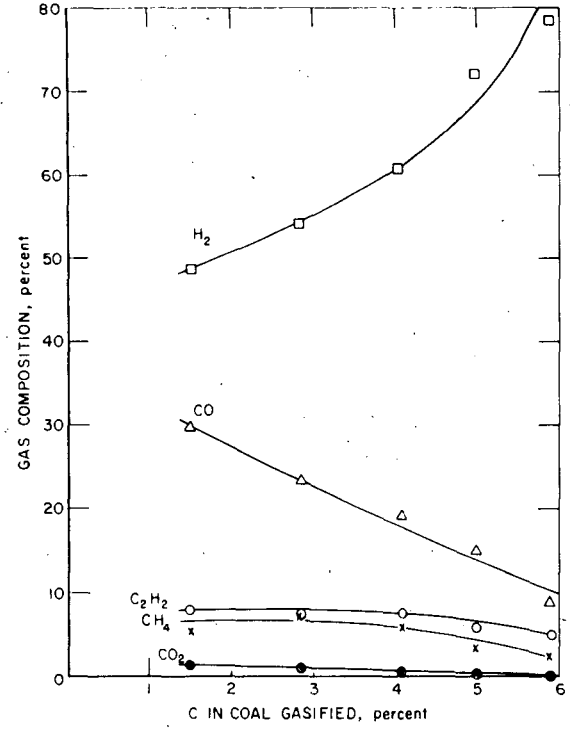


Figure 4.- Gas composition at various stages of discharge pyrolysis of hvab coal.

12-5-67 L-10290

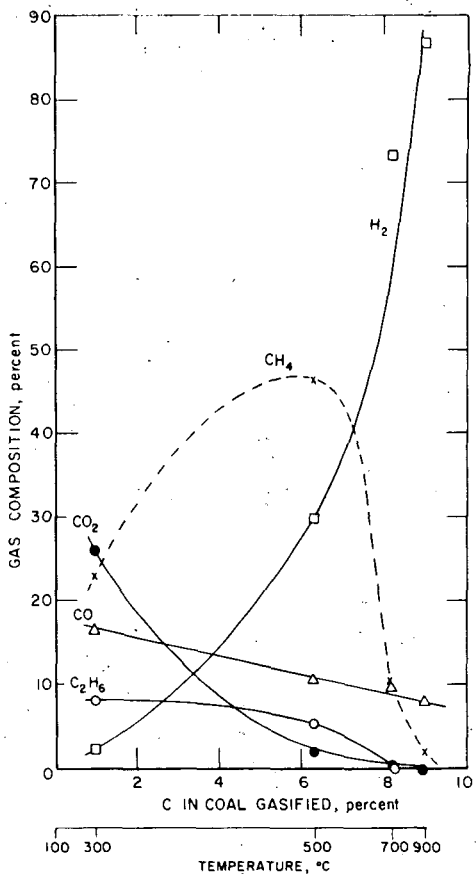


Figure 5.- Gas composition at various stages of thermal pyrolysis of hvab coal.

12-5-67 L-10291

# KINETICS OF HYDROCRACKING OF LOW TEMPERATURE COAL TAR

S. A. Qader, W. H. Wiser, and G. R. Hill

Department of Fuels Engineering,
University of Utah,
Salt Lake City, Utah

## Abstract

The results of hydrocracking of a low temperature coal tar in a batch autoclave over a catalyst containing sulphides of nickel and tungsten, supported on silica-alumina, indicated that gasoline can be obtained in a yield of 77% at 500°C and 3000 psi pressure. The highest quality product, containing 60% aromatics and 13% isoparaffins, was obtained at 450°C and 2000 psi but in a lower yield of 60%. Most of the sulfur, nitrogen, and oxygen present in the tar were removed. The gasoline formation, desulphurization, and denitrogenation reactions were all found to be of first-order with activation energies of 17,000, 14,500, and 15,000 calories per mole respectively. Linear relationships were found between rate constants for gasoline formation ($k_g$), desulphurization ($k_s$) and denitrogenation ($k_n$) as can be represented by the following equations:

$$k_g = 1.1371\ k_s - 0.1278$$

$$k_g = 2.11\ k_n - 0.0669$$

$$k_n = 0.5397\ k_s - 0.0837$$

Hydrocracking reactions involving the breakage of chemical bonds on the catalyst surface are rate-determining.

## Introduction

Hydrocracking has been investigated in recent years as a potential method for upgrading coal-derived liquids. The work reported so far is very much limited and the fundamental aspects of such processing are not well understood. Much of the earlier work was carried out in connection with the coal hydrogenation processes (Gordon, 1935, 1940, and 1947 and Pier, 1949) where a two-stage reaction was used in which the first stage liquified the coal and the second converted the resulting heavy distillates to gasoline by catalytic hydrocracking. Carpenter, et al (1963) reported the results of hydrocracking a lignite tar in a continuous fixed bed reactor over cobalt-molybdate and zinc chromite catalysts for producing gasoline. A maximum yield of 59% of gasoline was obtained at 477°C and 3000 psi pressure. Rutkowski

(1965) studied the influence of temperature, pressure, hydrogen-oil ratio, diluents, and catalysts on the hydrocracking of low temperature tars and reported minimum coke yields using tetralin and cyclohexane as diluents. Katsobashvili and Elbert (1966) reported a yield of 83.8% saleable products when a tar distillate boiling from 230° to 360°C was hydrocracked in a continuous fixed bed reactor at 500° to 550°C and 50 atmospheres under recycle conditions. The economic feasibility of producing gasoline from coal by the H-coal process, wherein the heavy oil produced in the first stage was hydrocracked in a subsequent stage, was demonstrated by the results published by Alpert, et al (1966). Zielke, et al (1966) investigated the suitability of zinc halide catalysts for hydrocracking coal extracts for the production of gasoline. The results indicated that a maximum yield of 68% of gasoline could be obtained at 427°C, 4200 psi pressure and 60 minutes reaction time. In the present communication, the results of hydrocracking of a low temperature coal tar in a batch autoclave over a catalyst containing sulphides of nickel and tungsten, supported on silica-alumina, are described. The influence of temperature and pressure on product distribution and kinetic evaluation of the data are presented.

## Experimental

### Materials.

Low temperature tar from a high volatile bituminous coal from Utah was prepared by carbonization at 550°C in a laboratory oven. The light oil boiling up to 200°C was separated from tar by distillation (Table I). The catalyst (commercial) contained 6% nickel and 19% tungsten, both as sulphides, supported on silica-alumina and had a surface area of 212 sq. meters per gram and size of -200 mesh. 5-A molecular sieves were of chromatographic grade.

### Equipment.

A 1-litre high pressure autoclave with a magnetic drive stirrer, pressure and temperature control devices, liquid and gas sampling lines, and water quenching system (Figure 1) and hydrogen cylinders with maximum pressure of 2300 psi were used.

### Procedure for hydrocracking experiments.

In each experiment 100 c.c of tar and 10 grams of the catalyst were used. The equipment was evacuated to remove most of the air, filled with hydrogen and heated to the desired temperature. The temperature rose to 300°C in 21 minutes and 500°C in 28 minutes. The reaction time was taken from the start of heating the equipment. When the reaction temperature was reached, the pressure was adjusted to the experimental value and maintained constant throughout except in experiments conducted at pressures higher than 2000 psi where there was a reduction in pressure of about 200 to 300 psi during

the course of the experiment. Experiments were conducted at different reaction times and 4 gas samples were taken out during each experiment. At the end of the reaction time, heating was stopped and the product was quenched rapidly by circulating water in the cooling coil immersed in it. It took 1 to 2 minutes to cool the product down to 250°C and 15 minutes to atmospheric temperature. The pressure was then released slowly and the autoclave opened. The product was transferred to a beaker, filtered to remove the catalyst, and the water separated to get the total oil product. The mechanical losses were found to be less than 1%. The yield of the product was taken as 100% and 100 minus the volume of the total oil product was taken as percent conversion to gas. A few c.c of the total oil product were used for sulfur and nitrogen analysis and the remainder was washed with 10% sodium hydroxide and 20% sulphuric acid to remove tar acids and bases respectively. The neutral oil was then distilled into a gasoline fraction boiling up to 200°C, a diesel oil fraction boiling from 200° to 360°C and residue. The volume of each fraction in c c obtained from the total oil product was taken as volume percent conversion to that particular fraction

Product analysis.

Sulfur was determined by the bomb method and nitrogen by the C-H-N chromatographic analyzer, F.M. Model 185. Tar acids and bases were estimated by extraction with 10% sodium hydroxide and 20% sulphuric acid respectively. Hydrocarbon-type analysis was done by the Fluorescent-Indicator-Adsoprtion method (ASTM, D1319-65T). For the estimation of naphthenes and isoparaffins, the saturated hydrocarbon portion was first separated from the mixture by sulphonation with a mixture of 70% concentrated sulphuric acid and 30% phosphorus pentoxide (ASTM, D1019-62). The naphthenes were estimated by the refractivity intercept method (ASTM, D1840-64). The N-paraffin content was determined by adsorption over 5-A molecular sieves in a glass column of 0.5-inch diameter and 1.5-foot length. The isoparaffins were obtained by the difference. The diesel index was calculated from API gravity and aniline point. The gas analysis was done by gas chromatography in the F.M. Model 720 dual column programmed temperature gas chromatograph.

Results and Discussion

Product distribution.

The yield of gasoline and gas and the iso-normal ratio in butanes increased with temperature whereas the diesel oil decreased while the residue remained almost the same (Figure 2). Tar acids and bases were removed completely along with most of the sulfur and nitrogen at 450°C and 1500 psi pressure (Table II). Isomerization increases with cracking and the gas yield and iso-normal ratio in butanes are qualitative indications of the extent of cracking reactions taking place leading to the formation of gasoline. A

pressure of 1500 psi is sufficient to suppress coke-forming reactions and the gasoline is formed mainly by the cracking of the diesel oil, thereby affecting the quantity and quality of the latter. The composition of gasoline obtained at different temperatures remains almost the same and the aromatics of the gasoline are mainly formed by the dealkylation of alkylbenzenes, hydrocracking of hydro-aromatics, and hydroremoval of sulfur, oxygen, and nitrogen compounds.

The gasoline yield increased at different rates with pressure (Figure 3). The rate of gasoline formation was high in the pressure range 1000 to 1500 psi, slowing down in the range 1500 to 2500 psi, and increasing again at higher pressures. The residue decreased rapidly in the range 1000 to 1500 psi but the decrease was small at higher pressures. On the other hand, the gas yield and iso-normal ratio in butanes remained almost constant up to a pressure of 1500 psi and increased at higher pressures (Figure 4). Pressure does not have a marked influence on cracking reactions in the range 1000 to 1500 psi but the increase in the yield of gasoline is due to the suppression of the coke-forming reactions. In the range 2000 to 2500 psi, partial hydrogenation of aromatics to hydro-aromatics takes place followed by the cracking of the latter which increases the yield of gasoline and the aromatic content (Figures 5 to 7). At higher pressures complete hydrogenation of aromatics to naphthenes takes place and increases the gasoline yield. The naphthenes in the gasoline increase with a corresponding decrease in the aromatics. Isomerization increases with pressure and temperature. High aromatic gasolines were obtained in the pressure range 1750 to 2500 psi (Table III). A maximum yield of 77% of gasoline was obtained at 500°C and 3000 psi pressure but the highest quality product containing 60% aromatics and 13% isoparaffins was formed at 450°C and 2000 psi pressure which can compare well with the premium grade gasoline from petroleum (Table IV).

Kinetics

Equilibrium was reached at different time periods at different temperatures with respect to gasoline formation but the conversion was 100% in the case of sulfur and nitrogen removal (Figures 8 to 10). The sulfur and nitrogen removal reactions are not governed by thermodynamic limitations but are limited only by kinetic factors under the experimental conditions employed. Plots of $\log \frac{a}{a-x}$ versus time (Figures 11 to 13), where "a" is the equilibrium conversion in case of gasoline and initial concentration in case of sulfur and nitrogen, are linear and the hydrocracking reactions with respect to gasoline formation and removal of sulfur and nitrogen are all first-order. The first-order rate constants are thus represented by equations 1 to 3.

$$\frac{d\,(\text{Gasoline})}{dt} = k_g\,(\text{Tar}) \qquad (1)$$

$$-\frac{d\,(\text{Sulfur})}{dt} = k_s\,(\text{Sulfur}) \qquad (2)$$

$$-\frac{d\,(\text{Nitrogen})}{dt} = k_n\,(\text{Nitrogen}) \qquad (3)$$

where "kg," "$k_s$," and "$k_n$" are rate constants for gasoline formation and removal of sulfur and nitrogen respectively. There was no change in the concentration of hydrogen in the system during the course of the reaction since the hydrogen pressure was maintained constant throughout. Hydrogen atoms may be involved in the rate-determining step but their concentration constitutes one of the constant factors in the rate constant term and does not show up in the rate equation. However, hydrogen actually takes part in the hydrocracking reactions and, hence, the reactions are considered pseudo-first-order

The hydrocracking reactions under study follow true Arrhenius temperature dependence (Figure 14) and the rate constants can be represented by equations 4 to 6.

$$k_g = 0.1567 \times 10^6\, e^{-17,600/RT} \text{ hrs.}^{-1} \qquad (4)$$

$$k_s = 0.2134 \times 10^5\, e^{-14,500/RT} \text{ hrs.}^{-1} \qquad (5)$$

$$k_n = 0.4738 \times 10^5\, e^{-15,900/RT} \text{ hrs.}^{-1} \qquad (6)$$

The following values of enthalpies and entropies of activation were calculated by the Eyring equation plotting log k'/T versus $\frac{1}{T}$ (Figure 15).

$$\Delta H_g = 16,200 \text{ cal /mole}, \quad \Delta S_g = -43.5 \text{ e.u.}$$

$$\Delta H_s = 12,200 \text{ cal /mole}, \quad \Delta S_s = -44.9 \text{ e.u.}$$

$$\Delta H_n = 14,900 \text{ cal /mole}, \quad \Delta S_n = -45.9 \text{ e.u.}$$

Linear relationship was found between $k_g$, $k_s$, and $k_n$ (Figure 16) and can be represented by equations 7 to 9

$$k_g = 1.1371\, k_s - 0.1278 \qquad (7)$$

$$k_s = 2.1100\, k_n - 0.0669 \qquad (8)$$

$$k_n = 0.5397\, k_s - 0.0837 \qquad (9)$$

A major part of the gasoline is expected to be formed by the cracking of hydrocarbons, but a minor part comes from the decomposition of some of the sulfur, oxygen, and nitrogen compounds. The yield of gasoline thus depends, to some extent, on the removal of sulfur and nitrogen and this may result in some sort of interrelationship between $k_g$, $k_s$, and $k_n$. The dissociation energies of the C-C, C-S, and C-N bonds may also have some influence on the above relationship, especially between $k_s$ and $k_n$. However, the results presented in this paper do not throw much light on the effect of other temperature and pressure conditions and equations 7 to 9 are not considered to be having much quantitative significance at this stage.

The energies and enthalpies of activation indicate that chemical reactions but not physical processes are rate-controlling. The probable chemical reactions occurring during hydrocracking are cracking, isomerization, hydrogenation, polymerization, condensation, and dehydrogenation, all taking place on the catalyst surface. Under the experimental conditions employed, polymerization, condensation, and dehydrogenation are very much suppressed and may be eliminated. It has been established by Weisz and Prater (1957) and Keulemans and Voge (1959) that reactions occurring on acidic sites of the dual-functional catalyst, like the one used in this investigation, are rate-determining which eliminates the possibility of hydrogenation reactions to be rate-limiting. Hence, cracking reactions involving the breakage of chemical bonds and the isomerization reactions, wherein skeletal rearrangement of carbonium ions takes place, must be rate-limiting. It is known that in catalytic hydrocracking, cracking precedes isomerization and only the isomerization of the cracked fragments occurs without any change of the uncracked material (Flinn, et al., 1960, and Archibald, et al., 1960). An excess of branched isomers than can be predicted by thermodynamic equilibrium are also formed; the latter can only happen if the isomerization of the cracked fragments can occur very rapidly and leave the catalyst surface without appreciable readsorption. Therefore, the isomerization is believed to be very rapid and cannot be rate-controlling. Hence, the cracking reactions, involving the breakage of chemical bonds on the catalyst surface, are rate-determining.

Acknowledgment

The research work reported in this paper was sponsored by the U. S. Office of Coal Research and the University of Utah.

Table I. Properties of Feed Material

| | |
|---|---|
| Sp. gr. (25°C) | 0.9942 |
| Tar acids, vol. % of feed | 30.0 |
| Tar bases, wt. % of feed | 3.5 |
| Sulfur, wt. % of feed | 0.6984 |
| Nitrogen, wt. % of feed | 0.4018 |
| Distillation data | |
| I.B.P., °C. | 200 |
| 50% distillate | 298°C |
| Pitch point | 360°C |
| Residue, vol. % of feed | 30.0 |
| Hydrocarbon types in neutral fraction 200° to 360°C, vol. % | |
| Saturates | 32.0 |
| Olefins | 19.0 |
| Aromatics | 49.0 |

Table II. Influence of Temperature on Product Distribution (Pressure, 1500 psi)

| Temp. (°C.) | 400 | 425 | 450 | 475 | 500 |
|---|---|---|---|---|---|
| Reaction Time, hrs. | 13 | 12 | 10 | 8 | 5 |
| Yield, vol. % of feed | | | | | |
| Gasoline | 45.0 | 51.0 | 56.0 | 61.0 | 64.0 |
| Diesel oil | 35.0 | 29.0 | 24.0 | 20.0 | 16.0 |
| Tar acids | 2.0 | 1.0 | -- | - | - |
| Tar bases | 1.0 | 0.5 | -- | - | - |
| Residue | 12.0 | 12.0 | 13.0 | 11.5 | 12.0 |
| Gas (including losses) | 4.5 | 6.5 | 7.0 | 7.5 | 8.0 |
| Sulfur, wt. % of feed | 0.0489 | 0.0210 | 0.014 | 0.0135 | 0.0136 |
| Nitrogen, wt. % of feed | 0.0924 | 0.0442 | 0.0321 | 0.0201 | 0.0163 |
| Composition of gasoline, vol. % | | | | | |
| Aromatics | 33.5 | 35.0 | 34.0 | 32.0 | 33.0 |
| Naphthenes | 10.0 | 9.0 | 10.5 | 10.0 | 10.0 |
| Olefins | 2.0 | 3.0 | 2.0 | 2.0 | 4.0 |
| Isoparaffins | 25.5 | 26.0 | 26.0 | 27.0 | 25.0 |
| N-paraffins | 29.0 | 27.0 | 27.5 | 29.0 | 28.0 |
| Diesel index of diesel oil | 40.0 | 37.5 | 34.0 | 31.0 | 28.0 |
| Isobutane / N-butane | 1.0 | 1.25 | 1.45 | 1.51 | 1.75 |

Table III. Influence of Pressure on Yield and Composition of Gasoline

| Yield and Hydrocarbon Types, Vol. % | Temperature, °C. | Pressure, psi. 1000 | 1250 | 1500 | 1750 | 2000 | 2250 | 2500 | 2750 | 3000 |
|---|---|---|---|---|---|---|---|---|---|---|
| Yield | 400 | 15.0 | 36.0 | 45.0 | 48.0 | 50.0 | 54.0 | 58.0 | 63.0 | 68.0 |
| Aromatics | 400 | 33.5 | 36.0 | 33.5 | 46.0 | 50.0 | 46.5 | 40.0 | 33.5 | 28.0 |
| Naphthenes | 400 | 10.0 | 9.5 | 10.0 | 10.5 | 10.0 | 18.5 | 24.0 | 28.5 | 31.0 |
| Olefins | 400 | 5.5 | 3.0 | 2.0 | 1.5 | 2.0 | 3.5 | 2.5 | 4.0 | 3.5 |
| Isoparaffins | 400 | 24.0 | 24.0 | 25.5 | 19.0 | 20.0 | 18.5 | 19.0 | 20.5 | 25.5 |
| N-paraffins | 400 | 27.0 | 27.5 | 29.0 | 23.0 | 18.0 | 13.0 | 14.5 | 13.5 | 12.0 |
| Yield | 450 | 36.0 | 49.0 | 56.0 | 58.0 | 60.0 | 62.0 | 66.0 | 69.0 | 73.0 |
| Aromatics | 450 | 36.0 | 32.5 | 34.0 | 44.0 | 60.0 | 56.0 | 47.0 | 39.0 | 33.0 |
| Naphthenes | 450 | 11.0 | 10.0 | 10.5 | 12.0 | 12.5 | 15.0 | 23.0 | 29.0 | 35.0 |
| Olefins | 450 | 3.0 | 3.5 | 2.0 | 1.0 | 1.0 | 1.0 | 1.0 | 1.0 | 1.0 |
| Isoparaffins | 450 | 23.5 | 26.5 | 26.0 | 21.0 | 13.0 | 14.0 | 15.5 | 19.0 | 22.0 |
| N-paraffins | 450 | 26.5 | 27.5 | 27.5 | 22.0 | 14.0 | 14.0 | 13.5 | 12.0 | 9.0 |
| Yield | 500 | 44.0 | 54.0 | 64.0 | 66.0 | 68.0 | 69.0 | 71.0 | 74.0 | 77.0 |
| Aromatics | 500 | 36.5 | 33.0 | 33.0 | 44.0 | 50.0 | 49.0 | 41.0 | 32.5 | 26.0 |
| Naphthenes | 500 | 11.5 | 10.0 | 10.0 | 11.0 | 12.5 | 13.0 | 19.0 | 25.5 | 34.0 |
| Olefins | 500 | 4.0 | 5.0 | 4.0 | 4.5 | 3.0 | 4.5 | 2.0 | 3.0 | 2.0 |
| Isoparaffins | 500 | 23.0 | 25.0 | 25.0 | 19.5 | 17.5 | 17.0 | 21.0 | 23.5 | 26.0 |
| N-paraffins | 500 | 25.0 | 27.0 | 28.0 | 21.0 | 17.0 | 16.5 | 17.0 | 15.5 | 12.0 |

Table IV. Comparison of Yield and Composition of Gasolines (Gasoline 1 at 450°C, 2000 psi, 10 hours and Gasoline 2 at 500°C, 3000 psi, and 5 hours, both from Tar)

| | Gasoline 1 | Gasoline 2 | Regular grade gasoline from petroleum | Premium grade gasoline from petroleum |
|---|---|---|---|---|
| Yield, vol. % of feed | 60.0 | 77.0 | - | - |
| Hydrocarbon composition, vol. % | | | | |
| Aromatics | 60.0 | 26.0 | 33.0 | 34.0 |
| Naphthenes | 12.5 | 34.0 | 18.0 | 12.0 |
| Olefins | 1.0 | 2.0 | 11.0 | 14.0 |
| Isoparaffins | 13.0 | 26.0 | 22.0 | 28.0 |
| N-paraffins | 14.0 | 12.0 | 16.0 | 12.0 |

Literature Cited

1. Gordon, K., J. Inst. Fuel 9, 69 (1935); 20, 42 (1946); 21, 53 (1947).

2. Pier, M., Z. ElectroChem. 53, No. 5, 291 (1949).

3. Weisz, P. B., Prater, C. D., Advan. Catalysis 9, 575 (1957).

4. Keulemans, A. I. M., Voge, H. H., J. Phys. Chem. 63, 476 (1959).

5. Flinn, R. A., Larson, O. A., Beuther, H., Ind. Eng. Chem. 52, 152 (1960).

6. Archibald, R. C., Greensfelder, B. S., Holzman, G., Rowf, D. H., Ibid., 52, 745 (1960).

7. Carpenter, H. C., Cottingham, P. L., Frost, C. M., Fowkes, W. W., Bureau of Mines Report of Investigation No. 6237 (1963).

8. Alpert, S. P., Johanson, E. S., Schuman, S. C., Chem. Eng. Progress 60, No. 6, 35 (1964).

9. Rutkowski, M., Zesz. Nauk. Politech. Wrol. Chem. 12, 3 (1965).

10. Katsobashvili, Ya. R., Elbert, E. I., Coke and Chemistry, U.S.S.R. 1, 41 (1966).

11. Zielke, C. W., Struck, R. T., Evans, J. M., Costanza, C. P., Gorin, E., Ind. Eng. Chem. 5, 151 and 158 (1966).

1 CERAMIC FURNACE
2 LIQUID SAMPLING TUBE
3 GAS SAMPLING TUBE
4 THERMOWELL
5 COOLING COIL
6 COOLING JACKET
7 MAGNETIC DRIVE ASSEMBLY
8 SHAFT
9 IMPELLER

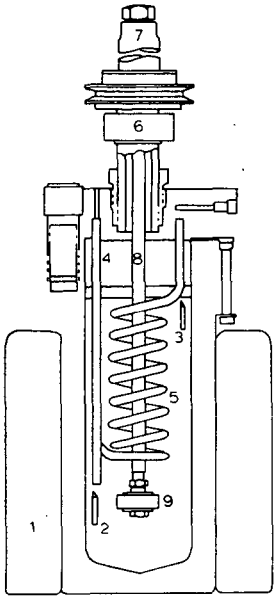


**Figure 1. Assembly of equipment**

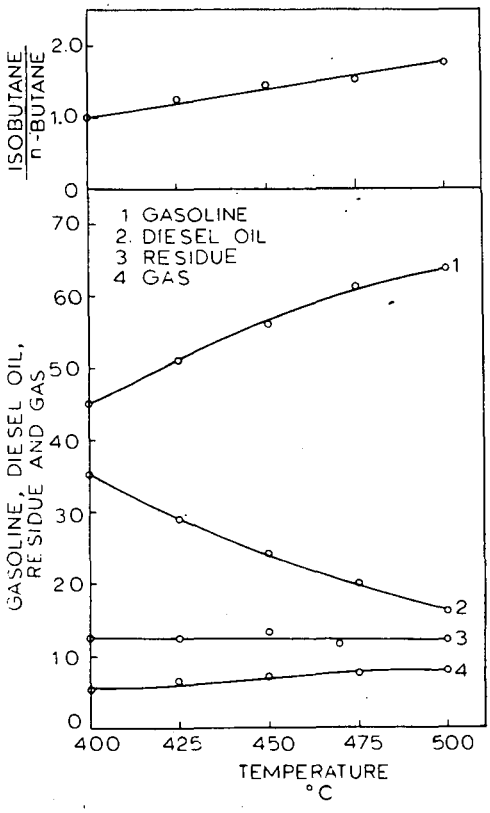


Figure 2. Effect of temperature on product distribution
Pressure, 1500 psi.
Reaction time, 13 hrs. at 400°C., 12 hrs. at 425°C.,
10 hrs. at 450°C., 8 hrs. at 475°C.,
5 hrs. at 500°C.

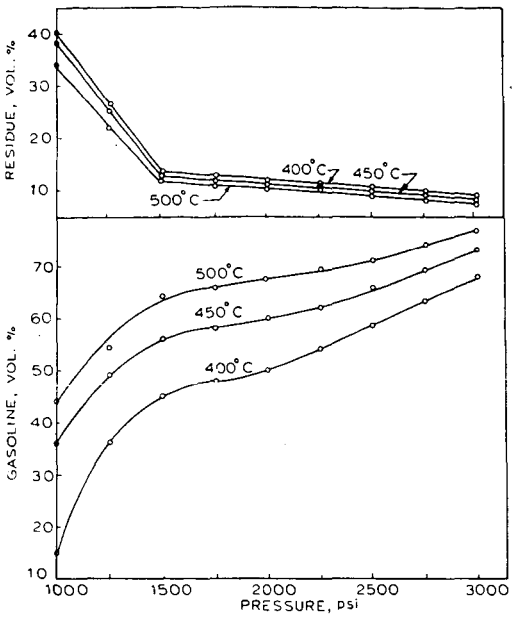


Figure 3. Effect of pressure on product distribution
Reaction time, 13 hrs. at 400°C.
10 hrs. at 450°C.
5 hrs. at 500°C.

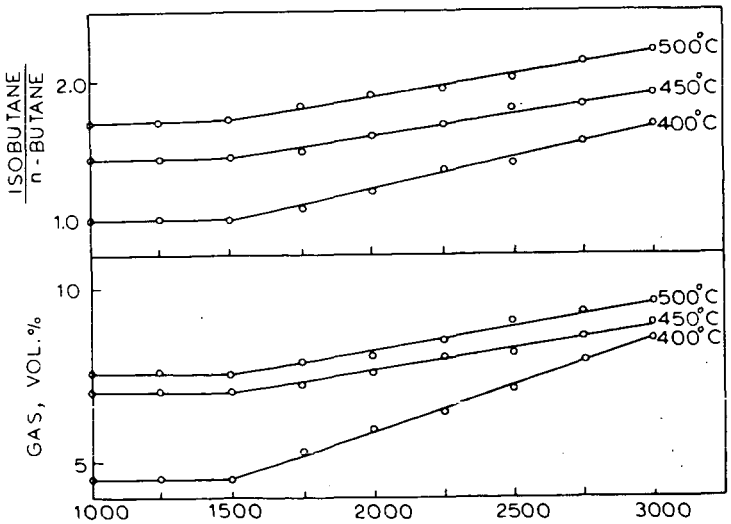


**Figure 4. Effect of pressure on product distribution**

**Reaction time, 13 hrs. at 400 C**
**10 hrs. at 450 C**
**5 hrs. at 500 C**

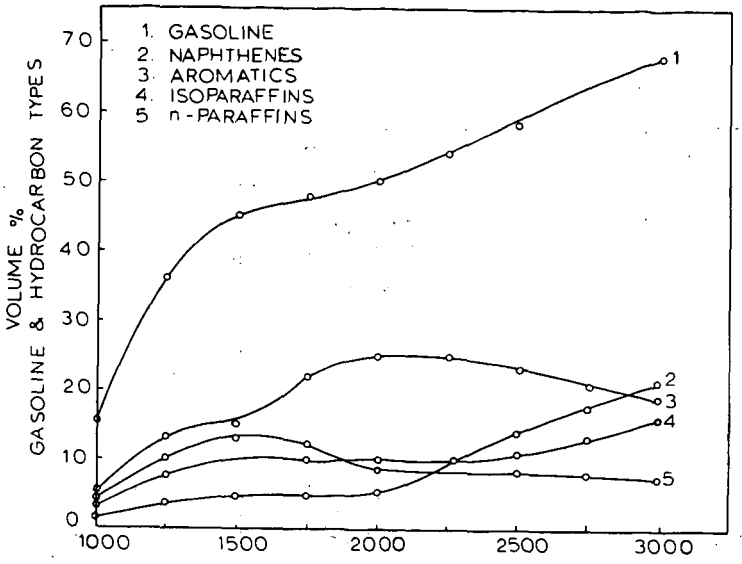


Figure 5. Effect of pressure on the yield of gasoline and hydrocarbon types - Temperature, 400 C

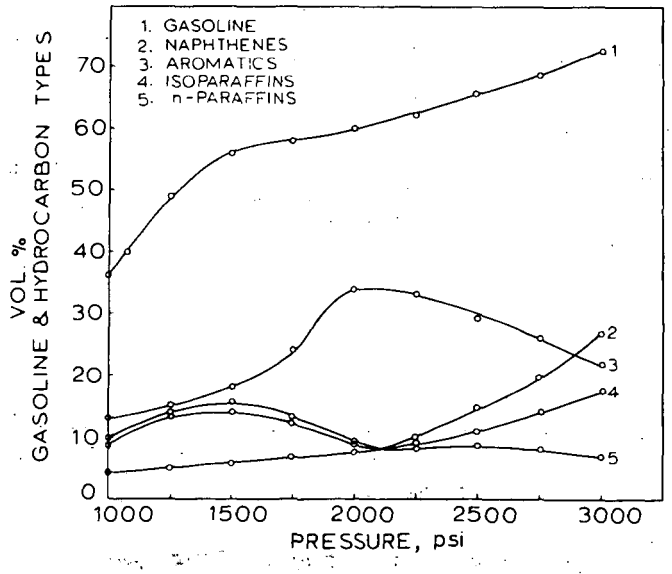


Figure 6. Effect of pressure on the yield of gasoline and hydrocarbon types - Temperature, 450 C

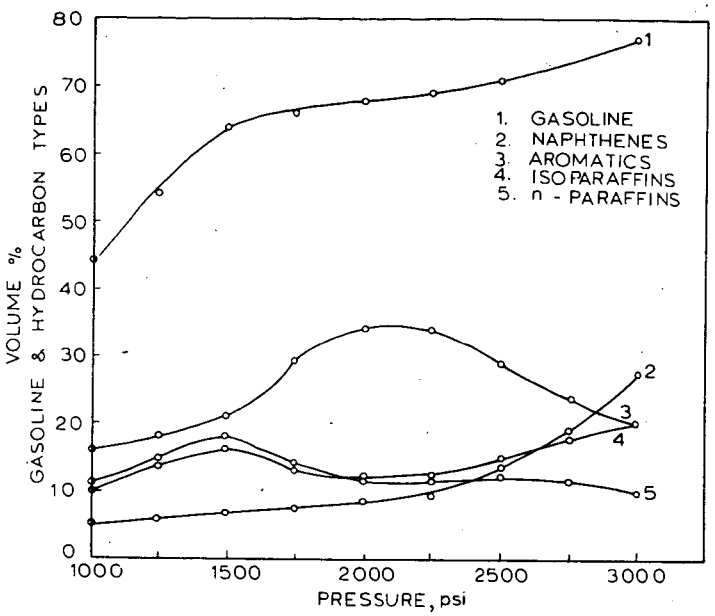


Figure 7. Effect of pressure on the yield of gasoline and hydrocarbon types - Temperature, 500 C

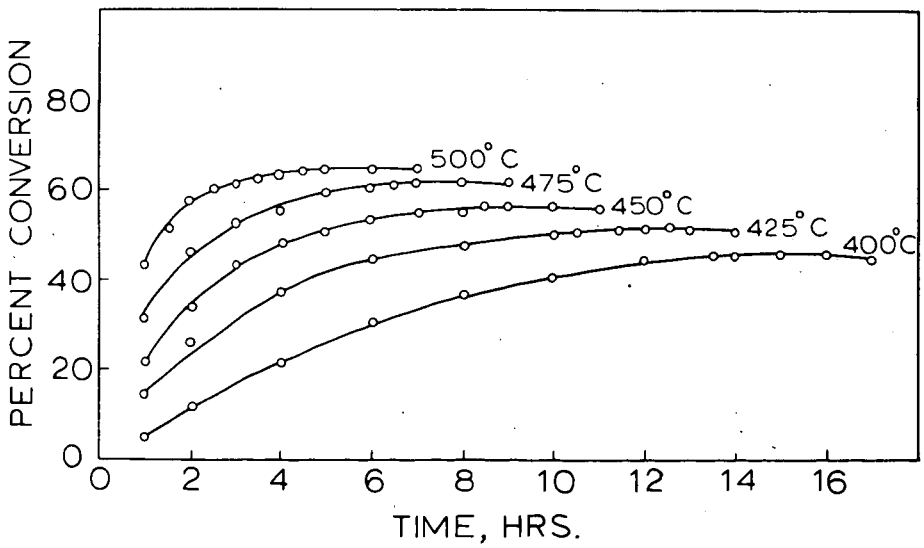


Figure 8. Effect of reaction time on gasoline formation Pressure, 1500 psi

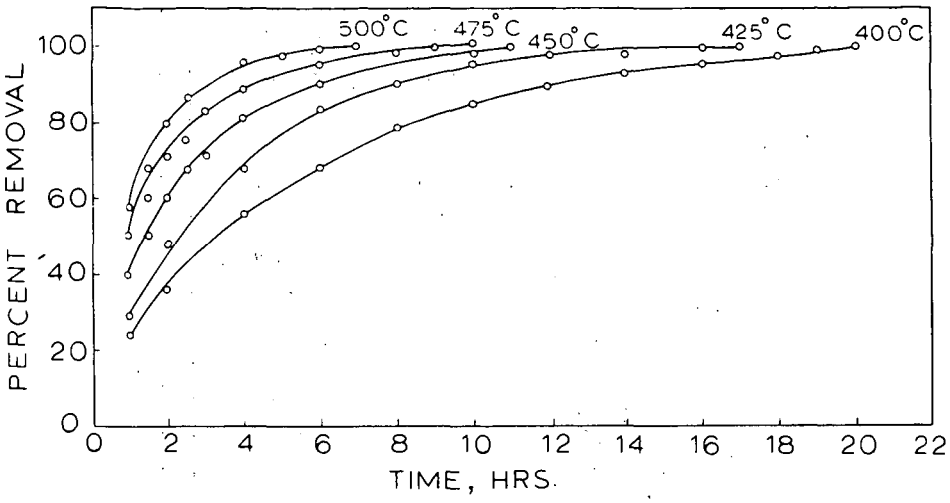


Figure 9. Effect of reaction time on desulphurization
Pressure, 1500 psi.

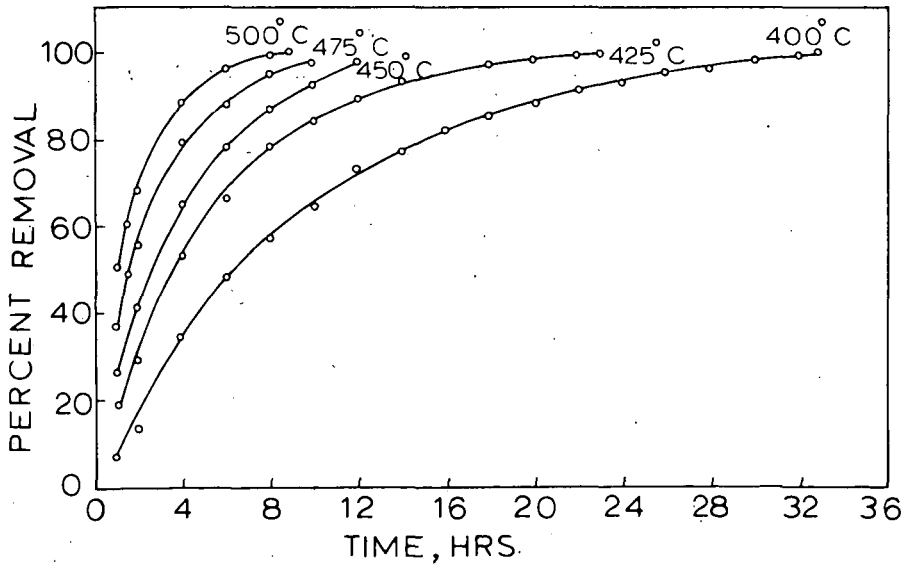


**Figure 10. Effect of reaction time on denitrogenation**
**Pressure, 1500 psi**

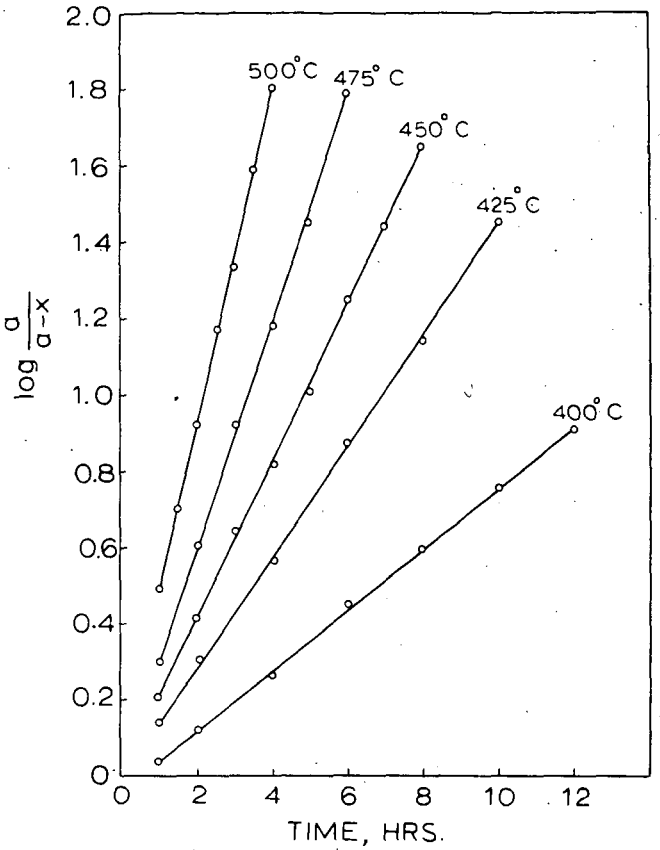


Figure 11. Plot of first-order equation for gasoline formation

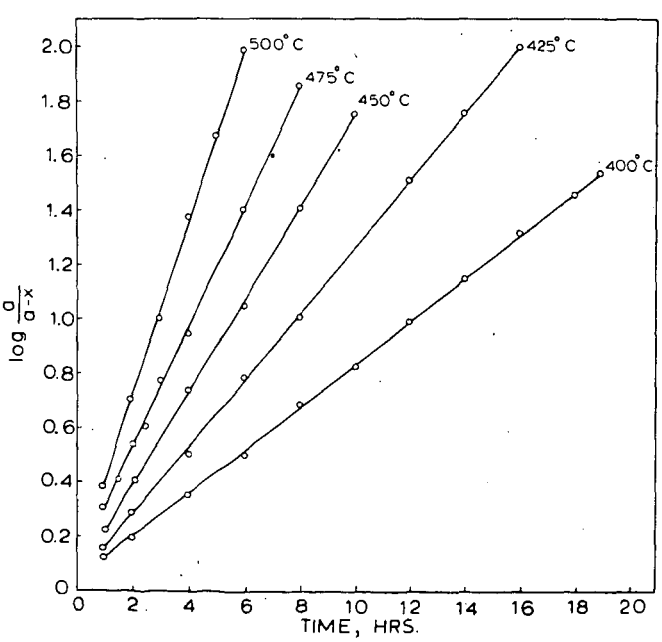


Figure 12. Plot of first-order equation for desulphurization.

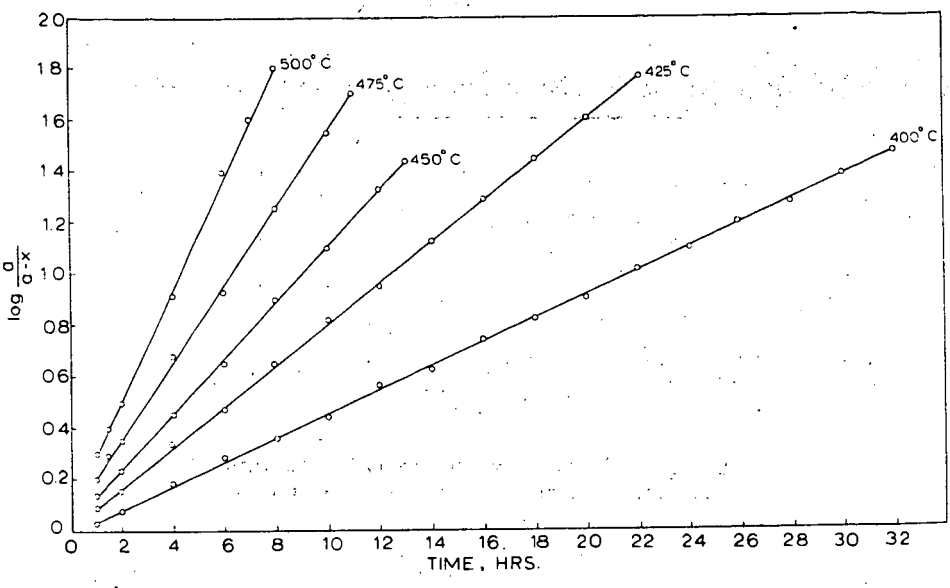


Figure 13. Plot of first-order equation for denitrogenation

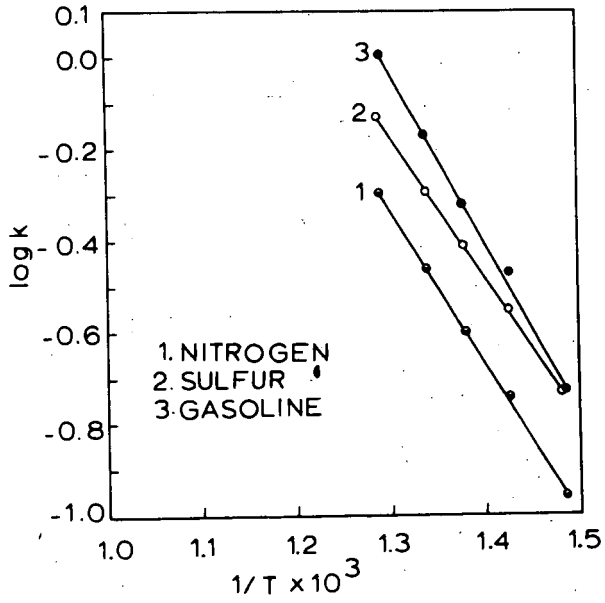


**Figure 14. Arrhenius plot for gasoline formation, desulphurization and denitrogenation**

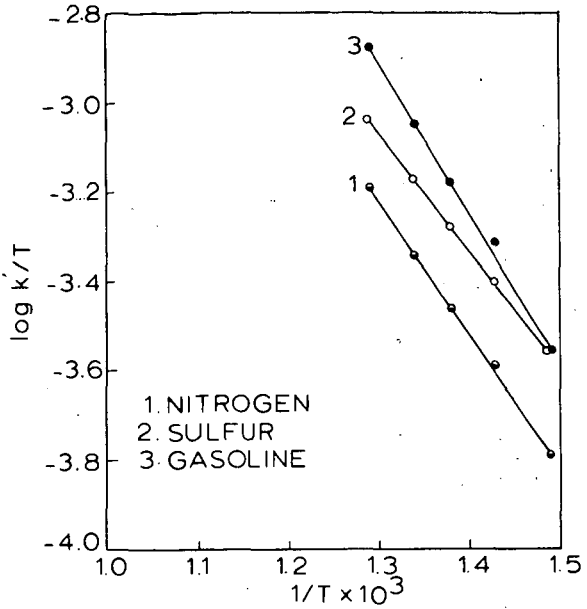


**Figure 15. Eyring plot for gasoline formation, desulphurization and denitrogenation.**

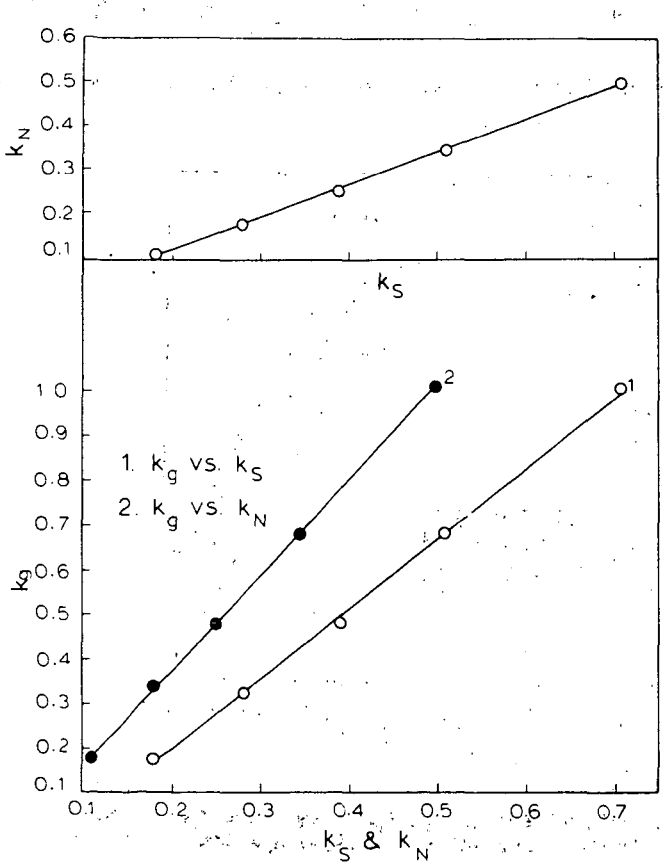


Figure 16. Relationship between rate constants
Pressure, 1500 psi.
Temperature, 400°, 425°, 450°, 475° and 500°C.

# DELAYED COKING OF LOW-TEMPERATURE LIGNITE PITCH

John S. Berber, Richard L. Rice, and Robert L. Lynch

U. S. Department of the Interior, Bureau of Mines,
Morgantown Coal Research Center, Morgantown, West Virginia

This paper is one of a series on the upgrading and utilization of various low-temperature tar fractions. Previous publications gave details on the preparation of biodegradable detergents from the olefin fraction (1), phthalic and maleic anhydrides from the neutral oil (3), and carbon electrode binders from the thermal cracking of the pitch (2).

Processing of petroleum residuals by delayed coking has been practiced commercially for a number of years (6). Pilot-plant studies have also been carried out on coke oven pitch (7) and a low-temperature tar topped to a temperature of 425° F (4). We believe this is the first effort to extend delayed coking to a low-temperature tar pitch.

## MATERIAL, EQUIPMENT, AND PROCESS DESCRIPTION

The tar was produced by the Texas Power & Light Company from a Texas lignite carbonized at 950° F in a fluidized bed. The pitch used in this study was obtained by distilling the crude tar under vacuum to an atmospheric boiling point of 630° F and amounted to 45 percent of the tar. Chemical and physical properties of the pitch are given in Table 1.

The delayed coking apparatus consists of a steel drum (C, see Figure 1) fabricated from a 5-foot length of 8-inch carbon steel pipe. The drum is flanged at the top and bottom ends to make the removal of the coke and cleaning easy. Coke removal is facilitated by use of a tilting drum. The coking drum is heated electrically (15.6 KW max). The pitch feed tank (A) was made from a 15-inch length of 8-inch carbon steel pipe and a cone, with a 1/2-inch coupling at the apex, is welded to the bottom of the 8-inch pipe and the top is open. The pitch tank is electrically heated by a 1.8 KW heater.

The pitch to be coked is ground and liquified in the pitch feed tank by heating to 400° F. The liquid pitch flows to the pitch feed pump (B), a small gear pump driven by an electric motor and hydraulic speed control (J), and is pumped through the pitch line preheater (F) which raises the temperature to about 485° F. The pitch is then fed to the delayed coking drum (C) which is maintained at the desired coking temperature. The pitch remains in the coking drum for several hours while the volatile matters are driven off. The volatiles are fed to an oil and gas condenser (D) and oil is collected in the bottom of the separator (E), and the gas is water scrubbed (H). The gas is then metered (G) and vented. A small tank (K) is tied into the pitch system in such a way that the pitch can be flushed out of the pump with a crude tar distillate fraction. Flushing the pump with crude tar before cooling prevents pitch solidification and simplifies restart.

A photograph of the apparatus is given in Figure 2.

The oil from the separator is vacuum distilled to about 750° F which yields an aromatic-rich distillate and a residue. The distillate can be catalytically oxidized to phthalic and maleic anhydrides while the residue, pitch, can be used as a binder for carbon electrodes, road paving, roofing, or piping material, depending on its specifications, such as softening point, carbon-hydrogen ratio, hydrogen content, and coking value.

## RESULTS AND DISCUSSION

This investigation was conducted at temperatures from 800° to 1,200° F and at atmospheric pressure. The coke yield ranged from 25 percent at 800° F to 45 percent at 1,200° F (Figure 3). This increase in yield is due to the higher degradation of the feed pitch at elevated temperatures. The product appeared darker, smoother, and char-like at 800° F, while at 1,200° F the coke had the silver-grey color typical of coke (Figures 4 and 5).

The ash content of the coke, as shown in Figure 6, was the same over the entire range of coking temperatures. The iron content of the coke (Figure 7) also was constant at all temperatures.

The sulfur content of the coke decreased slightly with the increasing temperature, Figure 8, indicating that, at higher temperatures, more of the sulfur was being converted to gas. It has been reported that delayed coke can be used as fuel for generating electric power (5). The relatively low sulfur content of this coke, 0.80 percent, should make it especially attractive as a fuel in view of present air pollution standards.

The coke obtained from this process can also be calcined and used as aggregate in the production of metallurgical electrodes, although the ash is slightly higher than the ash of petroleum coke which is currently used. It is desirable to have an ash content below 0.5 percent in the coke. The coke loses 15 percent by weight when calcined to 2,000° F.

The oil yield is a function of coking temperature and varied from 43 percent of the feed pitch at 800° F to 17 percent at 1,200° F (Figure 3). The specific gravity of the oil was about 0.95 at 800° F and 1.18 at 1,200° F (Figure 9). This oil, when distilled to 720° F, gave a distillate containing from 15 to 25 percent combined acids and bases with the remainder consisting of a neutral oil. The F.I.A. analysis of a typical neutral oil showed 89.2 percent aromatics, 6.9 percent olefins, and 3.9 percent paraffins. The vapor-phase catalytic oxidation of the neutral oil yielded better than 30 percent phthalic and maleic anhydrides. The distillation residue from the oil proved to be a suitable binder for metallurgical electrodes. A detailed evaluation of its use as a binder, as well as the coke as an aggregate, is in progress and will be reported in a future publication.

The gas yield was 17 percent at 800° F and increased to 39 percent at 1,200° F (Figure 3). The effect of coking temperature on the ethylene-to-ethane ratio is shown in Figure 10. This is probably due to dehydrogenation and thermal cracking. In addition, an increase in coking temperature is accompanied by a decrease in the methane-to-hydrogen ratio (shown in Figure 11). This ratio drops from 8:1 at 800° F to about 2:1 at 1,150° F. A typical analysis of gas obtained at 950° F is given in Table II.

## CONCLUSIONS

This work has shown that the commercial value of lignite pitch is increased by coking. The coking operation yields three products: oil, gas, and coke. The oil upon distillation is a valuable chemical intermediate. The coke could be used as an aggregate for metallurgical electrodes, other graphite products, and as a low-sulfur fuel. The gas is a possible substitute for natural gas or a source of hydrogen if subjected to a steam reforming process. Ethylene could also be recovered from the gas stream and used as a raw material.

## LITERATURE CITED

1. Berber, J. S., Rahfuse, R. V., Wainwright, H. W., Ind. Eng. Chem., Prod. Res. Develop. 4, 242 (1965).

2. Berber, J. S., Rice, R. L., Fortney, D. R., Ind. Eng. Chem., Prod. Res. Develop. 6, 197 (1967).

3. Berber, J. S., Rice, R. L., Hiser, A. L., Wainwright, H. W., Bur. Mines Rept. Invest. 6916, 1967, 17 pp.

4. Dell, M. B., Ind. Eng. Chem. 51, 1297 (1959).

5. Donnelly, F. J., Barbour, L. T., Hydrocarbon Process. 45, 221 (1966).

6. Martin, S. W., Wills, L. E., Ch. in "Advances in Petroleum Chemistry and Refining," v. II, ed. by J. J. McKetta, Jr., and K. A. Kobe, pp. 367-387, Interscience Publications, Inc., New York, 1959.

7. Ibid., pp. 379-380.

Table I. Properties of Pitch Feed

| | |
|---|---|
| Ultimate analysis: | As received |
| Carbon, % | 84.72 |
| Hydrogen, % | 8.53 |
| Nitrogen, % | 0.87 |
| Oxygen, % | 4.62 |
| Sulfur, % | 0.90 |
| Chlorine, % | 0.01 |
| Moisture, % | 0.00 |
| Flash point, ° F | 510 |
| Softening point (R & B) glycerin, ° C | 90 |
| Softening point (cube in glycerin), ° C | 105 |
| Penetration at 77 ° F, 100 grams, 5 seconds | 0 |
| Specific gravity, 25 ° C/25 ° C | 1.128 |
| Ash, % | 0.35 |
| Water, % | 0.00 |
| Ductility, cm at 77 ° F | 0 |
| Bitumen, soluble in $CS_2$ | 78.80 |
| Free carbon | 20.85 |
| Distillation: | |
| To 300 ° C, % | 6.40 |
| Softening point of residue (R & B), ° C | 90 |
| Sulfonation index of distillate to 300 ° C | 0 |
| Conradson carbon, % | 20.81 |

Table II. Composition of Gas at a Coking Temperature of 950° F

| Component | Volume-percent |
|---|---|
| $CO_2$ | 0.74 |
| CO | 4.91 |
| $H_2$ | 7.67 |
| $CH_4$ | 43.83 |
| $C_2H_6$ | 13.97 |
| $C_2H_4$ | 9.94 |
| $C_3H_8$ | 13.54 |
| $C_4^+$ | 5.40 |

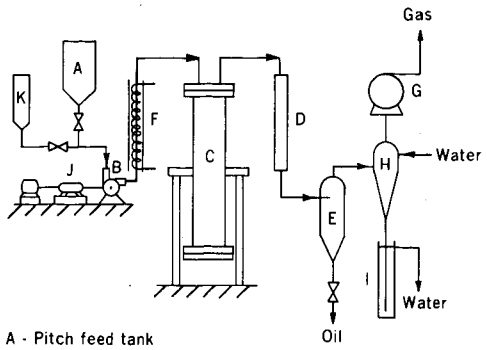


A - Pitch feed tank
B - Pitch feed pump
C - Delayed coking drum
D - Gas and oil cooler
E - Oil separator
F - Pitch line preheater
G - Wet test meter
H - Gas water scrubber
I - Scrubber seal pot
J - Hydraulic speed control
K - Pump flushing oil tank

FIGURE 1. - Flowsheet of Delayed Coking Process.

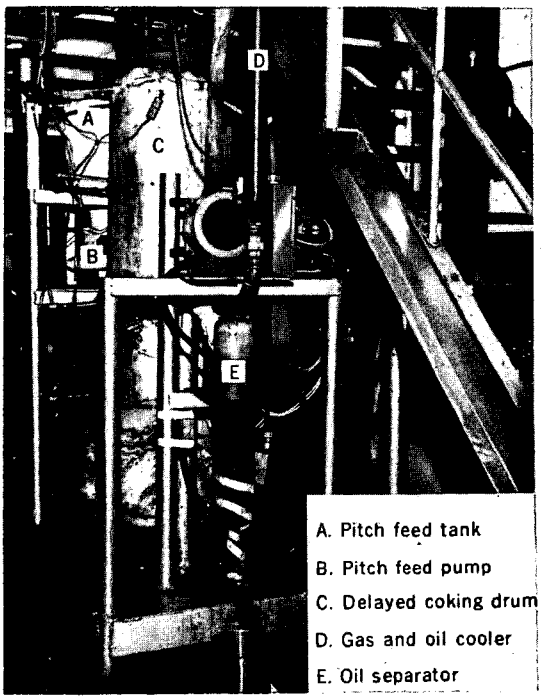


FIGURE 2. - The Delayed Coking Apparatus.

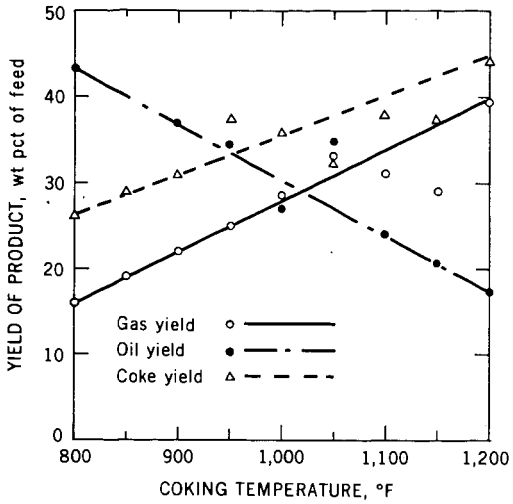


FIGURE 3. - Effect of Temperature on Product Distribution.

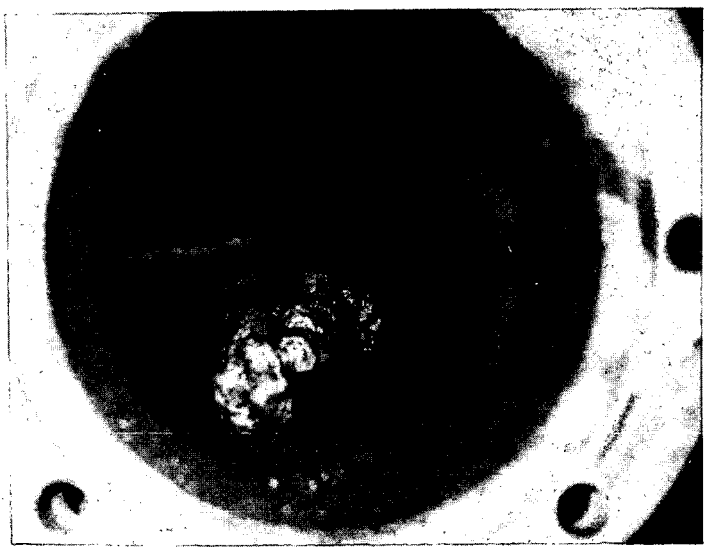

FIGURE 4. - Coke at the Top End of the Drum.

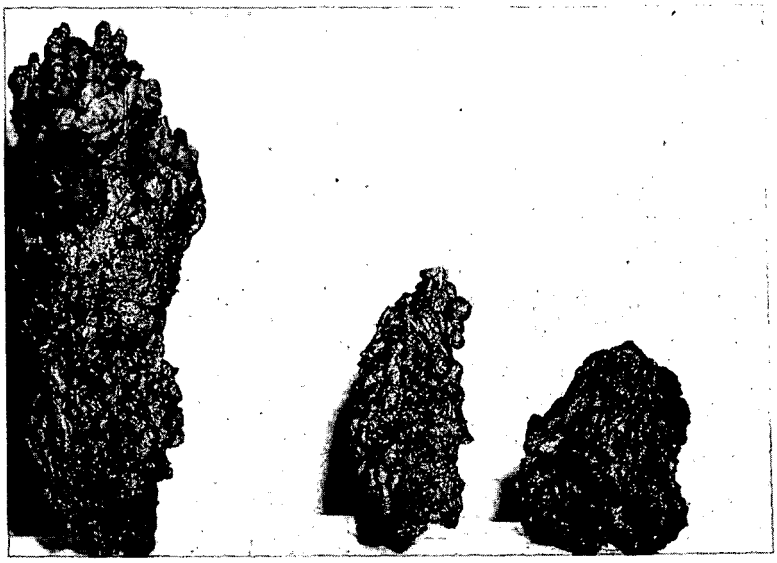

FIGURE 5. - Coke as Taken From Drum.

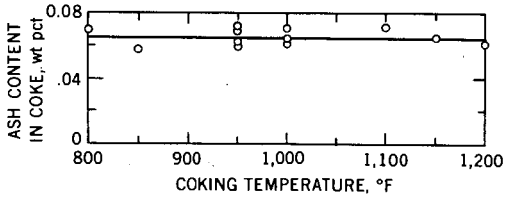


FIGURE 6. - Coking Temperature vs. Ash Content of Coke.

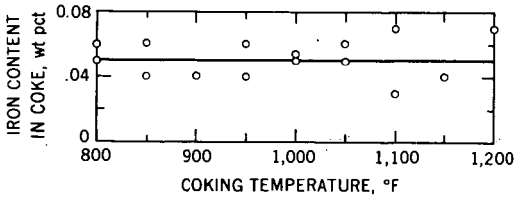


FIGURE 7. - Coking Temperature vs. Iron Content of Coke.

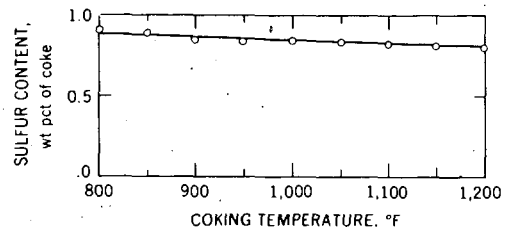


FIGURE 8. - Coking Temperature vs. Sulfur Content of Coke.

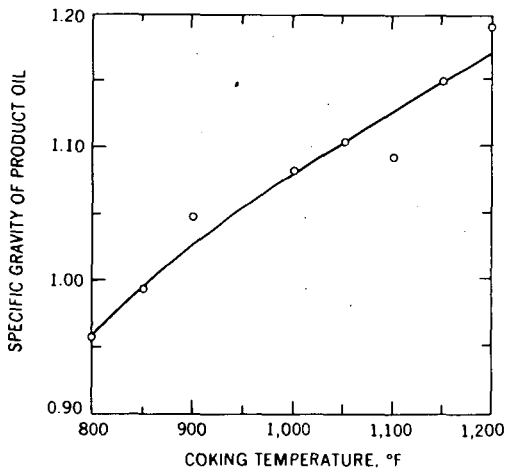


FIGURE 9. - Effect of Temperature on Specific Gravity of Product Oil.

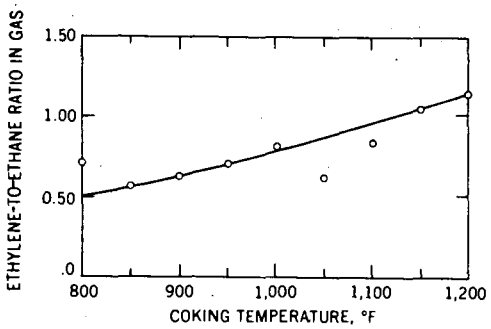


FIGURE 10. - Effect of Temperature on Ethylene-to-Ethane Ratio.

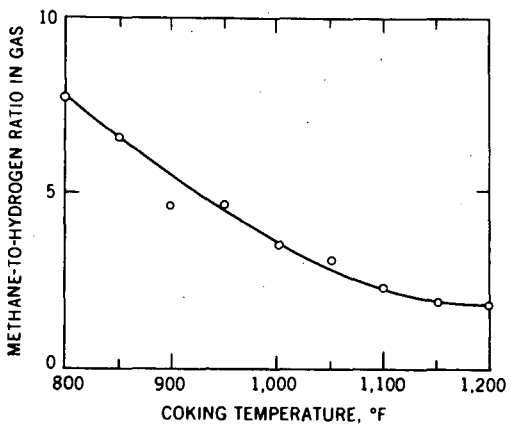


FIGURE 11. - Effect of Temperature on Methane-to-Hydrogen Ratio.

# FLUORODINITROETHANOL AND DERIVATIVES*

Henry J. Marcus

Aerojet-General Corporation, Azusa, California

## Introduction

The chemistry of 2-fluoro-2,2-dinitroethanol has been investigated for the past several years, and it is a privilege to present some of this material at this time. This paper presents a summary of a process evaluation study, and much of the chemistry involved will be reported in greater detail by the original authors in the coming months. It may be stated at the outset that the chemistry of fluorodinitromethyl compounds shows marked similarity to trinitromethyl or gem-dinitromethyl compounds, which are well-known in the literature.

## Synthesis of 2-Fluoro-2,2-dinitroethanol

One preparative method for 2-fluoro-2,2-dinitroethanol (FDNE) is based on the fluorination of the aci-sodium salt of dinitroethanol

$$F_2 (\text{or } ClO_3F) + \begin{matrix} NO_2^{\ominus}Na^{\oplus} \\ | \\ C - CH_2OH \\ | \\ NO_2 \end{matrix} \longrightarrow \begin{matrix} NO_2 \\ | \\ FC\ CH_2OH \\ | \\ NO_2 \end{matrix} \qquad (1)$$

I

The starting material for Reaction (1) is prepared *in situ* by the deformylation of 2,2-dinitro-1,3-propanediol with one mole of base

$$\begin{matrix} NO_2 \\ | \\ HOCH_2C\ CH_2OH \\ | \\ NO_2 \end{matrix} + NaOH \longrightarrow \begin{matrix} NO_2^{\ominus}Na^{\oplus} \\ | \\ C\ CH_2OH \\ | \\ NO_2 \end{matrix} \qquad (2)$$

II

Compound II is preferably prepared by the oxidative nitration of 2-nitro-1,3-propanediol (Reference 1). II is not isolated, but is partially purified by extraction from the aqueous reaction mixture with ethyl or isopropyl ether, followed by an extraction of the ether solution with aqueous base, which converts II to the aci-sodium salt of dinitroethanol. Although other methods of preparation of II are known, the route shown was the one of choice.

Conversion of II to FDNE was carried out by introducing fluorine gas, diluted 1:1 with nitrogen, into the aqueous solution of the aci-sodium salt at 15 to 25° (Reference 2). It was found that efficient dispersion of the fluorine is essential, and that stainless steel gas-inlet tubes with open ends of 1/4 or 3/8 in., or with various hole sizes of 0.016 to 0.040, are satisfactory in a 50-liter vessel. The smaller the diameter of the holes, however, the more frequently were they occluded by sodium fluoride. A rapid injection of water served to remove the obstruction.

* This report is based on work supported, in large part, by the AEC through the Lawrence Radiation Laboratory of the University of California.

Yields of 60 to 70% of FDNE were generally obtained, although about 100% of the theoretical quantity of fluorine was consumed. The pH of the solution was not a critical factor, so long as it was maintained at or above the 7.5 to 8.0 level. The same results were obtained whether the pH was maintained at 8.0 or whether fluorination was begun at a pH of about 11, and the solution allowed to go acid; in the latter case, however, it was sometimes necessary to add alkali and to continue the fluorination.

Ethyl ether was found to be very efficient in extracting FDNE from the aqueous fluorination mixture. However, it tends to extract some impurities along with the FDNE. For example, one of the contaminants found in the fluorination of II was identified as 2,2,4,4-tetranitro-1,5-pentanediol (Reference 3). It was obtained in rather significant quantity (3 to 5 percent) from an ether extract of FDNE, from a batch in which most of the FDNE had previously been extracted with methylene chloride. In actual practice, sodium chloride is added to decrease the solubility of FDNE in the aqueous medium, and methylene chloride, with a far less favorable distribution coefficient than ether, is used as the extractant. The crude product obtained by removing the solvent is generally 80 to 90 mole-percent pure, as analyzed by gas chromatography.

An alternate method for preparing FDNE consists of the fluorination of nitroform, followed by reduction with alkaline peroxide and the Henry reaction with formaldehyde (References 2 and 4).

$$HC(NO_2)_3 + F_2 \xrightarrow{OH^\ominus} FC(NO_2)_3 \qquad (3)$$

III

$$FC(NO_2)_3 + H_2O_2 + HCHO \xrightarrow{OH^\ominus} FDNE \qquad (4)$$

The fluorination of nitroform is carried out under conditions similar to those described for the aci-sodium salt of dinitroethanol, but the yields are superior (80 to 90% of theory), and the isolation of the product presents little difficulty; III is essentially insoluble in water, and, following mild washing, is obtained in 98 mole-percent purity (gas chromatography). A slight source of difficulty is presented by the emulsified interface, but this problem can be overcome by vacuum filtration and water-washing. Nitroform starting material may, if necessary, be prepared by the alkaline-peroxide reduction of tetranitromethane, and fluorinated <u>in situ</u>; in this case, yields of III from 65 to 70% (based on tetranitromethane) are obtained.

The route shown in (4) was discovered by workers at the U.S. Naval Ordnance Laboratory and substantial improvements since then, primarily by NOL, have made the process a very attractive one. The reduction of III, when carried out at -5 to -10°C in alkaline medium with a 20% excess of hydrogen peroxide and formaldehyde, gives yields of 90% FDNE in 95 mole-percent purity. The reaction can be effected in aqueous methanol in order to enhance the solubility of FTM in the reaction mixture, or, alternatively, a surface-active agent such as sodium p-tolunesulfonate or Triton X-100*, may be added to achieve the same result. The latter method is particularly advantageous when it is desired to use the solution of FDNE in the methylene

* An alkyl phenoxy polyethoxyethanol (Rohm & Haas Co.)

chloride extractant without other hydroxyl-containing impurities; water alone is readily removed from the solution, but a significant quantity of methanol, together with the attendant water, presents a more tedious problem.

Physical Characteristics of FDNE

Fluorodinitroethanol is a mobile, colorless liquid, b.p. 53° at 1 mm Hg, m.p. 9 to 10-1/2°C. Its density is 1.54 g/cc at 25°C. It can be vacuum-distilled with very minor decomposition (much less than 1%), but that slight decomposition does occur is indicated by small deposits of paraformaldehyde. Its refractive index is 1.4330 ($n_D^{25}$). It is a very strong vesicant, and skin contact is to be avoided. Values of its sensitivity to impact or shock are not very consistent, but certain evidence suggests that caution is in order. For example, a 70 weight-percent solution in methylene chloride had an impact sensitivity of less than 10 cm compared to 50 cm for neat FDNE (Olin Mathieson Tester, 2 Kg weight, 50% point; n-propyl nitrate = 8 cm).

Analysis of FDNE

Analysis of FDNE may be based on several criteria, of which purity by gas-chromatography is perhaps the most useful. Consistent results have been obtained with a 6-ring polyphenyl ether column in an Aerograph A90 gas chromatograph. An Aerograph Model 325 temperature programmer was attached to the oven heater, and by programming from 90 to 140°C at 6°C/min, very satisfactory separation of components was achieved.

FDNE may also be analyzed by measuring its absorbancy in dilute aqueous base at 382 mμ. For pure FDNE, log ε = 4.27. This determination must be made on fresh solutions, as the anion of fluorodinitromethane reacts with hydroxide ion.

A third method of analysis was developed by titration of FDNE in acetonitrile with 0.1N tetrabutylammonium hydroxide. Under these conditions, FDNE titrated as a dibasic acid, giving a single, sharp inflection.

Synthesis of bis(2-Fluoro-2,2-dinitroethoxy)methane

One of the more interesting derivatives of FDNE is its formal, bis(2-fluoro-2,2-dinitroethoxy)methane (FEFO) (Reference 5). Since conventional methods of acetal formation fail with electronegatively substituted alcohols such as trinitromethyl, gem-dinitro, and fluorodinitromethyl compounds, recourse was had to a method first developed at NOL (Reference 6), involving the use of concentrated sulfuric acid as the reaction medium

$$2x\ FC(NO_2)_2CH_2OH + (HCHO)_x \xrightarrow{H_2SO_4} x\ \underset{\text{IV (FEFO)}}{\left[FC(NO_2)_2CH_2O\right]_2CH_2} \qquad (5)$$

Under these conditions, FEFO is produced in 70 to 90% yields. The reaction may conveniently be carried out by adding concentrated sulfuric acid slowly to a solution of FDNE and s-trioxane in methylene chloride, but many variations yield equally satisfactory results. In place of trioxane, paraformaldehyde may be used, and the methylene chloride may be replaced by a similar solvent, or the reaction may be effected without the use of organic solvent by adding FDNE to a solution of formaldehyde (from either trioxane or paraformaldehyde) in sulfuric acid. A solvent may then be employed to assist in the isolation and purification of the product.

The effects of an excess of formaldehyde or an excess of FDNE on the yield and purity of FEFO were assessed in a series of runs in which the molar ratios of FDNE to formaldehyde were 2.5:1.0, 2.0:1.0, and 1.5:1.0, respectively. An additional run was made at the 2.0:1.0 ratio, in which the condensation medium was 100% sulfuric acid in place of the usual 95 to 98% acid. The results are summarized in Table 1.

TABLE 1

VARIATION OF REACTANT RATIO IN FEFO SYNTHESIS

| Case No. | Molar Ratio, FDNE:HCHO | % FEFO* | % Impurity of Higher GC Retention Time | % Yield |
|---|---|---|---|---|
| 1 | 2.5:1.0 | 99.2 | 0.8 | 88.0 |
| 2 | 2.0:1.0, conc $H_2SO_4$ | 98.2 | 1.8 | 82.9 |
| 3 | 2.0:1.0, 100% $H_2SO_4$ | 98.9 | 1.1 | 79.0 |
| 4 | 1.5:1.0 | 93.6 | 6.4 | 83.5 |

* GC assay

It is apparent that the reagents in stoichiometric ratio will yield good FEFO very effectively; that the higher purity FEFO obtainable with 100% sulfuric acid may compensate for the use of slightly less pure FDNE; and that even a 25% excess of formaldehyde can be tolerated, provided purification with sulfuric acid is added to the process (see below).

A series of runs (all with molar ratio 2.0:1.0) in which the reaction temperature was maintained for two hours at 0 to 10°C, 20 to 25°C, and 35 to 40°C, gave yields of 87.3, 87.8, and 84.0% FEFO, respectively, all of identical quality. The run at the highest temperature was carried out primarily to determine what, if anything, might occur if the reaction went out of control. Since methylene chloride served as the organic solvent in these runs, it apparently served to control the exotherm. This series further showed that product yield and purity are unaffected by reaction temperatures from 0° to at least 25°C.

In practice, the preparation of FEFO can be carried out conveniently by using the solution of FDNE in methylene chloride directly, without isolating the FDNE, although the solution is generally dried by passing through a silica gel-Drierite column, and a portion of the solvent is removed by distillation to avoid handling excessive volumes. The requisite amount of s-trioxane is then added to the solution, and concentrated sulfuric acid (approximately 1 ml acid per gram of FDNE) is then added dropwise with good agitation at 20 ± 5°C. The reaction mixture is stirred an additional 1 to 2 hours, and the methylene chloride (upper) layer is separated. The FEFO solution is then washed countercurrently or batchwise with 5% aqueous sodium hydroxide, and dried by percolation through a column of silica gel. Removal of the solvent under vacuum leaves the product as a clear, colorless liquid, generally 90 to 98 mole-percent pure, as analyzed by gas chromatography.

The contaminants in FEFO generally consist of several products of lower GC retention-times, and one or two of higher retention times.* The latter have been

* Referred to, for convenience, as "high-boilers"

identified (Reference 7) as the FEFO analogs with two and three methyleneoxy chains in the molecule, respectively.

$FC(NO_2)_2CH_2OCH_2OCH_2OCH_2CF(NO_2)_2$ and $\left[FC(NO_2)_2CH_2OCH_2O\right]_2\ CH_2$

V VI

Compounds V and VI seem to arise whenever the condensation medium is contaminated with water. If one is aware of this beforehand, the problem can be overcome by the use of fuming sulfuric acid, as shown in Table 2.

TABLE 2

EFFECT OF DILUTION WITH WATER ON FEFO SYNTHESIS

| Case No. | Conditions | Mole-% Components with lower GC retention time | % FEFO | % High-boilers | % Yield |
|---|---|---|---|---|---|
| 5 | Standard* | 3.6 | 93.4 | 3.0 | 92.5 |
| 6 | 10% $H_2O$ added to FDNE | 4.3 | 44.7 | 51.0 | 83.6 |
| 7 | As in 93, with 20-23% fuming $H_2SO_4$ in place of conc. $H_2SO_4$ | 2.9 | 93.4 | 3.7 | 77.7 |

* 2.0 moles of FDNE (distilled) per mole of formaldehyde

Results similar to those of Case No. 6 are obtained whenever the FDNE-methylene chloride solutions are inadequately dried.

If the FEFO product is still too highly contaminated with V and/or VI, purification may be effected by low-temperature crystallization from methylene chloride-hexane in a tedious, somewhat wasteful procedure, or by agitation with concentrated sulfuric acid. Results from the latter treatment are presented in Table 3.

TABLE 3

PURIFICATION OF FEFO WITH SULFURIC ACID

| Case No. | Mole-% Components with lower GC retention time | % FEFO | % High-Boilers V | % High-Boilers VI | % Recovery |
|---|---|---|---|---|---|
| 8, crude | 1.2 | 87.3 | 5.6 | 5.9 | - |
| 8, purified | 1.7 | 96.6 | 0.1 | 1.6 | 82 |
| 9, crude | 0.7 | 95.6 | 3.7 | - | - |
| 9, purified | 1.4 | 98.6 | - | - | 89 |

Extremely interesting results were obtained in the course of preparing FEFO from an FDNE-methylene chloride solution after attempted purification. This FDNE was prepared from fluorotrinitromethane in methanolic solution, and the FDNE-methylene chloride solution was later found to be highly contaminated with methanol and water. The crude FEFO-methylene chloride solution, following separation from the sulfuric acid layer, was divided into two equal portions. One portion was worked up in the usual manner, and the other was treated with two portions of concentrated sulfuric

acid before being worked up. The first portion gave a yield of 48 percent (calculated as FEFO), the second 42 percent. GC analysis showed the following results:

TABLE 4

IN-PROCESS PURIFICATION OF FEFO WITH SULFURIC ACID

| Case No. | Mole-% Components with lower GC retention time | % FEFO | % High-Boilers V | % High-Boilers VI |
|---|---|---|---|---|
| 10, treated as usual | 17.1 | 37.6 | 43.8 | 1.5 |
| 10, purified in process | 1.0 | 93.7 | 5.3 | - |

In spite of the fact that the conventionally-treated FEFO was apparently not completely freed of solvents, and the results are thus not strictly comparable, it is evident that a very high degree of purification was achieved. Since the yield of FEFO was nearly the same in both cases, it must be concluded that purification took place primarily other than through extraction of V and VI, and that the latter may have been converted into FEFO by a process indicated in the following sequence:

$$ROCH_2OCH_2OR + H^{\oplus} \rightleftharpoons ROCH_2\overset{H}{\overset{\oplus}{O}}CH_2OR \quad (6)$$

$$ROCH_2OCH_2OR \rightleftharpoons \left[ROCH_2^{\oplus}\right] + HOCH_2OR \rightleftharpoons ROH + HCHO$$

$$\left[ROCH_2^{\oplus}\right] + ROH \rightleftharpoons (RO)_2CH_2 + H^{\oplus}$$

The purification of FEFO with concentrated sulfuric acid immediately following separation of the FEFO-methylene chloride solution from the sulfuric acid reaction medium has consistently removed nearly all of the high-boiling contaminants, and has been made a standard procedure in FEFO preparation.

Several routes are known which yield FEFO from intermediates other than FDNE. One of these methods utilizes bis(2,2,2-trinitroethoxy) methane (VII) as the starting material (Reference 4)

$$\underset{\text{VII}}{\left[(NO_2)_3CH_2O\right]_2CH_2} \xrightarrow[H_2O_2,OH^{\ominus}]{} \underset{\text{VIII}}{\left[(NO_2)_2C^{\ominus}CH_2O\right]_2CH_2} \xrightarrow{F_2} \text{FEFO} \quad (7)$$

VII is reduced to the disodium salt (VIII) in the presence of alkaline peroxide in aqueous methanol. The organic solvent, added initially to ensure solubility and facilitate reaction of the starting material, must then be removed by vacuum distillation prior to fluorination. The product has been obtained in yields of up to 60% by this route. The sensitivity of VII, and the fact that large volumes and much time are required to effect the removal of the methanol, are severe disadvantages in this process.

Moderate yields of pure FEFO are obtained via another route which utilizes VII as the starting material:

$$\text{VII} \xrightarrow[H_2O_2,OH^{\ominus}]{} \text{VIII} \xrightarrow[H^{\oplus},HCHO]{} \underset{\text{IX}}{\left[HOCH_2C(NO_2)_2CH_2O\right]_2CH_2} \xrightarrow{OH^{\ominus}} \text{VIII} \xrightarrow{F_2} \text{FEFO} \quad (8)$$

The conversion of VIII, by means of the Henry reaction, to bis(3-hydroxy-2,2-dinitropropoxy)methane serves as a means of purification, and as a result the yields from IX

to FEFO are quite high (80 to 85%). The overall yield starting from VII, however, is 45 to 55%, and the large volumes and lengthy procedures decrease the utility of this method even further.

## Physical Characteristics of FEFO

FEFO is a colorless liquid, b.p. 120 to 124°C at 0.3 mm Hg, m.p. 14°C. Its density is 1.595 g/cc at 25°C, and its index of refraction $n_D^{25} = 1.4398$. It is soluble in the lower aliphatic alcohols and esters, and in most chlorinated solvents. It is stable to strong acids, and relatively stable to dilute aqueous alkali. Its sensitivity to impact has given values ranging from 11 cm (50% point, 2 Kg weight, RDX = 28 cm) to 40 to 50 cm (50% point, 2.5 Kg weight). Toxicity data are scanty but tend to indicate relatively low toxicity, at least by external exposure to skin or eye.

## Analysis of FEFO

Gas chromatography has been employed as the most suitable analytical method for FEFO assay. GC FEFO analyses are conducted with a six ring polyphenyl ether column and a sensitive flame ionization detector. A 2-minute isothermal run at 100°C is followed by a programmed increase of 6°C/minute to 200°C, and an additional 8 minutes at 200°C. All components are eluted within a 20-minute period. These operating conditions give well-resolved peaks with minimal tailing. Although sample sizes have been varied between 0.2 and 0.8 µl, 0.2 to 0.3 µl is preferred.

Preliminary studies suggested that chromatograph oven temperatures between 180 and 200°C would not cause measurable decomposition of FEFO. Therefore, to enhance volatilization and peak shape, a pre-heater temperature of 185°C was selected. However, at this temperature the area percents of the more volatile components did not reproduce well, although consistent data were obtained for the other impurities. A later series of tests of vaporizer temperatures from 150 to 200°C demonstrated the necessity of operating at 150°C because of an apparent degradation of FEFO at the higher temperatures. The data suggest that the apparent increase in impurities of low retention time at temperatures above 150°C is actually due to degradation of FEFO. Its assay decreases with the increase of these impurities attendant with the increased temperatures. By operating the vaporizer at 150°C, reproducible chromatograms are obtained without noticeably altering the elution times.

The anhydrous potentiometric titration applicable to FDNE may be used for FEFO also. FEFO can be titrated in acetonitrile with tetrabutylammonium hydroxide to give a single well-defined break corresponding to the removal of four protons per mole. A single sample assayed 88.8% FEFO, compared with 86.7% obtained by gas chromatography. Since the impurities in FEFO are also apt to have acidic properties, this method was not developed further.

## Acknowledgment

The author wishes to express his appreciation to Dr. M. J. Kamlet and Dr. H. G. Adolph of the U.S. Naval Ordnance Laboratory, White Oak, Maryland, and to Dr. K. Baum, Dr. V. Grakauskas, and Dr. F. E. Martin of the Aerojet-General Corporation for permission to present certain information prior to their own publications.

## REFERENCES

1. K. Klager, U.S. Patent 3,024,288 (1962).

2. V. Grakauskas and K. Baum, in press.

3. K. Klager, J. P. Kispersky, and E. E. Hamel, J. Org. Chem., 26, 4368 (1961).

4. M. J. Kamlet and H. G. Adolph, J. Org. Chem., in press.

5. F. E. Martin, patent applied for.

6. K. G. Shipp and M. E. Hill, J. Org. Chem., 31, 853 (1966).

7. H. G. Adolph, private communication.

# RECENT CHEMISTRY OF THE OXYGEN FLUORIDES

I. J. Solomon, A. J. Kacmarek, J. K. Raney, J. N. Keith

IIT Research Institute, Chicago, Illinois

Some of the recent chemistry of the oxygen fluorides will be discussed. The reaction of $OF_2$ and $SO_3$ has been studied by using $O^{17}$ labeled starting materials and $O^{17}$ NMR spectroscopy, and evidence for an OF transfer mechanism is presented. Similar experiments with $O^{17}$ labeled $SO_2$ and $O_2F_2$ have shown that the reactions of $O_2F_2$ can be explained in terms of an OOF transfer. The generality of this reaction is shown in that $CF_3CF(OOF)CF_3$ and $CF_3CF_2CF_2OOF$ are formed by the reaction of $O_2F_2$ and $CF_3CF{=}CF_2$.

# GAS GENERATOR PROPELLANTS

E. S. Sutton, C. W. Vriesen, and E. J. Pacanowsky

Thiokol Chemical Corporation
Elkton Division
Elkton, Maryland

The properties of ammonium perchlorate have made it the oxidizer of choice for composite solid propellants for the past 20 years. Its ability to produce propellant compositions with high flame temperatures and densities has made it extremely useful to the missile propulsion industry. Recently, it has become possible to convert this versatile oxidizer to another missile system application, that of warm gas generator propellants.

Warm gas generator propellants are required for driving turbine-alternator systems for electrical power generation, for actuating jet-controlled attitude control systems, and for propelling torpedo propulsion units. Despite the advantages of ammonium perchlorate, it has been difficult to utilize it in these applications, because of the inherently high flame temperature ($4500^{\circ}$ to $5500^{\circ}F$) of propellants based on it. Because of the materials of construction used in warm gas generator systems, the flame temperatures of these propellants are limited to values in the region of $2200^{\circ}$ to $2300^{\circ}F$.

In propellant technology, reduction of flame temperature is most conveniently obtained by reducing the oxidizer to fuel (O/F) ratio to a very low value, so that the composition is extremely fuel rich. In Figure 1 a plot is shown of flame temperature versus the weight percent of $NH_4ClO_4$ for a mixture of ammonium perchlorate and a typical low oxygen content, high fuel content polymeric hydrocarbon binder. Although aluminum powder is normally used as a fuel component in solid propellants, it has been omitted for two reasons: it increases flame temperature to still higher (and undesirable) values, while producing solid $Al_2O_3$ particles as an exhaust component. For most gas generator systems, the presence of solid particles in the combustion products is extremely undesirable because of the resultant clogging and erosion of the metallic portions of the system.

Examination of Figure 1 shows that the gradual reduction of the $NH_4ClO_4$ content from 90% to 70% reduces the flame temperature from $5000^{\circ}F$ down to the desired level of $2200^{\circ}F$, simply by greatly reducing the oxidation ratio of the system. The oxidation ratio decreases from 4.33 down to 1.15 for these two compositions, where oxidation ratio is defined as:

$$\text{Oxidation Ratio} = \frac{\Sigma O \text{ Atoms}}{\Sigma C \text{ Atoms} + \frac{1}{2} \Sigma H \text{ Atoms}}$$

Unfortunately, this reduction results in undesirably high levels of solid carbon in the combustion products when these are exhausted to the atmosphere. This can be seen in Table 1, where the level for the high fuel content binder is 6.45% solid carbon by weight. No carbon is found in the combustion chamber at 1000 psia, but expansion of the gases to 14.7 psia results in copious quantities of black smoke.

Two methods are applicable to the solution of this problem. The first of these involves substitution of much higher oxygen content binders for the polymeric fuel. In Figure 1 and Table I the results of substituting highly oxygenated polyester

polymers for the conventional fuel can be seen. Use of a carboxy-terminated polyester based on diethylene glycol and adipic acid, with an oxygen content of 37.0% results in almost a 50% reduction in solid carbon in the exhaust. The required amount of $NH_4ClO_4$ oxidizer for a 2200°F temperature is reduced to approximately 62%. For a 42.0% oxygen content binder, the amount of oxidizer for generation of 2200°F is reduced still further, to approximately 58%. Since one of the combustion products resulting from the use of $NH_4ClO_4$ is HCl, with its consequent erosivity of certain metals of construction, these reductions in oxidizer content are quite desirable, since they result in corresponding reductions in HCl content.

The second method of lowering flame temperature involves the addition of a third component to the system that is as low in energy content as possible and that has an internal oxidation ratio close to 1.0. Compounds with these high negative heats of formation and balanced stoichiometry are aptly designated as "coolants", since they are both poor fuels and poor oxidizers. A representative list of compounds of this type is shown in Table II. The oxidizers, ammonium perchlorate and ammonium nitrate, are included for comparison.

For each compound, the empirical formula, density, oxidation ratio, and heat of formation in kilocalories per gram are given. Because warm gas generating systems must be efficiently packaged, high density values are desirable. The advantage of possessing an oxidation ratio close to 1.0 has already been pointed out. Finally, since high flame temperatures result from either low negative or positive heats of formation, it is desirable that the value for $\Delta H_f/M$ be as large a negative number as possible, in order to produce low flame temperatures.

Examination of the compounds in Table II shows materials ranging from low oxidation ratio fuel-like compounds such as oxamide and azodicarbonamide, to more evenly balanced materials such as ammonium oxalate hydrate, oxalohydroxamic acid, and hydroxylammonium oxalate. Ammonium dihydrogen phosphate theoretically appears to be an oxidizer, like ammonium nitrate, and ammonium perchlorate; however, in actuality it serves only as a coolant, since the phosphate portion of the molecule is extremely stable at elevated temperatures, and is not a source of oxygen, unlike the nitrate and perchlorate structures.

As might be expected, the compounds in the middle of the list are the most desirable and useful coolants; in particular, oxalohydroxamic acid (also sometimes referred to as dihydroxyglyoxime-DHG) is of particular interest. Its high density, balanced stoichiometry and negative heat of formation are of importance in this regard.

Table III points out still another important factor in the selection of an effective coolant. A good coolant is thermally stable, but not too stable. Oxalohydroxamic acid is quite satisfactory in this respect, showing no endotherm or exotherm in differential thermal analysis below 300°F, but it completely fumes off at the slightly higher temperature of 338°F (dec.). Its ammonium salt, on the other hand, exhibits its first exotherm at a lower temperature than 300°F, but it is not completely decomposed until 400°F is reached. The other coolants shown are more stable in a thermal sense, but this frequently means that the amounts that can be added to a propellant formulation are limited to low levels because of difficulty in achieving combustion.

The effect of adding various amounts of coolant to typical warm gas generator propellant compositions is shown in Figure 2. At the same binder content of 26.5%, larger amounts of oxalohydroxamic acid (DHG) are required to reduce the flame temperature of the 43% oxygen content binder to the 2200°F level than for the 37% oxygen content binder. The more negative heat of formation of hydroxylammonium oxalate makes it possible to reach the 2200°F level with even less coolant. The

overall effectiveness of these coolants is realized when the flame temperatures of the same compositions without coolant are compared, for these are 4250°F and 3900°F, respectively, for the 42% and 37% oxygen binders. Hydroxylammonium oxalate (HAO) is especially effective in improving the cleanliness of the exhaust for only 22% of this coolant produces a 2278°F flame temperature with no solid carbon in the exhaust products.

In addition to the foregoing methods of reducing carbon in the exhaust products, it is also possible to effect a reduction by reducing the pressure at which the combustion reaction is carried out. An indication of the extent of this factor can be seen in Figure 3, where the weight percent of solid carbon formed in the Exhaust is plotted as a function of the combustion pressure for a single composition over the pressure range of 100 psia to 20,000 psia. At 20,000 psia, the carbon content of the exhaust is over 5% by weight, while at pressures below 500 psia, 0% carbon results. A reduction in flame temperature also results, with the value of 2374°F for the 20,000 psia level decreasing to 2058°F at 100 psia.

In addition to the formation of solid carbon, it is also possible for ammonium chloride to condense in solid crystalline particles during the reduction of flame temperature resulting from expansion of the combustion gases through a nozzle or turbine system. The presence of chlorine in the ammonium perchlorate leads to the formation of HCl as one of the combustion products; this in turn reacts with traces of $NH_3$ in the composition products to form $NH_4Cl$ when the temperature of the system falls below the value at which the vapor pressure of $NH_4Cl$ is equal to the pressure of the system. A plot of the vapor pressure - temperature relationship for $NH_4Cl$ is shown in Figure 4. If the temperature and pressure of the system fall above the line, solid $NH_4Cl$ will not form; when either the temperature or the pressure or both are reduced sufficiently to fall below the line, formation of solid particles will occur. In general, the higher the pressure in the system, the less likely it is that $NH_4Cl$ will deposit on cold walls or surfaces in the system.

Another problem resulting from the presence of HCl in the combustion products is the reaction of small amounts of this acid with the metallic materials of construction in systems using warm gas generators of this type. The metal chlorides formed from these reactions are undesirable for two reasons: changes in the dimensions of the attacked metal surfaces result from a volatilization of the chlorides, and later on deposition of metal chloride particles can occur in unwanted locations as the temperature of the gas is reduced.

Table IV shows the deposition temperature (melting point) for several of these metallic chlorides at a pressure of 1000 psia (68.05 atmospheres). They are arranged in order of increasing volatility. Although the rate of erosion of surfaces of most of these metals is extremely slow, as shown by the data on loss rate, the amounts of the chlorides formed are still of concern in some applications. The use of carbon steel is undesirable, but some stainless steels are satisfactory due to the protective action of chromium and nickel. The use of molybdenum and its alloys results in good erosion resistance and volatile chlorides for the reaction products.

Finally, it should be pointed out that a general correlation exists for a great many of the specific compositions described in this paper between theoretical flame temperature and % solid carbon in the exhaust. This can be seen in Figure 5, for with a few exceptions, all of the compositions previously discussed fall within a single band. Above a flame temperature of approximately 2550°F, no carbon forms; while below this temperature the amount formed is inversely related to the temperature.

In summary, two general methods of obtaining low flame temperature propellant compositions have been described that do not result in the production of large (over 6%) quantities of solid carbon in exhaust products. These are the use of highly oxygenated polyester binders and the use of "coolant" compounds with large negative values of $\Delta H_f/M$ and oxidation ratios close to 1.0. Two useful compounds of this type are oxalohydroxamic acid and hydroxylammonium oxalate.

The effects of varying combustion pressure over the range of 100 to 20,000 psia have been described. Effects related to the presence of HCl in the system, including the conditions controlling solids such as $NH_4Cl$ and various metallic chlorides in the system have also been discussed.

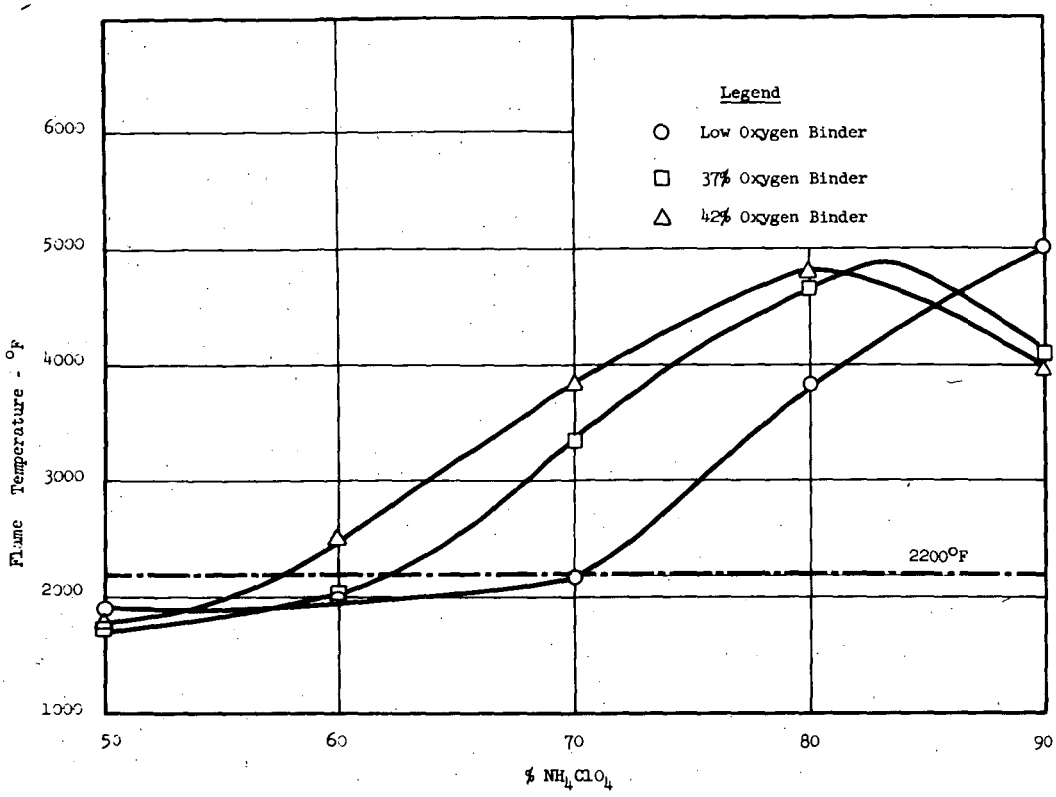


Figure 1. Effect of Oxygen Content on Flame Temperature

Table I

Reduction of Carbon Content
of
Combustion Products

| Binder | Wgt. % Oxidizer/Coolant | Flame Temp. ($^{o}$F) | Oxidation Ratio | Wgt.% $C_{(s)}$ in Exhaust |
|---|---|---|---|---|
| Low Oxygen Content | 70/0 | 2186 | 1.15 | 6.45 |
| 37% Oxygen Content | 60/0 | 2028 | 1.56 | 3.52 |
| 37% Oxygen Content | 43.5/30 | 2138 | 1.69 | 1.99 |
| 42% Oxygen Content | 37.5/36 | 2175 | 1.74 | 1.88 |

Table II

Coolants

| Compound | Empirical Formula | Density (g/cc) | Oxidation Ratio | $\frac{\Delta H_f}{M}\left(\frac{kcal}{g}\right)$ |
|---|---|---|---|---|
| Azodicarbonamide | $C_2H_4O_2N_4$ | 1.68 | 0.5 | -0.60 |
| Oxamide | $C_2H_4O_2N_2$ | 1.667 | 0.5 | -1.375 |
| Ammonium Oxalate Hydrate | $C_2H_{10}O_5N_2$ | 1.50 | 0.715 | -2.40 |
| Oxalohydroxamic Acid | $C_2H_4O_4N_2$ | 1.85 | 1.0 | -1.138 |
| Hydroxylammonium Oxalate | $C_2H_8O_6N_2$ | 1.60 | 1.0 | -1.85 |
| Ammonium Dihydrogen Phosphate | $NH_4H_2PO_4$ | 1.803 | 1.33 | -3.02 |
| Ammonium Nitrate | $NH_4NO_3$ | 1.725 | 1.5 | -1.09 |
| Ammonium Perchlorate | $NH_4ClO_4$ | 1.95 | 2.0 | -0.60 |

Table III

Differential Thermal Analysis

of Coolants

| Coolant | Endotherm (°F) | Exotherm (°F) | Fumes (°F) |
|---|---|---|---|
| Oxalohydroxamic Acid | None | 311.0 | 338.0 |
| Ammonium Oxalohydroxamate | None | 266.0 | 401.0 |
| Hydroxylammonium Oxalate | 271.4 | 348.8 | 399.2 |
| Azo-dicarbonamide | None | 372.2 | 451.4 |
| Ammonium Oxalate Hydrate | 192.2 + 413.6 (dec.) | None | None |

Table IV

Formation and Deposition of Metallic Chlorides

| Metal | Milligrams of Loss per 10 grams | Highest Melting Chloride | |
|---|---|---|---|
| | | Chloride | Melting Point (°C) |
| Cr | 0 (1) | $CrCl_3$ | 1150 |
| Ni | --- | $NiCl_2$ | 1001 |
| Fe | 3.6 | $FeCl_2$ | 670-674 |
| Ti | 2.7 | $TiCl_3$ | dec. 440 |
| Zr | --- | $ZrCl_4$ | 437 |
| W | --- | $WCl_6$ | 275 |
| Nb | 0 | $NbCl_5$ | 204.7 |
| Mo | 0 | $MoCl_5$ | 194 |

(1) 304 Stainless Steel

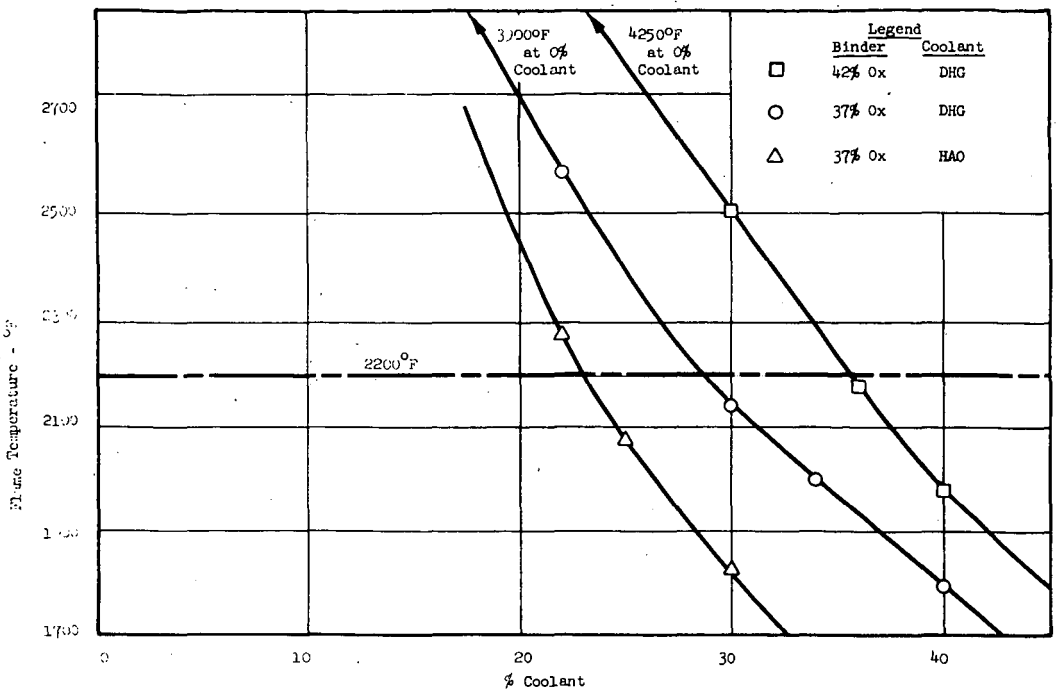


Figure 2. Effect of Percentage of Coolant on Flame Temperature

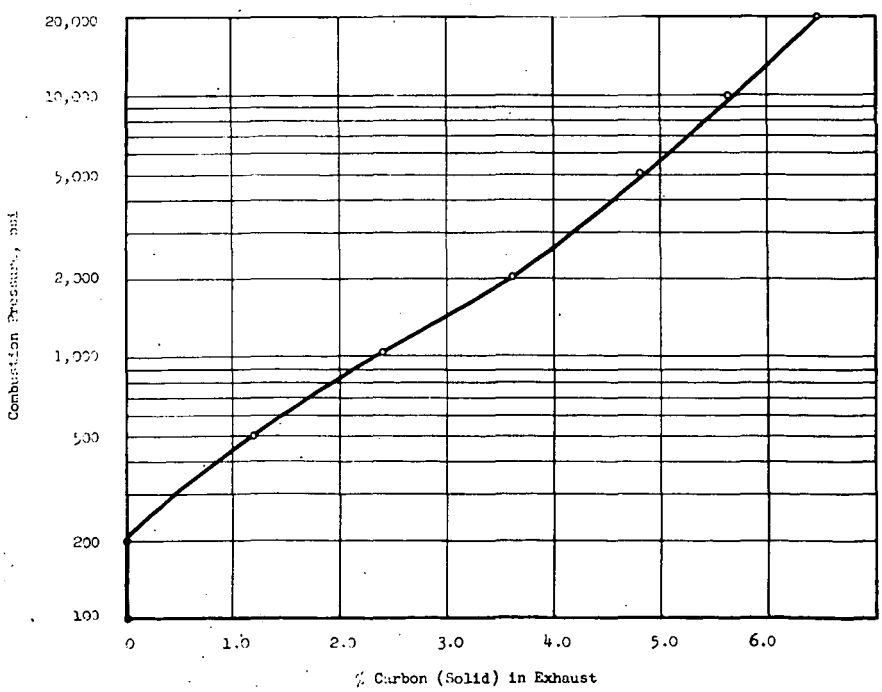


Figure 3. Effect of Pressure on % Carbon(s)

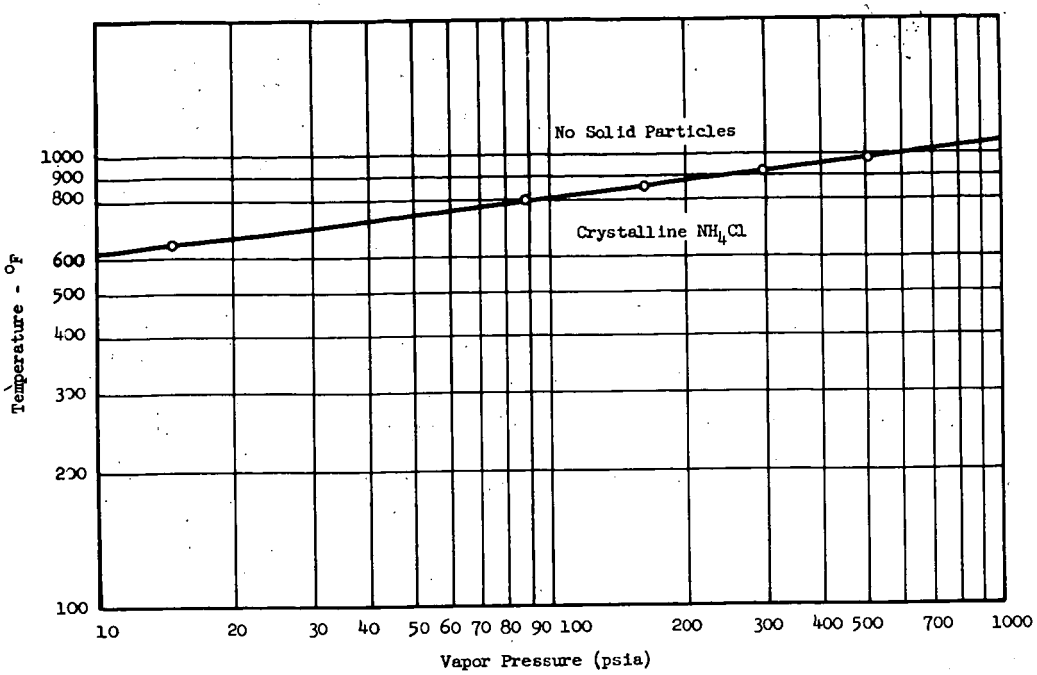


Figure 4. Vapor Pressure of $NH_4Cl$

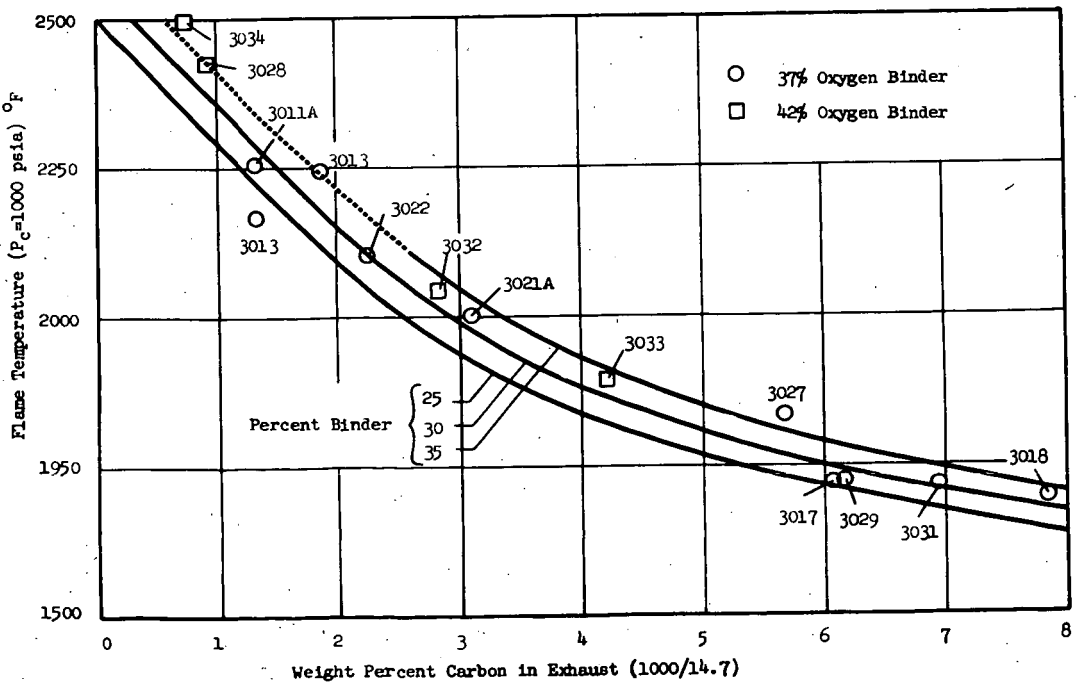


Figure 5. Temperature vs. Carbon Content of Q Series DHC-AP Propellant Compositions

# THE SYNTHESIS OF FLUORAMMONIUM SALTS[1]

Vytautas Grakauskas, Allen H. Remanick, and Kurt Baum

Contribution from Chemical & Biological Processes,
Aerojet-General Corporation, Azusa, California 91703.

Of the four possible fluorine-substituted ammonium ions, only the tetrafluoro derivative has been reported as a stable salt.[2,3] Difluoramine and trifluoramine have been reported to form reversible complexes with Lewis acids at low temperatures. Fluoramine was claimed to be a by-product of the electrolysis of ammonium bifluoride[5,6] but the results have been shown to be in error.[7] Dimethylfluoramine was synthesized by the fluorination of unsymmetrical dimethylsulfamide and the compound was sufficiently basic to form a stable hydrochloride.[8] Fluorimonium salts prepared by the rearrangement of alkyldifluoramines[9] can also be considered as alkylidene derivatives of substituted fluoramines.

Simple salts of fluoramine have now been prepared by the reaction of alkyl N-fluorocarbamates with strong acids. The starting materials are synthesized readily by the fluorination of alkyl carbamates.[10]

Fluorammonium Bisulfate. Fluorimonium salts have been prepared and characterized in sulfuric acid. Under these conditions, the hydrolysis of N-fluorocarbamates in sulfuric acid would be expected to give the fluorammonium ion, which also should be stable.

When a solution of ethyl N-fluorocarbamate in concentrated sulfuric acid was heated at 85 to 90°, carbon dioxide and ethylene were evolved. The $F^{19}$ nmr spectrum of the sulfuric acid solution consisted of a quartet at 36.8 ppm relative to external trifluoroacetic acid, with a coupling constant of 38 cps. Thus, the fluorine was coupled to three equivalent hydrogens, and it is noteworthy that the hydrogens did not exchange rapidly with the solvent. By contrast, the $F^{19}$ spectrum of an unheated solution of ethyl N-fluorocarbamate in sulfuric acid consisted of a single broadened signal at 27.5 ppm; the NH protons of the starting material thus exchanged with the solvent rapidly by the nmr time scale.

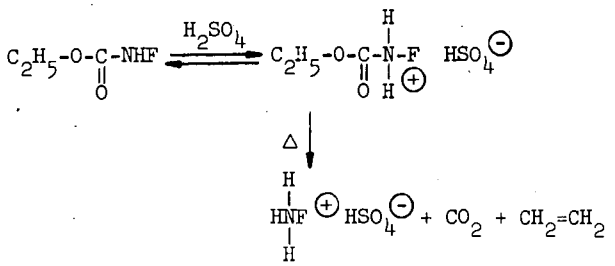

Additional evidence for the fluorammonium ion structure was obtained from reactions with carbonyl compounds. The reaction of cyclohexanone with a sulfuric acid solution of fluorammonium bisulfate gave ϵ-caprolactam, isolated by quenching the mixture with ice. A probable intermediate was α-fluoraminocyclohexanol, which could lose a fluoride ion and undergo nucleophic ring expansion. Alternatively, the dehydration of this alcohol could give fluoriminocyclohexane, which in turn, would undergo a similar ring expansion. The Beckmann fragmentation of fluorimines has been reported recently.[11]

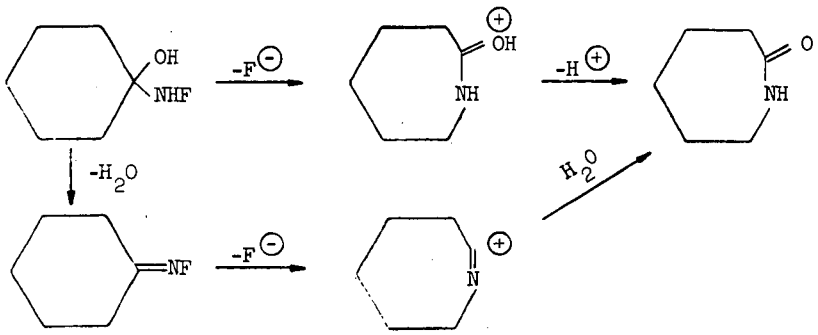

When n-butyraldehyde was treated similarly with the fluorammonium bisulfate solution, n-butyronitrile was formed. A related reaction, carried out in the presence of base instead of acid is the synthesis of nitriles from aromatic aldehydes and chloramine.[12]

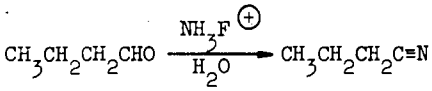

Attempts to isolate pure fluorammonium bisulfate, by diluting the sulfuric acid solution with organic solvents, were unsuccessful.

Fluorammonium Perchlorate. Perchloric acid, which is more volatile than sulfuric acid, appeared to offer better possibilities for the isolation of a pure fluorammonium salt. Accordingly, a solution of ethyl N-fluorocarbamate in 70% perchloric acid was heated until gas was evolved (68°), and the excess perchloric acid was then removed under vacuum. However, the product was contaminated by organic material of low volatility. Isopropyl N-fluorocarbamate reacted with 70% perchloric acid at a lower temperature than the ethyl ester (35 to 40°), and gave a less contaminated, but still unsatisfactory product. Unexpectedly, fluorammonium perchlorate was found to have appreciable vapor pressure, subliming slowly at 46°/.02 mm; the sublimed salt was analytically pure.

It is well-recognized that the maximum acid strength of a solution is limited by the acidity of the conjugate acid of the solvent. For this reason, perchloric acid is a stronger acid in acetic acid that in aqueous solution.[13] Perchloric acid is soluble in chloroform[14]; therefore, this solvent, which has very low basicity, should enhance the acidity. Indeed, isopropyl N-fluorocarbamate reacted more rapidly with a 10% solution of anhydrous perchloric acid in chloroform, than with the 70% commercial reagent. An additional advantage was that fluorammonium perchlorate was insoluble in chloroform. Analytically pure product was isolated directly in quantitative yield. The fate of the isopropyl group was not determined, but inasmuch as carbon dioxide free of propylene was liberated, it appears likely that isopropyl perchlorate was formed; if it was formed, it would remain in solution.[15]

$$(CH_3)_2CHOCNHF + 2\ HClO_4 \xrightarrow[42\text{-}43^\circ]{CHCl_3} (CH_3)_2CHOClO_3 + CO_2\uparrow + \underline{NH_3FClO_4}$$

Fluorammonium perchlorate was a white solid which melted with decomposition at 104 to 105°. Differential thermal analysis showed a sharp exotherm at this temperature. The impact sensitivity was the same as that of RDX. The salt was hygroscopic and decomposed rapidly in the presence of atmospheric moisture. Although the synthesis and isolation was carried out in glass equipment under an atmosphere of dry nitrogen, some etching of the glass was visible after several hours of contact with the salt. However, samples have been stored at room temperature for several months, without decomposition, in fluorocarbon or passivated-nickel containers.

Fluorammonium perchlorate was insoluble in hydrocarbons and halocarbons; it was soluble in simple esters, nitriles, nitroalkanes, and in such ethers as monoglyme and tetrahydrofuran. It formed a 1:1 complex with dioxane. Concentrated solutions (e.g., 30 to 50%) in any solvents were unstable, and in several instances, fumed off shortly after they were prepared. Addition of chloroform to the ethyl acetate solution precipitated unchanged fluorammonium perchlorate.

The fluorine nmr spectrum of fluorammonium perchlorate in sulfuric acid consisted of a quartet ($J$ = 44.1 cps) at 34.3 ppm from trifluoracetic acid ($\phi$ = 110.8), while the proton spectrum showed a doublet ($J$ = 44 cps) at 10.28 $\delta$.[16] However, when acetonitrile was used as the nmr solvent, the proton spectrum gave a broadened singlet at 10.7 $\delta$, while the fluorine spectrum gave a slightly unsymmetrical singlet at 122.4 $\phi$. In ethyl acetate, the proton signal was a sharp singlet at 11.5 $\delta$, and the fluorine signal was a sharp singlet at 122.8 $\phi$. Thus, rapid hydrogen exchange took place in the organic solvents but not in sulfuric acid. If the mechanism of exchange were direct displacement of protons, a higher rate could be expected in sulfuric acid than in the organic solvents. The more basic solvents apparently allow dissociation of fluorammonium perchlorate, to a small extent, to fluoramine and perchloric acid. The high volatility of fluorammonium perchlorate, compared to that of ammonium perchlorate might also be the result of dissociation.

$$H_3\overset{\oplus}{N}F\ ClO_4^{\ominus} \rightleftharpoons H_2NF + HClO_4$$

Fluorammonium Methanesulfonate - Fluorammonium methanesulfonate was synthesized by heating ethyl N-fluorocarbamate and methanesulfonic acid at 90°. The salt was precipitated by the addition of ether. The melting point and dta exotherm were essentially the same as those of the perchlorate, and of the perchlorate-dioxane complex; this temperature range appears to be the stability limit of the fluorammonium ion.

$$(CH_3)_2CHOCNHF + CH_3SO_3H \longrightarrow H_3NF \oplus CH_3SO_3^{\ominus}$$

The infrared spectrum is described in the Experimental Section.

Methylfluorammonium Bisulfate - To determine whether substituted fluorammonium salts could be prepared by these methods, the reaction of ethyl N-fluoro-N-methylcarbamate with sulfuric acid was studied. Gas was evolved at 85 to 95°. The $F^{19}$ nmr spectrum of the sulfuric acid solution consisted of an incompletely resolved triplet of quartets at -29.5 ppm (external trifluoroacetic acid reference), with coupling constants of 42 cps to the $NH_2$ and 28 cps to the methyl.

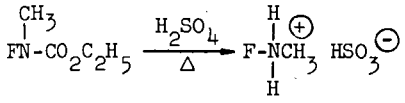

A sulfuric acid solution prepared in this manner reacted with cyclohexanone and water to give N-methylcaprolactam.

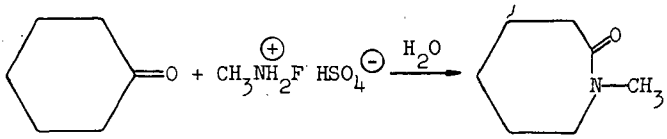

These reactions are analogous to those of the unsubstituted fluorocarbamates and indicate broad applicability of the synthesis methods.

Acknowledgement. The authors wish to thank Dr. H. M. Nelson and Mr. L. A. Maucieri for the nmr spectra, and Mr. K. Inouye for the elemental analysis.

## REFERENCES


1. This work was supported by the Office of Naval Research and the Advanced Research Projects Agency.

2. W. E. Tolberg, R. T. Rewick, R. S. Stringham, and M. E. Hill, Inorg. Chem., 6, 1156 (1967).

3. J. P. Guertin, K. O. Christe, and A. E. Pavlath, Inorg. Chem., 5, 1961 (1966).

4. A. D. Craig, Inorg. Chem., 3, 1628 (1964).

5. O. Ruff and L. Staub, Z. Anorg. Allg. Chem., 198, 32 (1931).

6. M. Schmeisser and P. Sartori, Angew. Chem., 71, 523 (1959).

7. C. B. Colburn, "Advances in Fluorine Chemistry," Vol. 3, M. Stacey, J. C. Tatlow, and A. G. Sharpe, editors, Butterworth & Co., Washington, D.C. (1963), p. 108.

8. R. A. Wiesboeck and J. K. Ruff, Inorg. Chem., 5, 1629 (1966).

9. K. Baum and H. M. Nelson, J. Am. Chem. Soc., 88, 4459 (1966); K. Baum, J. Org. Chem., 32, 3648 (1967).

10. V. Grakauskas, Third International Fluorine Symposium, Munich, Sept. 1965; R. E. Banks, R. N. Haszeldine, and J. P. Lalu, J. Chem. Soc. (C), 1966, 1514.

11. T. E. Stevens, Tetrahedron Letters, 1967, 3017.

12. R. C. Hauser and A. G. Gillaspie, J. Am. Chem. Soc., 52, 4517 (1930).

13. G. Schwarzenbach and P. Stensby, Helv. Chim. Acta, 42, 2342 (1959).

14. J. W. Mellor, "A Comprehensive Treatise on Inorganic and Theoretical Chemistry," Vol. II, Longmans, Green & Co., New York, 1946, p. 380.

15. J. Meyer and W. Sporimann, Z. Anorg. Allgem. Chem., 228, 341 (1936).

16. One member of the doublet was obscured by the solvent signal in concentrated sulfuric acid, but was visible using 101% sulfuric acid.

# PREPARATION AND POLYMERIZATION OF $NF_2$-CONTAINING MONOMERS

Eugene L. Stogryn

Esso Research & Engineering Co., Linden, New Jersey

Polymeric compositions normally employed to hold the oxidizer and fuel components of solid rocket propellant system do not contribute to the energetics of the propellant. In advanced solid propellants use of non-energetic binders is particularly deleterious to the attainment of high Isp. Preparation of binders containing the energetic difluoramino group was studied. Introduction of this group into polymer monomers was realized by the free radical addition of $N_2F_4$ to olefins. The difluoramino oxiranes synthesized for this work were obtained by either of the illustrated routes.

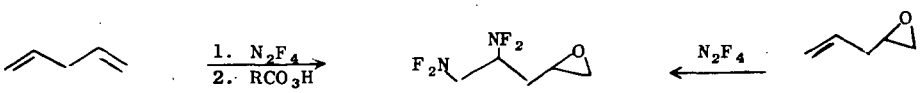


Attempts to difluoraminate vinyl oxiranes in which the vinyl function is directly attached to the ring were unsuccessful. These systems yield free radical induced rearrangements involving the olefinic and the oxirane functions.

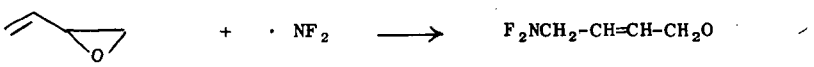


These rearrangements will be discussed. Difluoramination of 3-methylene oxetane yielded a mixture of the expected product together with a difluoramino aldehyde. Polymerization of the $NF_2$-oxiranes and oxetane will be described.

# KINETICS OF THE GAS PHASE PYROLYSIS OF CHLORINE PENTAFLUORIDE[1]

by A. E. Axworthy and J. M. Sullivan

Rocketdyne, A Division of North American Rockwell Corporation
6633 Canoga Avenue, Canoga Park, California 91304

The kinetics of the photochemical formation of chlorine pentafluoride from $ClF_3$ and $F_2$ has been studied recently by Krieger, Gatti, and Schumacker.[2] We report herein the results of our investigation of the gas phase thermal decomposition of $ClF_5$.

## EXPERIMENTAL

The electrically-heated stirred flow reactor (91-ml, monel) employed is described elsewhere.[3,4] Chlorine pentafluoride vapor of 98 weight percent purity (containing about 1.3% HF and 0.7% $ClF_3$) was passed through the reactor at an initial partial pressure of 32 mm in a mixture with helium. The total pressure was 1 atm. The reactor was equipped with a by-pass to allow measurement of the $ClF_5$ concentration in the entering gas stream.

The gases leaving the reactor (or the by-pass) were passed through a 10-cm nickel infrared cell with AgCl windows. The $ClF_5$ concentration was followed by measuring the absorbance at 12.5 microns. The flow rates were measured with a soap bubble flow meter connected to the exit stream. The measured flow rates and reactor volume were corrected to reactor temperature. No correction was made for the partial dissolution of reactants and products in the soap solution or for the presence of water vapor.

Infrared analysis of the exit gas showed $ClF_3$ and $ClF_5$ as the major absorbers, with ClF present in trace quantities. Fluorine does not absorb in this range (2-15 microns). These results indicate that the stoichiometry is mainly:

$$ClF_5 \rightarrow ClF_3 + F_2 \qquad \Delta H = +18.5 \text{ kcal/mole}^5 \tag{1}$$

## RESULTS

The results obtained for the thermal decomposition of $ClF_5$ over the temperature range 252-307° are presented in Table 1. For a stirred flow reactor, the rate constants for a simple order, single-reactant reaction are given by the equation:

$$k_n = (P^\circ - P)/(P^n\tau) \tag{2}$$

where $P^\circ$ and P are the partial pressures, respectively, of reactant entering and

---

1. This work was supported by the United States Air Force under Contract No. AFO4(611)-10544.
2. R. L. Krieger, R. Gatti, and H. J. Schumacker, Z. Phys. Chem., 51, 240 (1966).
3. J. M. Sullivan and T. J. Houser, Chem. Ind. (London), 1057 (1965).
4. J. M. Sullivan and A. E. Axworthy, J. Phys. Chem., 70, 3366 (1966).
5. JANAF Thermochemical Tables, Quarterly Supplement No. 7.

leaving the reactor, $\tau$ is the average residence time in the reactor, and n is the order of the reaction.[4] It can be shown from eq 2 that for a first-order reaction, a plot of $\alpha/(1-\alpha)$ vs $\tau$, where $\alpha$ is the fraction reacted, should be linear with a slope equal to the rate constant. Figure 1 shows that the decomposition of $ClF_5$ follows first-order kinetics up to 80% reaction at 293°. The data in Figure 1 were obtained at temperatures of 291.5-294.0°, and corrected to 293.0° using an activation energy of 41 kcal/mole. The rate constant, $k_1$, from each experiment is listed in Table 1. The best first-order rate constant, $k_1^A$, at each temperature, obtained from a plot of the type shown in Figure 1, is given in the last column of Table 1 and plotted in the Arrhenius form in Figure 2. A least squares fit of the data to the Arrhenius expression yields the line shown in Figure 2 which represents the rate expression:

$$k_1 = 10^{14.61} \exp(-41{,}330/RT) \text{ sec}^{-1} \qquad (3)$$

The uncertainty in activation energy is about 2 kcal/mole.

The mixing requirements for a stirred flow reactor do not allow a convenient procedure for varying widely the surface-to-volume ratio, but the high values of the activation energy and preexponential factor suggest that the reaction is homogeneous in nature. Also, it was found that the rates were unchanged after the reactor, containing products of reaction, had been allowed to sit at 280° for 1 month.

## DISCUSSION

Three possible mechanisms may be written which are compatible with the observed rate expression, i.e., first order in $ClF_5$ with no apparent inhibition as the products accumulate:

A) Unimolecular Elimination of $F_2$

$$ClF_5 \rightarrow ClF_3 + F_2 \qquad (4)$$

B) Non Chain Radical Mechanism

$$ClF_5 \rightarrow ClF_4 + F \qquad (5)$$
$$ClF_4 \rightarrow ClF_3 + F \qquad (7)$$
$$F + F + M \rightarrow F_2 + M \qquad (9)$$

C) Long Chain Radical Mechanism

$$ClF_5 \rightarrow ClF_4 + F \qquad (5)$$
$$F + ClF_5 \rightarrow ClF_4 + F_2 \qquad (6)$$
$$ClF_4 \rightarrow ClF_3 + F \qquad (7)$$
$$F + ClF_4 \rightarrow ClF_3 + F_2 \qquad (8)$$

The long chain mechanism (C) may be questioned on the basis of the observed rate parameters A and E. Mechanism (C) requires that

$$A = \left(\frac{A_5 A_6 A_7}{A_8}\right)^{\frac{1}{2}} \quad \text{and} \quad E = \tfrac{1}{2}\left(E_5 + E_6 + E_7 - E_8\right)$$

The A factors for the individual steps can be estimated from the generalizations proposed by Benson and Demore[6]. Thus,

6. S. W. Benson and W. B. Demore, Ann. Rev. Phys. Chem., 16,426 (1965).

$\left(\frac{A_5 A_6 A_7}{A_8}\right)^{\frac{1}{2}} \sim \left(\frac{10^{14}\ 10^{14}\ 10^{10}}{10^{10}}\right)^{\frac{1}{2}} \sim 10^{14}$. This value is in good agreement with the observed value of $10^{14.6}$. $E_5 + E_7$ are assumed equal to $\Delta H^\circ + E_{-7}$, where $\Delta H^\circ$ is the heat of reaction for $ClF_5 \rightarrow ClF_3 + 2F$ ($\Delta H^\circ$ = 57 KCal/mole)[4] and $E_{-7}$ is the activation energy for the reverse of reaction (7). Semenov's approximation[7] gives $E_{-7}$ = 2.5 KCal/mole and $E_6$ = 11.0 KCal/mole. The radical-radical reactions (-5) and (8) are assumed to have zero activation energies. Therefore $E = \frac{1}{2}(57.0 + 2.5 + 11.0\text{-}0) \sim 35$ KCal/mole. This value is somewhat lower than the observed value of 40.3 KCal/mole and suggests that the long chain mechanism (C) probably is not important in the decomposition of $ClF_5$.

Unfortunately the data do not allow a choice to be made between the molecular elimination mechanism (A) and the non chain mechanism (B). Thermochemical data[5] give $K_{eq} = 10^{-8.85} 10^{\frac{18.5}{\theta}}$ for the reverse of reaction (4). Therefore, $k_{-4} = 10^{5.8} \exp(-22{,}800/RT)$ liter/mole sec. The A factor $10^{5.8}$ liter/mole sec is not unreasonable for a bimolecular reaction. Hence, the molecular elimination reaction (A) cannot be eliminated.

If the non chain radical mechanism (B) is correct, then the measured activation energy, 40.3 KCal/mole, is equal to the bond dissociation energy for the first Cl-F bond in $ClF_5$. This value seems reasonable since the average bond energy in $ClF_5$ is 36 KCal/mole[5]. Further support for the non chain radical mechanism is given by the generalization of Benson and DeMore[6] that the A factor of unimolecular reactions involving the splitting off of atoms are in the range of $10^{14}$ to $10^{15}$ sec$^{-1}$.

It now remains to discuss the recent photochemical investigation by Krieger et al.[2] They studied the kinetics of the photochemical formation of $ClF_5$ from $ClF_3$ and $F_2$ (365 mμ, 16-70°) and obtained the complex rate expression:

$$\frac{d(ClF_5)}{dT} = kI_a \left[\frac{k'(ClF_3)}{M} + 1 + \frac{k''}{M}\right]^{-1}$$

Their somewhat unusual mechanism involves the formation of an activated $ClF_5$ molecule which can (1) be collisionally deactivated to $ClF_5$, (2) react directly with $ClF_3$ to form 2 $ClF_4$ radicals, or (3) split into $ClF_4$ + F. In order to explain their observed results (quantum yield dependent on inert gas pressure and on $ClF_3$ pressure), all three of these processes must occur to an appreciable extent in each of their experiments.

These photochemical results indicate that the $ClF_5$ activated molecule decomposes more rapidly than classical theory would predict. Also, the thermal decomposition of $ClF_5$ should be pressure dependent and accelerated by the presence of the product $ClF_3$.

The thermal and photochemical results can be shown to be compatible in two ways. First, it can be calculated from the photochemical rate constants that the accelerating effect of $ClF_3$ would not be sufficient to appreciably affect the first-order plot shown in Fig. 1. Thermal experiments would have to be run with added $ClF_3$ and at various total pressures to determine if the decomposition is dependent on the

7. N. N. Semenov, "Some Problems in Chemical Kinetics and Reactivity," Volume I, Princeton University Press, Princeton, New Jersey, 1958, P 29.

concentration of $ClF_3$ and added inert gases.

If it turns out that the thermal decomposition rate is unaffected by added $ClF_3$ and inert gases, it could be argued that the activated complex in the photochemical reaction differs in average energy from the thermally-formed activated complex. The fluorine atoms formed in the photochemical decomposition of $F_2$ must contain considerable translational energy since there are no accessible electronic states. If a portion of this translational energy is converted to internal energy in the $ClF_5$ complex ($F + ClF_4 \rightarrow ClF_5^*$), the stability of the complex would be greatly reduced. For example, an additional 10 KCal/mole of activation energy would decrease the predicted half-life of the complex from about $10^{-8}$ to about $10^{-10}$ sec, and might also account for its reactivity toward $ClF_3$.

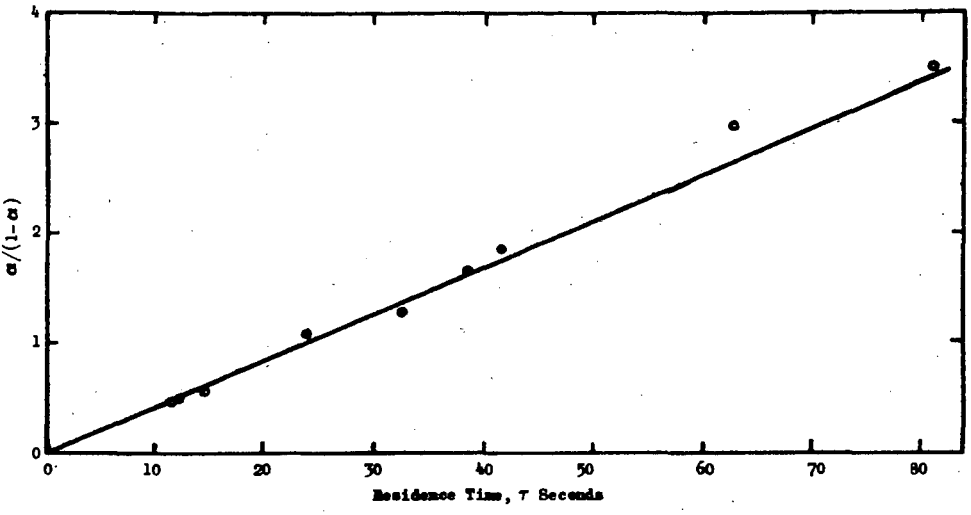


Figure 1. First-Order Plot of $ClF_5$ Decomposition Data at 293 C

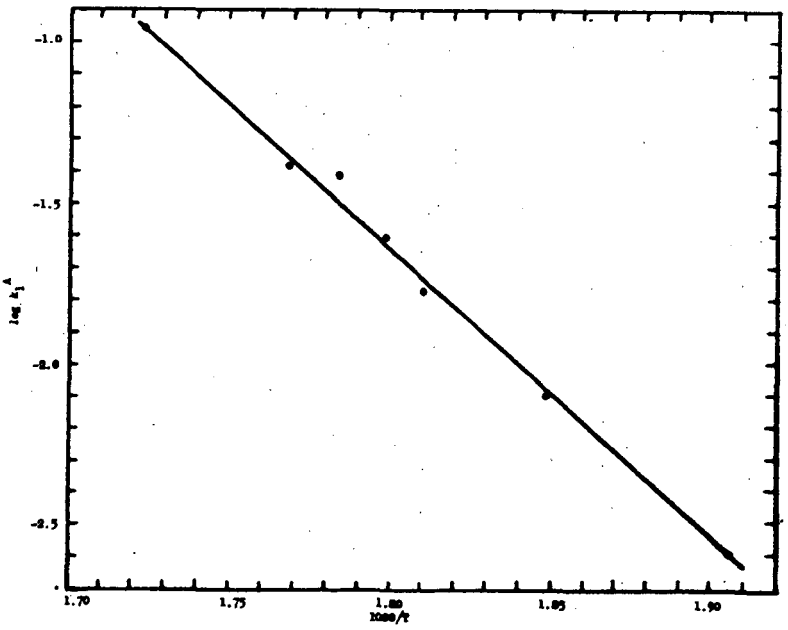


Figure 2. Arrhenius Plot

Table 1. Experimental Kinetic Data for the Pyrolysis of Gaseous Chlorine Pentafluoride

| Temp, °C | $\tau$, sec | Fraction Reacted, $\alpha$ | $k_1$, $sec^{-1}$ | $k_1^A$, $sec^{-1}$ |
|---|---|---|---|---|
| 252.2 | 24.9 | 0.068 | 0.00292 | 0.00260 |
| 252.2 | 113.0 | 0.254 | 0.00300 | |
| 252.2 | 281.5 | 0.375 | 0.00213 | |
| 252.2 | 449.0 | 0.525 | 0.00246 | |
| 268.5 | 196.8 | 0.612 | 0.00803 | 0.00803 |
| 279.4 | 36.2 | 0.381 | 0.0170 | 0.0164 |
| 279.4 | 115.3 | 0.646 | 0.0158 | |
| 283.2 | 23.6 | 0.371 | 0.0250 | 0.0251 |
| 283.0 | 36.3 | 0.477 | 0.0252 | |
| 287.4 | 24.4 | 0.465 | 0.0357 | 0.0385 |
| 288.2 | 40.4 | 0.625 | 0.0413 | |
| 287.4 | 42.4 | 0.629 | 0.0398 | |
| 287.6 | 55.0 | 0.716 | 0.0459 | |
| 291.8 | 11.9 | 0.312 | 0.0380 | 0.0417 |
| 291.5 | 24.1 | 0.499 | 0.0413 | |
| 293.0 | 11.6 | 0.312 | 0.0391 | |
| 293.0 | 14.6 | 0.364 | 0.0394 | |
| 293.3 | 32.4 | 0.570 | 0.0408 | |
| 293.0 | 38.4 | 0.624 | 0.0432 | |
| 293.5 | 41.7 | 0.658 | 0.0462 | |
| 293.0 | 62.8 | 0.749 | 0.0476 | |
| 294.0 | 81.3 | 0.790 | 0.0464 | |
| 307.5 | 7.96 | 0.433 | 0.0959 | 0.113 |
| 306.8 | 9.76 | 0.529 | 0.115 | |
| 307.0 | 11.93 | 0.595 | 0.123 | |
| 307.5 | 12.9 | 0.583 | 0.109 | |

# Redox in the $Cl_2O$–$AsF_5$ System

C. J. Schack and D. Pilipovich

Rocketdyne, a Division of North American Rockwell Corporation
Canoga Park, California 91304

Dichlorine oxide (or chlorine monoxide) has been reported to form a complex with $AsF_5$ at $-78^\circ$ and at about $-50^\circ$ formed an odd molecule, $ClOAsF_5$, through elimination of $Cl_2$.[1] Inference of the structure as being the postulated odd molecule was drawn from the observed reaction stoichiometry and the fact that the postulated odd molecule reacted with $NO_2$ to give $ClNO_3$.

We were interested in studying various aspects of the proposed odd molecule particularly as a ready source of the ClO radical. However, we felt that, prior to utilizing $ClOAsF_5$ as an intermediate, a more complete characterization was in order.

## Experimental

Materials. Chlorine monoxide was prepared from $Cl_2$ and yellow HgO using a modified procedure.[2] Arsenic pentafluoride was purchased from Ozark-Mahoning and used without purification after gas chromatography indicated a purity of better than 99.5%. Chloryl fluoride was prepared from $KClO_3$ and $F_2$[3] and purified by fractional condensation. Nitrogen tetroxide was purchased from the Matheson Co. and purified by fractional condensation. Phosphorus dichloride trifluoride was formed[4] from $PF_3$ and $Cl_2$.

Apparatus. Experiments were conducted in two vacuum systems, one constructed of glass, the other of stainless steel-Teflon. Solids were handled in an inert atmosphere glove box. Infrared spectra were taken on a Perkin-Elmer 137 Infracord using 5-cm gas cells fitted with AgCl windows or halocarbon oil mulls between AgCl plates. Debye-Scherrer powder X-ray diffraction patterns were obtained with a G. E. XRD5 instrument using $CuK\alpha$ radiation.

Vapor phase chromatography of reactants and products was carried out on a column packed with 50% w/w of Halocarbon Oil 4-11V and Kel-F low density molding powder according to Dayan and Neale.[5]

(1) M. Schmeisser, W. Fink and K. Brandle, Angew. Chem. 69, 780 (1957).

(2) C. J. Schack and C. B. Lindahl, Inorg. and Nucl. Chem. Letters, 3, 387 (1967).

(3) A. Engelbrecht, Angew. Chem., 66, 442 (1954).

(4) R. R. Holmes and W. P. Gallagher, Inorg. Chem., 2, 433 (1963).

Reactions of $Cl_2O$ and $AsF_5$. Measured quantities of $Cl_2O$ (117 cc, 5.22 mmoles) and $AsF_5$ (85.0 cc, 3.79 mmoles) were separately condensed into the reactor (glass or Teflon tubes) at -196°. The temperature was changed to -78° and it was observed that the mixed reactants gradually developed a dark red color. Pumping on the mixture after a few hours at -78° resulted in the recovery of some of the starting materials and much $Cl_2$. Subsequent warming of the reaction to ambient temperature gave additional small amounts of gaseous materials and a white solid. Little or no -196° non-condensable gases were observed throughout the reaction. In all, 111 cc of volatile products were obtained. Infrared and gas chromatographic analysis indicated these products to be a mixture of $AsF_5$ (17.5 cc, 0.78 mmole) and $Cl_2$ (93.5 cc, 4.17 mmoles) with a trace of $ClO_2$ and no $Cl_2O$. The observed reactant-product ratio of $Cl_2O$:$AsF_5$:$Cl_2$ was 5.00:2.89:4.01. Similar reaction ratios were obtained when $Cl_2O$ was used as the excess reagent. The solid product showed two infrared bands 1280 $cm^{-1}$ (m, doublet) and 690 to 700 $cm^{-1}$ (s. broad). Based on the observed stoichiometry of the reaction and the known infrared frequencies of Cl-O[6] and AsF[7] compounds, it appeared the solid might be principally $ClO_2AsF_6$. Accordingly, an authentic sample was prepared.

Preparation of $ClO_2AsF_6$. Chloryl fluoride (111 cc, 4.96 mmoles) and $AsF_5$ (63.7 cc, 2.84 mmoles) were separately condensed into a Teflon ampoule at -196°. After 1 hour at room temperature, the unreacted gases were removed and measured (48.0 cc, 2.14 mmoles). An infrared spectrum showed only $FClO_2$. The white solid product had an infrared spectrum identical to that of the solid from the $Cl_2O$-$AsF_5$ reaction. In addition, both solids fumed in air and exploded on contact with water. Powder X-ray patterns of both solids were obtained and were identical. The observed spacings and relative intensities are given in Table 1.

Reaction of $ClO_2AsF_6$ and $NO_2$. Weighed amounts of $ClO_2AsF_6$ and excess $NO_2$ gas were reacted for 1 hour at 0°. The expected displacement[8] of $ClO_2$ was achieved but in poor yield; 20% for the solid from the $Cl_2O$ reaction and 35% for the solid from the $FClO_2$ reaction.

---

(5) V. H. Dayan and B. C. Neale, Advances in Chemistry Series, No. 54, American Chemical Society, Washington, D. C., 1966, p. 223.
(6) E. A. Robinson, Can. J. Chem., 41, 3021 (1963).
(7) R. Peacock and D. Sharp, J. Chem. Soc., 2766 (1959).
(8) M. Schmeisser and W. Fink, Angew. Chem., 69, 780 (1957).

TABLE 1

X-RAY POWDER DIFFRACTION DATA FOR $ClO_2AsF_6$

| d, Å | Relative Intensity | d, Å | Relative Intensity |
|---|---|---|---|
| 7.50 | 30 | 2.30 | 10 |
| 5.55 | 30 | 2.08 | 60 |
| 5.10 | 30 | 2.05 | 60 |
| 4.40 | 70 | 1.95 | 40 |
| 4.02 | 40 | 1.87 | 10 |
| 3.65 | 100 | 1.84 | 10 |
| 3.57 | 90 | 1.80 | 10 |
| 3.49 | 10 | 1.76 | 10 |
| 3.03 | 50 | 1.70 | 20 |
| 2.87 | ≤ 10 | 1.59 | 15 |
| 2.76 | ≤ 10 | 1.55 | 10 |
| 2.69 | ≤ 10 | 1.53 | 10 |
| 2.54 | ≤ 10 | | |

Reaction of $PF_3Cl_2$ and $Cl_2O$. A 1:1 mixture of $PF_3Cl_2$ and $Cl_2O$ was allowed to warm to room temperature at which point an infrared spectrum was taken. The only infrared absorbing material present was $POF_3$. None of the $PF_3Cl_2$, a strong infrared absorber, remained. The by-product $Cl_2$ was revealed by its color when frozen. No non-volatile solids were observed.

## Results and Discussion

The reaction of $Cl_2O$ with $AsF_5$ does not give the odd molecule $ClOAsF_5$ but gives instead the salt $ClO_2AsF_6$. Further, the reaction appears to follow the stoichiometry shown in equation 1:

$$5Cl_2O + 3AsF_5 \longrightarrow 2ClO_2AsF_6 + 4Cl_2 + AsOF_3 \qquad (1)$$

The reaction stoichiometry does not appear to be dependent on the experimental reactant ratios. The formation of $ClO_2AsF_6$ was confirmed by preparing an authentic sample and comparing their X-ray patterns.

$$FClO_2 + AsF_5 \longrightarrow ClO_2AsF_6 \qquad (2)$$

In the reaction of $Cl_2O$ with $AsF_5$, the evolution of $Cl_2$ apparently involves a much more complex process than a simple Cl-O bond rupture. The equation reported[1] for this process at -50° is shown in equation 3:

$$Cl_2O{\cdot}AsF_5 \longrightarrow ClOAsF_5 + 1/2\ Cl_2 \qquad (3)$$

We would prefer to propose an initial step that infers an ionization of $Cl_2O$, i.e., an ionic complex is obtained, perhaps $ClO^+AsF_5Cl^-$:

$$Cl_2O + AsF_5 \longrightarrow ClOAsF_5Cl \qquad (4)$$

The oxidation of the $ClO^+$ species could then proceed with additional $Cl_2O$:

$$Cl_2O + ClOAsF_5Cl \longrightarrow ClO_2AsF_5Cl + Cl_2 \qquad (5)$$

This step (equation 4) should not be considered unusual inasmuch as other chlorine oxides are capable of redox (e.g., $ClO_2$ gives some $Cl_2O_6$ on photolysis[9]).

The most difficult rationale is the formation of the $AsF_6^-$ in the reaction. Admittedly a multiplicity of diverse reaction sequences could be proposed most of which would be difficult to experimentally verify. One possible path offered involves the dissociation of $ClO_2AsF_5Cl$ into its components with the subsequent reactions noted:

$$ClO_2AsF_5Cl \longrightarrow FClO_2 + AsF_4Cl \quad (6)$$

$$2AsF_4Cl \longrightarrow AsF_3Cl_2 + AsF_5 \quad (7)$$

$$AsF_5 + FClO_2 \longrightarrow ClO_2AsF_6 \quad (8)$$

$$AsF_3Cl_2 + Cl_2O \longrightarrow AsF_3O + 2Cl_2 \quad (9)$$

It is readily seen that the sum of equations 4 through 9, suitably weighted, gives equation 1.

The identity of $AsOF_3$ was not established as a product since it is a non-volatile[10] X-ray amorphous solid. In addition, we did not wish to further complicate matters by studying the reaction of $AsF_3Cl_2$ with $Cl_2O$ as a test of equation 8 inasmuch as $AsF_3Cl_2$ "goes ionic" and is formulated as $AsCl_4^+AsF_6^-$[11]. We did feel, however, that a suitable test of equation 8 would be the reaction of $PF_3Cl_2$ and $Cl_2O$. Indeed, the rapid conversion of $PF_3Cl_2$ to $POF_3$ and $Cl_2$ as in equation 10:

$$PF_3Cl_2 + Cl_2O \longrightarrow POF_3 + 2Cl_2 \quad (10)$$

strongly suggests that "covalent" $AF_3Cl_2$ would react similarly. The reaction conditions are such that the reorganization of $AsF_4Cl$, postulated as an intermediate in equation 6, would give initially the covalent structure.

The initial report on the preparations of "$ClOAsF_5$" did offer the reaction of $NO_2$ as a proof of the radical present[11]:

$$ClOAsF_5 + 2NO_2 \longrightarrow NO_2AsF_5 + ClNO_3 \quad (11)$$

The existence of $NO_2AsF_5$ has already been questioned seriously and apparently disproved[12]. Further, the formation of some $ClNO_3$ should be expected from $ClO_2AsF_6$ and $NO_2$ inasmuch as the reaction of $ClO_2$ and $NO_2$ gives $ClNO_3$[13]. It is quite likely that the reaction observed by Schmeisser et al.

(9) H. J. Schumacher, and G. Stiezer, Z. Physik, Chem., 37, 363 (1930).

(10) K. Dehnicke and J. Wiedlein, Z. Anorg. allg. chem., 342, 225 (1966).

(11) H. M. Dess, R. W. Parry, and G. L. Vidall, J. Am. Chem. Soc., 78, 5730 (1956).

(12) S. I. Morrow and A. R. Young, Inorg. and Nucl. Chem. Letters, 2, 349 (1966).

(13) H. Martin and Th. Jacobsen, Angew. Chem., 67, 524 (1955).

was the initial displacement of $ClO_2$ from $ClO_2AsF_6$ by $NO_2$ followed by a reaction of $ClO_2$ with $NO_2$, the overall reaction being:

$$ClO_2AsF_6 + 2NO_2 \longrightarrow NO_2AsF_6 + ClNO_3 + 1/2\ O_2 \qquad (12)$$

Except for the formation of the oxygen, the reaction in equation 12 has the same stoichiometry of $NO_2$ to "solid" as that reported in equation 11. Thus, the proof of "$ClOAsF_5$" through its reactions or its synthesis is not conclusive.

# DENSITY, VISCOSITY AND SURFACE TENSION OF $O_3$-$OF_2$

Charles Hersh

IIT Research Institute, Chicago, Illinois

# FREEZING POINT DEPRESSION IN $LF_2$ SYSTEMS

By W. D. English, W. A. Cannon and W. E. Crane

Astropower Laboratory, McDonnell Douglas Corporation
Newport Beach, California

## INTRODUCTION

In some test programs at Douglas using liquid fluorine and liquid hydrogen, we found it was desirable to lower the freezing point of fluorine without appreciably affecting its chemical reactivity. The use of a eutectic mixture with another cryogenic oxidizer seemed the method of choice, and consideration of physical and chemical properties led us to select oxygen difluoride, $OF_2$, for the other component. Oxygen was also suggested, but was not used because of reports of the quenching effect oxygen has on the fluorine-hydrogen reaction (Reference 1), an effect we also found in our research on the ignition of the $LF_2$-$LH_2$ reaction in $LH_2$ (Reference 2) and which has also been reported in the $OF_2$-$H_2$ reaction (Reference 3). $LO_2$ was therefore dropped from further consideration.

Theoretical calculations of the freezing point depression in the $F_2$-$OF_2$ system were carried out. These suggested that experimental investigation was warranted.

## THEORETICAL

The equilibrium or phase diagram of a two-component solid-liquid system may assume several general forms according to the nature of the components (Reference 4); these forms may be classified as follows:

1. Eutectic Systems
   - a. Simple eutectic
   - b. Monotectic (special form of simple eutectic)
   - c. Compound formation with congruent melting point
   - d. Compound formation with incongruent melting point
2. Completely Miscible Solid Solutions
   - a. Continuous solid solution
   - b. Minimum melting solid solution
   - c. Maximum melting solid solution
3. Partially Miscible Solid Solutions
   - a. Peritectic solid solution
   - b. Eutectic solid solution

In order for nonpolar compounds to form solid solutions, the following conditions must generally be satisfied:

1. Analogous chemical constitutions
2. Similar crystal structures
3. Nearly equal molecular volumes

While little is known of the crystal structures of $F_2$ and $OF_2$, it is certain that conditions 1 and 3 are not satisfied, and it is unlikely that solid solutions will form. Furthermore, there is no known tendency toward compound formation between $OF_2$ and $F_2$. Thus simple eutectic or monotectic systems are probable -- and the latter are rarely encountered.

If it is assumed that the system would be a simple eutectic, with the solution of each component in the other obeying Raoult's Law, and the liquidus curves conforming to equations for ideal solutions, the following considerations will apply:

From the Clausius-Clapeyron equation it can be shown that for equilibrium between solid solvent and vapor, at constant pressure,

$$\frac{d\ell nP_s}{dT} = \frac{L_s}{RT^2}$$

For an equilibrium between liquid and vapor, the corresponding equation is

$$\frac{d\ell nP_L}{dT} = \frac{L_e}{RT^2}$$

If it is assumed that the equations hold for supercooled solution in contact with solid, then

$$\frac{d\ell n(P_s/P_L)}{dT} = \frac{L_s - L_e}{RT^2} = \frac{L_f}{RT^2}$$

At the freezing point of the solution, the vapor pressure of the solid solvent must equal that of the solution, hence

$$\frac{d\ell n(P_1/P_L)}{dT} = \frac{L_f}{RT^2}$$

Since $P_1/P_L = X_1$ (mole fraction of solvent in solution) if Raoult's Law is applicable, then

$$\frac{d\ell nX_1}{dT} = \frac{L_f}{RT^2}$$

If this is integrated between T and $T_o$ (where $X_1 = 1$)

$$\ell nX_1 = \frac{L_f}{R}\left(\frac{1}{T} - \frac{1}{T_o}\right)$$

where T is the freezing point of the solution at solvent concentration $X_1$. This assumes that $L_f$ is independent of temperature, which is not strictly true, but this approximation was used, since the normal variation of $L_f$ with temperature would increase the freezing point depression in contrast to the real nonideality of the solutions, which tends to decrease the depression.

Using the last equation, the freezing point, T, was calculated for various concentrations of $F_2$ in $OF_2$ and $OF_2$ in $F_2$. A value of 122 cal/mole was used for the heat of fusion of $F_2$ (Reference 5). No value for the heat of fusion of $OF_2$ could be found in the literature, so it was estimated that the entropy of fusion was 6.5, which implies a heat fusion of 320 cal/mole. This value was used for the calculations

involved for constructing the phase diagram. A minimum freezing temperature of 39°K at an $F_2$ mole fraction of 0.65 resulted.

Solid fluorine is reported to undergo a transition at 45.55°K with a heat of transition of 173.9 cal/mole (Reference 5). Inasmuch as the solid fluorine can exist in two forms above the predicted eutectic temperature, the equilibrium diagram becomes more complicated. The theoretical phase diagram was recalculated using a value of 122 cal/mole as the heat of fusion of fluorine until the transition temperature was reached, after which the liquidus curve was assumed to undergo a change in slope corresponding to the heat of fusion plus the heat of transition. This curve was continued to meet the $OF_2$-rich liquidus curve leading to a theoretical minimum freezing point of 40°K at 0.54 mole fraction $F_2$.

## APPARATUS

A Pyrex apparatus was designed and built for this experiment. It is illustrated in Figures 1 and 2. It consists of a central volume for the test chamber, fitted with inlet tubing, a solenoid operated stirrer, and a thermowell. The central tube is surrounded by several annuli arranged concentrically in the following order -- an annulus in which the pressure can be controlled to control heat transfer rates, an annulus for liquid helium to cool the fluids in test, an evacuated annulus, an annulus for liquid nitrogen (heat shield) and another evacuated annulus. The evacuated annuli were silvered except for strips for observation of the interior.

Liquid helium is supplied to the cooling bath from 25 liter transport Dewars connected to the apparatus by insulated lines. Liquid nitrogen was poured into the heat shield when needed.

Temperatures were measured with a copper-constantan thermocouple inserted in the thermowell with an external reference junction at liquid nitrogen temperature. Thermoelectric potentials were measured with a Grey type E-3067 potentiometer and temperatures estimated from the tables and data of Powell, Bunch, and Corruccini (Reference 6). The thermocouple calibration was checked against boiling liquid nitrogen and hydrogen as fixed points. At 50°K the thermoelectric emf for copper-constantan is about 12.1 microvolts per degree. With a sensitivity of 5 microvolts or better for the potentiometer, the sensitivity of temperature reading is about 0.4°.

## MATERIALS

The oxidizers tested were obtained in the gaseous state from commercial suppliers. Fluorine supplied by Air Products and Chemicals was passed over an NaF absorption scrubber to reduce the HF content to 0.02 vol %. Oxygen difluoride supplied by Allied Chemical Division of General Chemical was also treated with NaF to remove HF.

## PROCEDURE

The quantities of fluorine and oxygen difluoride were measured by volume in the liquid state; weights were calculated from reported (References 7 and 8) densities. A glass ampul of calibrated volume was attached to the oxidizer supply manifold. The system was evacuated, the measuring apparatus and the ampul were chilled with $LN_2$ to 77°K, the test apparatus was valved off, and the oxidizer supply was valved open. When sufficient oxidizer had condensed in the ampul, the supply was shut off, the line to the test unit was valved open, and the $LN_2$ was removed from around the ampul, causing the oxidizer to distill into the test apparatus. When distillation was complete, the ampul was valved off.

After condensation of oxidizer was complete, the solenoid stirrer was activated, liquid helium was supplied to the cooling bath, and the pressure in the heat-transfer annulus adjusted to attain a cooling rate of about 1°K/minute. The emf of the thermocouple was continuously monitored, and the value recorded at 30 second intervals. The appearance of the oxidizer was observed visually during the experiment.

The experiments were conducted with $F_2$, with $OF_2$, and with several mixtures of $F_2$ and $OF_2$. The recorded thermocouple potentials were converted to temperatures from which cooling curve graphs (temperature vs. time) were plotted for each solution concentration. Figure 3 is a typical example. Temperatures at which breaks in the curves occurred were identified, and these were plotted on a temperature vs. concentration graph to provide a typical phase diagram (Figure 4). The data used for plotting the phase diagram are tabulated in Table I.

## RESULTS AND DISCUSSION

It was determined that, within the accuracy of the experiments, the binary system $F_2$-$OF_2$ exhibited typical eutectic formation with a probable break in the fluorine-rich liquidus curve due to a solid phase transition at 45 ± 0.5°K. The accuracy of the temperature measurements was ± 0.5°K. When the temperature-composition curves were plotted and extrapolated to their intersection (the eutectic), the error in composition was ± 2 mole %. This variation is indicated on the graphs by the bars through the experimental points. The errors in quantities of components used are believed to be considerably less than these. The eutectic temperature is estimated to be 43 ± 0.5°K and the eutectic composition 0.59 ± 0.02 mole fraction fluorine.

TABLE I

OBSERVED FREEZING POINTS -- $OF_2$-$F_2$ MIXTURES

| | Mole % $F_2$ | Initial F. P. °K | Transition Temp. °K | Eutectic F. P. °K |
|---|---|---|---|---|
| 1. | 100.0 | 53.0 | - | - |
| 2. | 80.0 | 48.3 | 45.0 | 43.5 |
| 3. | 69.5 | - | 45.0 | 42.4 |
| 4. | 46.0 | 45.6 | - | 43.3 |
| 5. | 28.0 | 47.8 | - | 43.4 |
| 6. | 0 | 49.2 | - | - |

## ACKNOWLEDGMENT

Work presented in this paper was conducted by the Douglas Aircraft Company, Missile and Space Systems Division, under company-sponsored research and development funds.

## GLOSSARY

P = vapor pressure
L = latent heat
R = gas constant
T = temperature, °K

## SUBSCRIPTS

s = solid state or solid-gas transition
L = liquid state or liquid-gas transition
e = evaporation
f = fusion
l = solution
o = freezing point of pure solvent

REFERENCES

1. Levy, J. B. and Copeland, B. K. W., J. Phys. Chem., 67, 2156, 1963, 69, 408, 1965. Brokaw, R. S., Ibid., 69, 2488, 1965; 69, 2808, 1965.

2. Cady, E. C. and Black, W. G., Personal Communication, March 1966.

3. Solomon, W. C., et al, Exploratory Propellant Chemistry, Semiannual Report, Air Force Rocket Propulsion Laboratory, Edwards, California, AFRPL-TR-66-238, October 1966.

4. Glasstone, S., Textbook of Physical Chemistry, D. Van Nostrand & Co., New York, 1940, Chapter X.

5. Jih-Heng, H., White, D., and Johnston, H. L., J. Am. Chem. Soc., 75, 5642-5, 1953.

6. Powell, R. O., Bunch, M. O., and Corruccini, R. J., Cryogenics, 2, 139-50, 1961.

7. Jarry, R. L. and Miller, H. C., J. Am. Chem. Soc., 78, 1553, 1956.

8. Anderson, R., Schinzlein, J. G., Toole, R. C., and O'Brien, I. d., J. Phys. Chem., 56, 473, 1952; Ruff, O. and Menzel, W., Z. Anorg. Chem., 198, 39, 1932.

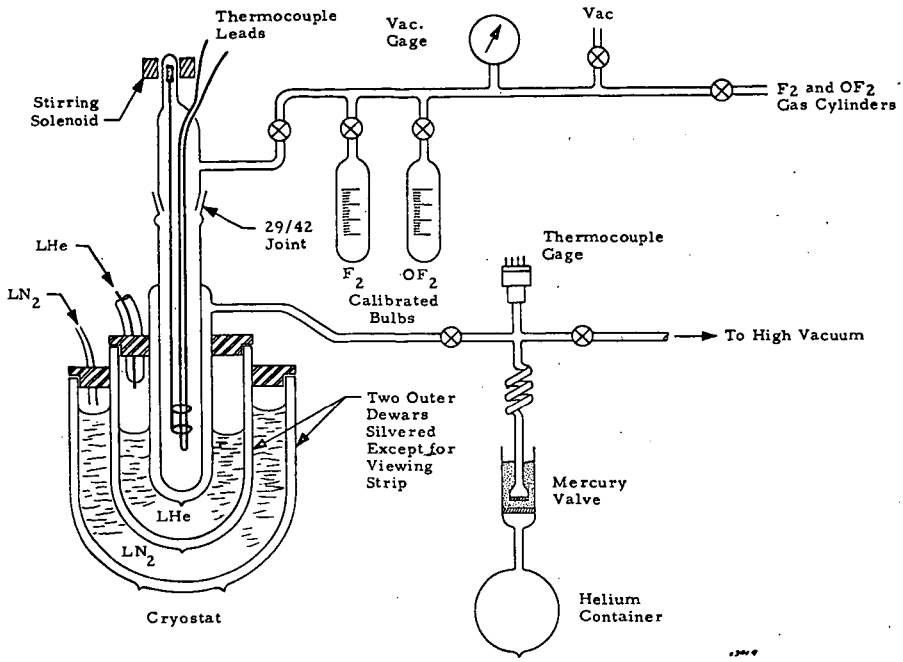


Figure 1. Freezing Point Apparatus

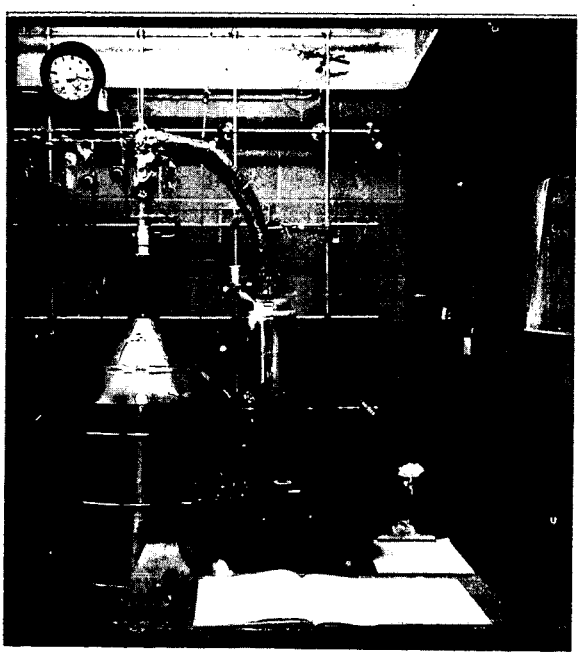

Figure 2. Freezing Point Apparatus

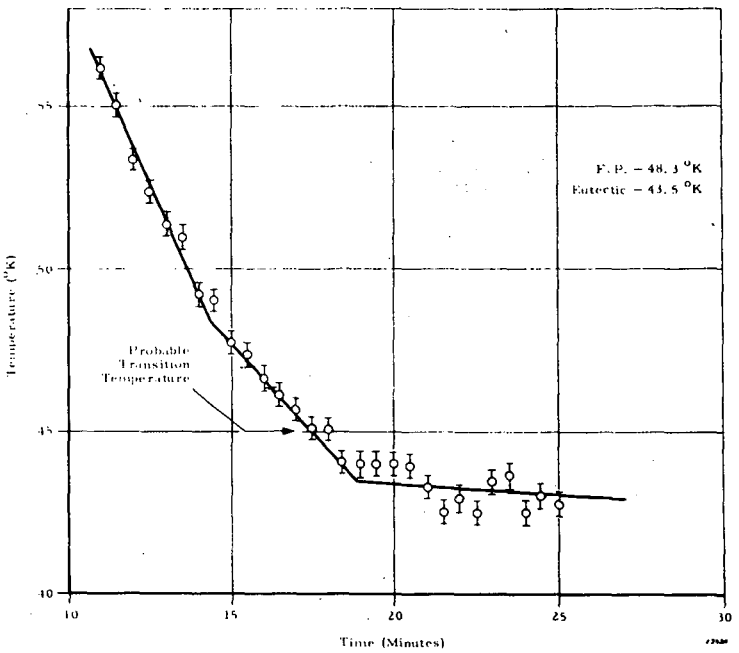


Figure 3. Cooling Curve — 80 mole % $F_2$, 20 mole % $OF_2$

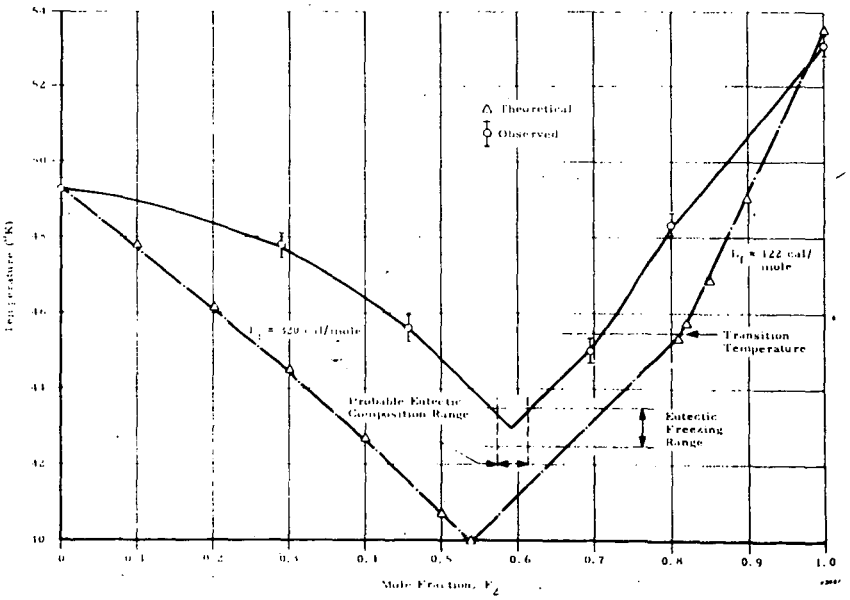


Figure 4. Phase Diagram, $OF_2$-$F_2$

# REACTIONS OF OXYGEN TETRAFLUOROBORATE

C. T. Goetschel, V. A. Campanile, C. D. Wagner, and J. N. Wilson

Shell Development Company, Emeryville, California

## Introduction

Recently we developed an efficient method of preparing $F_2O_2$. This compound is known to react with boron trifluoride[1] to produce $O_2^+BF_4^-$. Little is known of the reaction of $O_2^+BF_4^-$ itself. It is relatively stable at room temperature, but reacts readily with organic compounds. For instance, tiny particles dropped into benzene or isopropyl alcohol instantly ignite fires. The only known inorganic reaction[1] is with $NO_2$ where oxygen is displaced giving $NO_2^+BF_4^-$. This paper describes some additional reactions of $O_2^+BF_4^-$ with inorganic as well as some organic compounds.

## Results and Discussion

### A. Inorganic Reactants

#### 1. Xenon

Since xenon has nearly the same ionization potential as $O_2$, and since $Xe^+$ should be smaller than $O_2^+$, we felt that possibly xenon would replace oxygen to give the novel $Xe^+BF_4^-$. When liquid xenon (165°K) and solid $O_2^+BF_4^-$ ($Xe/O_2^+BF_4^- = 15$) were mixed in an evacuated tube, oxygen was released. The reaction was accomplished by allowing the xenon alternately to vaporize and condense around the $O_2^+BF_4^-$. After several minutes the sample was cooled in liquid nitrogen and any non-condensable gases were expanded into a fixed volume. The mass spectrum of the expanded gases showed only oxygen. The oxygen was pumped off; the reaction tube was warmed enough to liquefy the xenon and the procedure was repeated. This was continued until no further oxygen was obtained (about 85% of theory). Then the xenon was vaporized at 173°K (any $BF_3$ would also vaporize at this temperature) and expanded into a fixed volume. The loss of xenon (the amount reacted) was the same as the amount of oxygen collected. The mass spectrum indicated essentially no $BF_3$ was in the expanded xenon.

After removing all the xenon, the remaining white solid was slowly warmed. Decomposition became appreciable at 253°K with complete decomposition at room temperature. The mass spectrum of the gases showed Xe, $BF_3$, and $F_2$ with a $Xe:BF_3$ ratio of 1; we believe this to be evidence for the existence of $Xe^+BF_4^-$. Some $O_2$ was observed as well. The oxygen could have come from the decomposition of some unreacted $O_2^+BF_4^-$, or possibly from a xenon-oxygen compound of low stability. It is a firm conclusion that xenon reacts with $O_2^+BF_4^-$ at temperatures as low as 165°K to give free oxygen and a xenon compound.

#### 2. Chlorine Dioxide

Chlorine dioxide was prepared by dropping sulfuric acid onto a mixture of $KClO_3$ and glass chips. The $ClO_2$ generated was then diluted in a stream of $CO_2$ and passed first through a drying tube ($P_2O_5$), then through a sample of

$O_2^+BF_4^-$ which was supported on a glass frit and cooled to 195°K. An immediate reaction occurred, releasing oxygen. Within minutes the reaction was completed. The product, a light-yellow solid, was unstable at room temperature. The mass spectrum of its decomposition products showed only m/q peaks for fragment ions from $ClO_2$, $BF_3$ and $F_2$. The product $ClO_2^+BF_4^-$ has previously been reported[2] from the reaction of chloryl fluoride with boron trifluoride.

3. Chlorine, Chlorine Trifluoride, and Ammonia

In hopes of preparing the novel $Cl_2^+BF_4^-$, $ClF_3^+BF_4^-$, and $NH_3^+BF_4^-$, we passed the corresponding gases through $O_2^+BF_4^-$. In each case oxygen was displaced. However, the products were not stable at the reaction temperature (223°K to 195°K).

4. Cyanogen

At 248°K, $O_2^+BF_4^-$ dissolved in liquid cyanogen to give a clear, colorless solution. However, no oxygen was displaced and $O_2^+BF_4^-$ was recovered after removal of the cyanogen.

B. Organic Reactants

Although benzene and isopropyl alcohol spontaneously inflame when a milligram of $O_2^+BF_4^-$ is added, we felt that reactions with other specific organic compounds (in particular perhalogenated materials) could be studied under carefully controlled conditions.

Indeed, when liquid $CCl_4$ was condensed around $O_2^+BF_4^-$ at 250°K, a smooth reaction occured to liberate $O_2$, $Cl_2$, and $BF_3$, forming $CFCl_3$ and $CF_2Cl_2$. In a like manner, $O_2^+BF_4^-$ reacted with $CF_2Cl_2$ at 233°K to form $CF_3Cl$, essentially quantitatively. No $CF_4$ was detected. Hexafluorobenzene also reacted with $O_2^+BF_4^-$ at 298°K to give $O_2$, $F_2$, $BF_3$, and fluorinated hydrocarbons with the following prominent ions in the mass spectrum: $CF_3^+$, $C_2F_4^+$, $C_2F_5^+$, and $C_3F_5^+$. Some oxygen was converted to $CO_2$ and $COF_2$. It was also found that methane and ethane will inflame at 195°K. However, there was no reaction between perfluorocyclobutane and $O_2^+BF_4^-$.

Of the compounds that were found to react readily with $O_2^+BF_4^-$, both methane and $ClF_3$ have higher ionization potentials than that of $O_2$ (12.2 ev). Cyanogen, with both unsaturation and a higher ionization potential, did not react. In the case of compounds with ionization potentials below or equal to that of $O_2$, a reasonable mechanism for reaction is electron transfer to liberate $O_2$ and form a new ion which may or may not react further.

It should be noted that no $CF_4$ was formed from the reaction of $O_2^+BF_4^-$ with $CCl_2F_2$, whereas $CCl_2F_2$ was a product from the reaction with $CCl_4$. This would be expected if the primary products from the unstable $CCl_2F_2^+BF_4^-$ and $CCl_4^+BF_4^-$ were $CClF_3$ and $CCl_3F$, respectively. The former product has a higher ionization potential (12.9 ev)[3][4] than $O_2$ and is less likely to react with $O_2^+BF_4^-$. Therefore no $CF_4$ was observed. On the other hand, $CCl_3F$ has a favorable ionization potential, and further reaction with $O_2^+BF_4^-$ is possible, giving $CCl_2F_2$.

Acknowledgement

This work was supported by the Advanced Research Projects Agency under the research contract No. DA31-124-ARO(D)-54, monitored by the U.S. Army Research Office, Durham, North Carolina.

References

1. I. J. Soloman, R. I. Brabets, R. K. Uenish, J. N. Keith, and J. M. McDonough, J. Inorg. Chem. 3, 457 (1964).

2. A. A. Woolf, J. Chem. Soc., 4113 (1954).

3. J. W. Warren and J. D. Craggs, Mass-Spectrometry, Institute of Petroleum, London (1952), p. 36.

4. R. Bralsford, P. V. Harris, and W. C. Price, Proc. Roy. Soc. [A] 258, 459 (1960).

# PREPARATION OF FLUORINE PEROXIDES AND DIOXYGEN TETRAFLUOROBORATE BY LOW TEMPERATURE RADIOLYSIS

C. T. Goetschel, V. A. Campanile, C. D. Wagner, and J. N. Wilson

Shell Development Company, Emeryville, California

## Introduction

More than three decades have elapsed since it was shown that oxygen and fluorine could be combined by passage through an electrical discharge. The product, condensed on a very cold surface, was dioxygen difluoride, $O_2F_2$.[1] More recently, higher oxides of fluorine have been similarly prepared; these have been claimed to be $O_3F_2$,[2] $O_4F_2$,[3] $O_5F_2$ and $O_6F_2$.[4] The existence of $O_4F_2$ appears to be well established; however, there has been some controversy concerning the existence of $O_3F_2$ as a molecular species.[5]

Although $O_2F_2$ and $O_4F_2$ are stable only at very low temperatures, considerable evidence has been acquired concerning their physical[6-10] and chemical[11-16] properties. With all these studies the method of preparation of the oxygen fluorides has remained the same. No work has been reported on the radiation-induced reaction of oxygen and fluorine in a condensed phase.

The present study describes the reaction of these materials in the liquid phase at 77°K. Reactions were induced by high intensity 3 Mev bremsstrahlung.

## Procedure

Except for certain cases, ca 1.0 ml samples (28 mmoles) were irradiated in vacuo in stainless steel or sapphire vessels at 77°K for 1-2 hr at dose rates up to 100 megarads/hr of 3 Mev bremsstrahlung. The high-intensity 3 Mev bremsstrahlung was generated by directing the 3 Mev, 1 ma unscanned electron beam from a Van de Graaff accelerator onto a water-cooled gold target.[17] Following the irradiation the reaction vessel was attached to a vacuum line with provisions for expanding into a predetermined volume, measuring the pressure and analyzing with a mass spectrometer.[18] With this equipment the total volume and composition of gases from decompositions of products could be measured.

In experiments where $BF_3$ was added to the irradiated sample, the $BF_3$ was condensed in the top of the irradiated sample tube. The dewar of liquid nitrogen surrounding the tube was then slowly lowered to distill the $BF_3$ to the bottom of the tube. By this method any material deposited on the walls of the reaction vessel could react with the $BF_3$. The excess oxygen and fluorine were removed at 77°K; the sample tube was warmed to 195°K and the unreacted $BF_3$ was pumped off.

## Results and Discussion

The initial mixtures of $F_2$ and $O_2$ had a yellow color; after irradiation a reddish-brown solid was observed on the walls of the sapphire tube. The solid is presumed to be a mixture of $F_2O_2$ and $F_2O_4$ with possibly other oxides of fluorine. In each of the experiments described below (Table 1), excess $F_2$ and $O_2$ were removed at 77°K, first by evaporation into the calibrated

volume and then by pumping to a few microns pressure; this treatment would also remove $F_2O$. The sample was then warmed cautiously to decompose the $F_2O_4$ to $F_2O_2$; the $O_2$ released was measured gasometrically. This operation was carried out most successfully by removing the liquid nitrogen bath until a small increase in pressure was observed, replacing the liquid nitrogen, and repeating the process until the $F_2O_2$ could be melted (113°K) without further oxygen evolution. The oxygen thus evolved was mass spectrometrically free of $F_2$ (however, this was not a very sensitive test because the mass spectrometer inlet system was somewhat reactive with small quantities of fluorine). The blood-red liquid $F_2O_2$ was then frozen at 77°K (orange solid) and the residual $O_2$ was pumped away. Subsequent remelting at 113°K resulted in no further release of $O_2$. The sample was then warmed slowly to room temperature to decompose the $F_2O_2$ and measure the $F_2 + O_2$.

This procedure was occasionally unsuccessful in cases with the initial mole ratio $F_2/O_2$ of 1.0 or 3.0, because a minor explosion ("pop") would be heard during the decomposition of $F_2O_4$, accompanied by a sudden rise in pressure. The gasometric data indicated that in these cases some of the $F_2O_2$ was decomposed during the sudden decomposition of $F_2O_4$. Because of this, the apparent yields of $F_2O_4$ and $F_2O_2$ reported in Table 1 are taken only from experiments in which there was no audible evidence of explosion. Nevertheless, the reported yields of $F_2O_4$ may be slightly too high in some cases because of some decomposition of $F_2O_2$ during the decomposition of $F_2O_4$.

The data reported in Table 1 show several unusual features. First, in the mixtures containing only $F_2$ and $O_2$, the number of millimoles of oxygen converted to $F_2O_2$ and $F_2O_4$ remain nearly constant despite a large variation in the initial ratio of $F_2$ to $O_2$, even when the major part of the oxygen was consumed. The G-value for products also remained constant at a value that is several-fold higher than the values that are usually found for non-chain reactions.[8] These observations suggest that the formation of $F_2O_2$ under these conditions involves a short chain process that is initiated with approximately equal efficiency whether the initial absorption of energy is done by oxygen or by fluorine.

Another observation is that the ratio of $F_2O_4$ to $F_2O_2$ in the products displays no obvious trend with the initial ratio of $F_2/O_2$. The possible chain

$$\begin{array}{ccccccc} F\cdot & \xrightarrow{O_2} & FO_2\cdot & \xrightarrow{O_2} & FO_4\cdot & \xrightarrow{O_2} & FO_6\cdot \\ \downarrow F\cdot & & \downarrow F_2 & & \downarrow F_2 & & \downarrow F_2 \\ F_2 & & F_2O_2 + F\cdot & & F_2O_4 + F\cdot & & F_2O_6 + F\cdot \end{array}$$

would not lead to these results in a homogeneous system, but the kinetics are probably complicated by the fact that the products precipitate as solids.

The experiments in which the reactants were diluted with argon show that the presence of argon had a small positive effect on the total conversion of oxygen, whereas dilution with nitrogen does not appear to effect the yield. Some energy transfer from argon seems indicated.

---

a) G for ion pair formation is expected to be about 4; for radicals it often ranges from 6-10.

One experiment was done with a large excess of oxygen ($F_2/O_2$ = 1/6). The unreacted $F_2$ and $O_2$ (21.6 mmoles out of an initial 28) were removed and the reaction tube evacuated to < 5 μ. The color of the solid remaining in the sapphire tube was very dark brown. When the liquid nitrogen bath was momentarily removed and the sample was illuminated briefly with a flashlight, the product detonated violently and shattered the sapphire tube. Whether the detonation was due to the presence of a large amount of $F_2O_4$ or to $F_2O_6$ is not known. It is unlikely that the detonation was due to $O_3$ since its vapor pressure is well above 5 μ at 77°K and should have been pumped off. The very unstable $F_2O_6$ (dark brown in color) has been reported to explode on illumination or sudden warming. It is claimed to decompose thermally about 90°K.

In the experiments listed in Table 1, some $F_2O$ was formed in addition to $F_2O_2$ and $F_2O_4$; the amount was relatively small and was not studied systematically. The presence of $F_2O$ was detected by mass spectrometric analysis.

Experiments With Added $BF_3$

It has been shown by others[15] that $BF_3$ reacts with $F_2O_2$ at low temperatures to form the ionic compound $O_2^+BF_4^-$. We therefore added $BF_3$ to irradiated mixtures of $O_2$ and $F_2$ in order to explore the radiation route to $O_2^+BF_4^-$ and possibly to $O_4^+BF_4^-$.

Boron trifluoride (3.5 mmoles) was condensed in the top of the irradiation tube containing the formed fluorine peroxides (ca 1.7-2.0 millimoles) suspended in the excess fluorine and oxygen. The $BF_3$ was distilled to the bottom of the tube and the contents mixed by alternately vaporizing and condensing a portion of the excess fluorine and oxygen. In this manner the $BF_3$ was better able to contact the reddish-brown peroxide. The excess fluorine and oxygen were then removed under vacuum at 77°K. When the contents were warmed to 113°K, a rapid reaction occurred, and the color changed to orange. This suggests that much of the $F_2O_4$ decomposed without reacting with $BF_3$. The orange color changed to white when the temperature was raised to 143°K; this corresponds to the conversion of the $F_2O_2$ to $O_2^+BF_4^-$. Further warming to 240°K led to slight decomposition; the remaining solid was relatively stable, decomposing only very slowly at room temperature and atmospheric pressure. The decomposition is much more rapid under reduced pressure, indicating a reversible step with a gaseous product in the decomposition. The yield was measured by recovering the solid in a dry box and weighing it.

The gases evolved upon warming to 240°K consisted of $O_2$, $F_2$, and $BF_3$. Irradiation of various fluorine-oxygen mixtures followed by addition of $BF_3$ gave gases for this low-temperature decomposition in the ratio of $(O_2 + F_2)/BF_3$ of 1.9 ± .35. There is a systematic tendency for this ratio to be higher when the total volume of gas liberated is low. These findings correspond to decomposition of an oxygen-rich compound, probably $O_4^+BF_4^-$, with simultaneous induced decomposition of some of the $O_2^+BF_4^-$. (Evidence for the formation of $O_4^+BF_4^-$ from $F_2O_4$ has also been obtained in an independent investigation by Soloman and his colleagues.)[19]

The more stable product (presumed to be $O_2^+BF_4^-$) decomposed rapidly above 300°K to give $O_2$, $F_2$, and $BF_3$. The elemental analysis of the solid was F, 62.6%; B, 8.6%; theory, F, 63.7%; B, 9.2%). The infrared spectrum of the powder between silver chloride plates exhibits the characteristic absorption frequencies[20] of the $BF_4^-$ ion. No absorption band attributable to $O_2^+$ was observed, but this ion should have no dipole moment.

The x-ray powder pattern (Table 2) is very similar to that of the likely isomorphous $NO^+BF_4^-$ compound. (The nitrosyl and dioxygenyl cations are similar in size.)[21] A comparable correlation[14] was found for $NO^+AsF_6^-$ and $O_2^+AsF_6^-$.

The EPR spectrum of the solid at 77°K was a broad signal with a G-value of 1.94 and a peak-to-peak separation in the derivative mode of about 382 gauss. Kirshenbaum and Grosse[22] found similar results in HF solution. Soloman, et al[15][23] reported similar results for the solid.

The yields of $O_2^+BF_4^-$ recovered from various experiments are listed in Table 3. Comparison of the yields after 1 hr irradiation time in the experiments listed in Tables 1 and 3 indicates that a little less than two moles of $F_2O_2$ are required to produce one mole of $O_2^+BF_4^-$. Either some decomposition of $F_2O_2$ occurred during the process of warming to the temperature of reaction with $BF_3$, or the formation of $O_2^+BF_4^-$ is accompanied by a side reaction that decomposes part of the $F_2O_2$. It will also be noted that in the single experiment with a large excess of oxygen present during irradiation ($F_2/O_2 = 1/6$), the excess $F_2$ and $O_2$ were successfully removed without detonation after $BF_3$ was added. The yield of $O_2^+BF_4^-$ was relatively small, but there was evidence for the formation of larger amounts of a less stable compound. One other observation of interest is that when $BF_3$ is present during the irradiation, the yield of $O_2^+BF_4^-$ finally recovered is relatively small.

Acknowledgements

This work was supported by the Advanced Research Projects Agency under the research contract No. DA31-124-ARO(D)-54, monitored by the U.S. Army Research Office, Durham, North Carolina. Gratitude is also expressed to Dr. R. M. Curtis for performing the x-ray studies on $O_2^+BF_4^-$, to Dr. E. E. Genser for obtaining the EPR spectrum of $O_2^+BF_4^-$, and to Mr. E. Wong for his assistance with the Van de Graaff accelerator.

Table 1. YIELDS OF $F_2O_2$ AND $F_2O_4$ FROM IRRADIATION[a] OF FLUORINE/OXYGEN MIXTURES

| Mole Ratio, $F_2/O_2$ | Amount Irradiated, millimoles | | | | Yield,[b] millimoles | | Ratio, $F_2O_4/F_2O_2$ | Oxygen Consumed | | G-Value (c) |
|---|---|---|---|---|---|---|---|---|---|---|
| | $F_2$ | $O_2$ | Ar | $N_2$ | $F_2O_2$ | $F_2O_4$ | | mmole | % | |
| 1 | 14.0 | 14.0 | - | - | 1.50 | 0.13 | 0.087 ± 0.02 | 1.72 | 12.3 | 17.5 |
| 3 | 21.0 | 7.0 | - | - | 1.72 | 0.085 | 0.05 ± 0.02 | 1.89 | 27.0 | 18.5 |
| 5 | 22.8 | 4.6 | - | - | 1.93 | 0.105 | 0.055 ± 0.02 | 2.14 | 46.6 | 21.2 |
| 7 | 24.5 | 3.5 | - | - | 1.86 | 0.14 | 0.075 ± 0.015 | 2.14 | 61.2 | 20.6 |
| 1 | 10.5 | 10.5 | - | 7.0 | | (d) | n.d. | 1.26 | 12.0 | 13.5 |
| 1 | 10.5 | 10.5 | 7.0 | - | | (d) | n.d. | 1.73 | 16.5 | 17.1 |
| 1 | 10.5 | 10.5 | 7.0 | - | 1.65 | 0.07 | 0.042 ± 0.02 | 1.79 | 17.1 | 17.6 |
| 3 | 15.7 | 5.3 | 7.0 | - | 1.62 | 0.14 | 0.09 ± 0.02 | 1.90 | 35.9 | 18.2 |
| 5 | 17.5 | 3.5 | 7.0 | - | 1.62 | 0.105 | 0.065 ± 0.02 | 1.83 | 52.3 | 17.3 |
| 7 | 18.4 | 2.6 | 7.0 | - | 1.62 | 0.09 | 0.055 ± 0.02 | 1.79 | 68.9 | 16.8 |

a) 77°K, 100 megarads, 1 hr.
b) Yield data accurate to ca ± 0.03 mmole.
c) Molecules of product formed per 100 ev absorbed energy.
d) Amount of $F_2O_4$ not reliably determined because of a slight detonation on warming the system to decompose $F_2O_4$.

Table 2. DIFFRACTION PATTERNS OF $NO^+BF_4^-$ AND $O_2^+BF_4^-$

| $NO^+BF_4^-$ | | $O_2^+BF_4^-$ | | |
|---|---|---|---|---|
| Interplanar Spacing A | Intensity of Reflection | Interplanar Spacing A | Intensity of Reflection | hkl |
| 5.50 | 24 | 5.50 | 16 | 110 |
| 4.41 | 40 | 4.33 | 34 | 101 |
| 3.96 | 8 | 3.91 | 5 | 111 |
| 3.76 | 12 | 3.74 | 9 | 120 |
| 3.51 | 100 | 3.47 | 100 | 021 |
| 3.25 | 12 | 3.27 | 16 | 210 |
| 3.13 | 80 | 3.10 | 88 | 121 |
| 2.82 | 60 | 2.82 | 75 | 211 |
| 2.75 | 12 | 2.74 | 12 | 220 |
| 2.52 | 40 | 2.49 | 44 | 112 |
| 2.40 | 3 | 2.43 | 7 | 131 |
| 2.39 | 8 | 2.35 | 7 | 022 |
| 2.26 | 60 | 2.24 | 63 | 122 |

Table 3. PREPARATION OF $O_2^+BF_4^-$ [a]

| Irradiation Time, min[b] | Ratio $F_2:O_2$ Irradiated[c] | $O_2^+BF_4^-$ Produced, mg | %m $O_2^+BF_4^-$ Based on Oxygen | G-Value Total[g] |
|---|---|---|---|---|
| 15 | 1:1 | 27 | 1.6 | 8.9 |
| 30 | 1:1 | 53 | 3 | 8.8 |
| 60 | 1:1 | 96 | 6 | 7.9 |
| 60 | 2:1 | 129 | 12 | 11.0 |
| 60 | 3:1 | 134 | 16 | 10.6 |
| 60 | 5:1 | 127 | 24 | 10.5 |
| 60 | 7:1 | 113 | 27 | 8.8 |
| 60 | 1:6 | 44[d] | 1.5 | 4.1 |
| 60[e] | 1:1 | 45 | 2.7 | 14.9 |
| 120 | 3:1 | 216 | 26 | 8.6 |
| 180 | 1:1 | 231 | 14 | 6.3 |
| 180 | 5:1 | 248 | 47 | 6.9 |
| 120[f] | 3:1 | 21 | 2.6 | 0.2 |

a) 14 mmoles of $BF_3$ was added after irradiation.
b) Dose rate of 100 megarads/hour.
c) Millimoles of oxygen used with $F_2:O_2$ ratios was: 1:1 = 14 mmoles; 2:1 = 8.75 mmoles; 3:1 = 7.0 mmoles; 5:1 = 4.4 mmoles; 7:1 = 3.5 mmoles; 1:6 = 21.9 mmoles.
d) A second compound was formed which decomposed at 133°K yielding about 3 mmoles of noncondensable gases.
e) Dose rate of 25 megarads/hour.
f) 10.5 mmoles of $BF_3$ added to the reaction tube before irradiation.
g) Molecules of product formed per 100 ev absorbed energy.

## REFERENCES


1. O. Ruff and M. Menzel, Z. Anorg. Chem. 211, 204 (1933).

2. A. D, Kirshenbaum and A. V. Grosse, J. Am. Chem. Soc. 81, 1277 (1959).

3. A. V. Grosse, A. G. Streng, and A. D. Kirshenbaum, ibid. 83, 1004 (1961).

4. A. G. Streng and A. V. Grosse, ibid. 88, 169 (1966).

5. I. J. Solomon, Adv. Oxid. Research, U.S. Dept. Comm., AD 640405, (1966), Ill. Inst. of Tech. or Chem. Abst. 66, 82006f, (1967).

6. A. D. Kirshenbaum, A. V. Grosse, and J. G. Aston, ibid. 81, 6398 (1959).

7. A. D. Kirshenbaum and A. G. Streng, J. Chem. Phys. 35, 1440 (1961).

8. A. G. Streng, Chem. Revs. 63, 607 (1963).

9. T. J. Malone and H. A. Mc Gee, Jr., J. Phys. Chem. 69, 4338 (1965).

10. T. J. Malone and H. A. Mc Gee, Jr., ibid. 71, 3060 (1967).

11. A. G. Streng and A. V. Grosse, Adv. in Chem. Series, No. 36, Am. Chem. Soc., Washington, D.C., 1962, pp. 159-164.

12. M. S. Cohen, J. Inorg. Chem. 1, 972 (1962).

13. A. G. Streng, J. Am. Chem. Soc. 85, 1380 (1963).

14. A. R. Young, II, T. Hirata, and S. I. Marrow, ibid. 86, 20 (1964).

15. I. J. Soloman, R. I. Brabets, R. K. Uenishi, J. N. Keith, and J. M. Mc Donough, J. Inorg. Chem. 3, 457 (1964).

16. S. I. Marrow and A. R. Young, II, ibid. 4, 759 (1965).

17. C. D. agner and V. A. Campanile, Nucleonics 17, (7), 99 (1959).

18. Quad 200 Quadrupole Mass Spectrometer, Electronic Associates Inc., Palo Alto, California.

19. I. J. Soloman, Illinois Institute of Technology, Research Institute, private communication, October 1967, in press.

20. N. N. Greenwood, J. Chem. Soc., 3811 (1959).

21. N. Barlett and D. Lohman, J. Chem. Soc., 5253 (1962).

22. A. D. Kirshenbaum and A. V. Grosse, unpublished work under Air Force Contract No. AF04(611)-9555, Temple University, December 1965.

23. I. J. Soloman, et al, unpublished work under Air Force Contract No. AF49(638)-1175, Illinois Institute of Technology, Research Institute, December 1962.

# REVIEW OF ADVANCED INORGANIC OXIDIZERS

Edward W. Lawless and Robert J. Rowatt

Midwest Research Institute, Kansas City, Missouri

## I. Introduction

In this paper the properties and chemistry of advanced inorganic oxidizers will be reviewed with emphasis on recent developments. The classes of compounds will be limited to the oxygen fluorides, the nitrogen fluorides, the nitrogen fluoride oxides, the halogen fluorides and the halogen fluoride oxides. In general, all of the compounds described here are highly reactive, toxic materials, and very volatile except for ionic derivatives. The growth of chemistry involving O-F, N-F and Cl-F compounds has been remarkable: from about nil in 1946 to over 1000 today.

## II. Oxygen Fluorides and Derivatives

The reported oxygen fluorides, their derivatives and some of their properties are summarized in Table I. Oxygen difluoride is the only binary compound of this type which is stable at room temperature, but $O_2F_2$ is stable below about -80°C and is well characterized. A reasonably good understanding has been gained recently of the apparent equilibrium system $O_4F_2 \rightleftharpoons 2O_2F$.

The existence of $O_3F_2$ as a separate entity is in doubt, and the natures of the reported "$O_5F_2$" and "$O_6F_2$" are quite uncertain. Oxygen difluoride is commercially available, while the others are prepared by electrical discharge at low temperatures from appropriate $O_2$-$F_2$ mixtures.

The structures of $OF_2$ and $O_2F_2$ have been determined and are compared in Figure 1 with those of related compounds. The abnormally long O-F distance and the greatly shortened O-O bond in $O_2F_2$ have led Linett to formulate its structure as having an essentially four-electron O-O bond (as in $O_2$ itself, 1.21 Å bond length) and a one-electron O-F bond (resonating between the two positions). Dioxygen difluoride can, therefore, readily dissociate at the O-F bond to give F atoms and the stable $O_2F$ radical:

$$O_2F_2 \longrightarrow O_2F\cdot + F\cdot$$

and is an extremely energetic fluorinating agent. At low temperatures it is more reactive than fluorine itself and far more reactive than $OF_2$. The latter compound begins to decompose near 200°C and many of its reactions require activation by heat or light. The $O_2F\cdot$ radical can be generated by ultraviolet radiation of liquid $OF_2$, of $OF_2$-$O_2$, $F_2$-$O_2$ or $F_2$-$N_2O$ mixtures in a matrix, at 4°K, by the decomposition of $O_4F_2$ or $FSO_2OOF$, and in the reaction of $CF_4$ with $O_2$. The OF radical has never been detected in the gas or liquid phase despite an intensive search.

The reactions of the oxygen fluorides are usually simple fluorinations, but oxygen addition by $OF_2$ can occur especially in aqueous solution or in reactions

TABLE I

OXYGEN FLUORIDES AND DERIVATIVES

| Compound | Properties | | | | |
|---|---|---|---|---|---|
| | MP, °C | BP, °C | Decomp. Temp. | $^{19}F$ NMR[a] | Infrared[b] |
| OF· | Observed in $N_2$ or Ar matrix at 4°R | | | -- | 1028 |
| $OF_2$ | -223.8 | -144.8 | ~200 | -249 liq.<br>-248 g | 1740, 929, 909, 880, 826, 461 |
| $O_2F_2$ | -163.5 | -57 dec. | -78 | -865<br>-825 | 1024, 628, 463 |
| $O_4F_2 \rightleftharpoons 2O_2F\cdot$ | -191 | -80 ext | -183 | -- | 1519, 588 ($O_4F_2$)<br>1494, 484 ($O_2F\cdot$) |
| "$O_3F_2$" | -189 to 190 | -60 dec. | <-158 | -857 | -- |
| "$O_5F_2$" | <-196 | -- | -- | -- | -- |
| "$O_6F_2$" | <-213 | -- | -- | -- | -- |
| $CF_3OF$ | <-215 | -95 | -- | 72, -147 | 1282, 1259, 1223, 1217, 945, 880, 679 |
| $CF_2(OF)_2$ | -- | -62.5 | -- | -159 tr, +84.2 tr | 1300, 1270, 1150, 950 qt |
| $CF_3C(O)OF$ | -- | -21<br>-21.5 | -- | -- | -- |
| $SF_5OF$ | -86 | -35 | -- | -189 | 935, 888, 614, 585 |
| $NO_2OF$ | -175 | -45.9 | -- | -- | 1760, 1300, 920, 810, 708 |
| $ClO_3OF$ | -167.3 | -15.9 | -- | -226 | 1298, 1049, 666 |
| $FSO_2OF$ | -158.5 | -31.3 | -- | -244.9, -36.2 | -- |
| $CF_3OOF$ | -- | -50 (est) | -- | +69.2 db, -291.5 qt | 1290, 1175, 955, 755, 725 |
| $C_2F_5OOF$ | -- | -15 (est) | -- | +84.1 db of tr ($CF_3$)<br>+97.4 db of qt ($CF_2$)<br>-291.6 tr of qt | 1380, 1285, 1235, 1175, 740 |
| $FSO_2OOF$ | -- | 0 | -- | -- | -- |

a/ $^{19}F$ chemical shift (ppm vs. $CFCl_3$=0) for fluorine of -OF group.
b/ Positions ($cm^{-1}$) for O-F stretching fundamental.

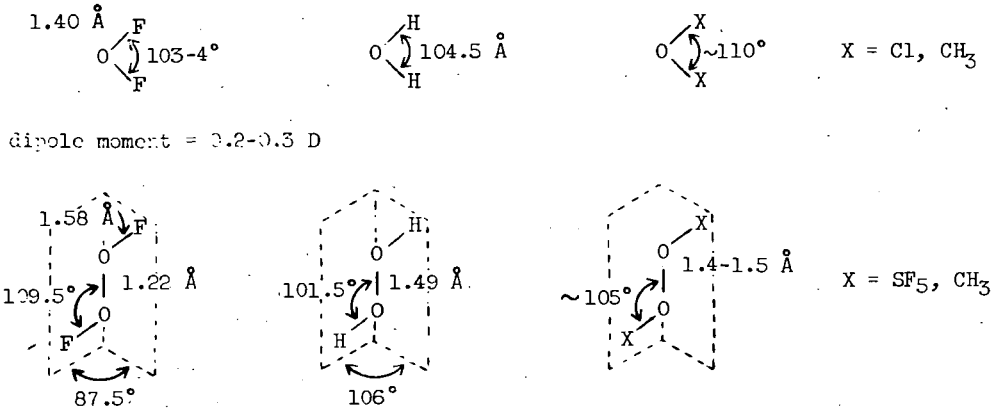


Figure 1 - Comparison of Structures of $OF_2$, $O_2F_2$ and Related Compounds

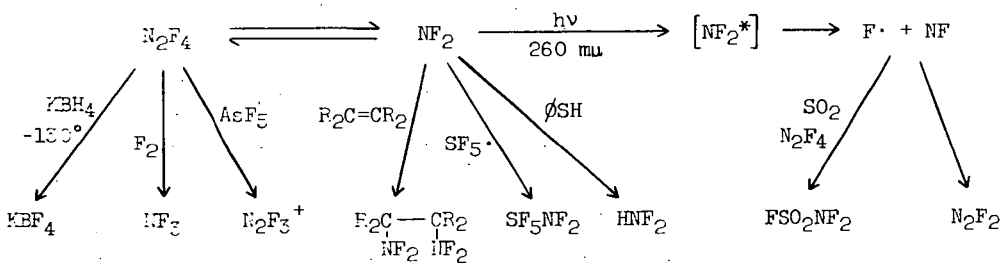


Figure 2 - Examples of Reaction Types for $N_2F_4$

with some nitrogen, chlorine, or sulfur-containing materials. Dioxygen difluoride (or the $O_2F$ radical) undergoes the fluoride abstraction reaction with strong Lewis acids at low temperatures to give stable dioxygenyl salts. Oxygen difluoride undergoes a similar reaction at elevated temperatures.

$$O_2F_2 + BF_3 \xrightarrow{-140^\circ} O_2BF_4 + 1/2F_2$$

$$2OF_2 + SbF_5 \xrightarrow{200^\circ} O_2SbF_6 + F_2$$

Although considerable doubt now exists about the existence of trioxygen trifluoride, the trifluoromethyl derivative $CF_3OOOCF_3$ is known as well as the peroxide $CF_3OOCF_3$. The authors are not aware of reports of the simple ether $(CF_3)_2O$, although the sulfide $(CF_3)_2S$ is stable at 400°C.

## III. Nitrogen Fluorides and Derivatives

The reported nitrogen fluorides, their derivatives and some of their properties are summarized in Table II.

The NF molecule is known only as a reactive intermediate which dimerizes readily to $N_2F_2$. It has been observed by flash photolysis of the $NF_2$ radical in an argon matrix at 4°K and by pyrolysis of $N_2F_4$ at high dilution in argon at 2550°K.

The $NF_2$ radical is well established to exist in equilibrium with $N_2F_4$ in analogy to the $N_2O_4$-$NO_2$ equilibrium

$$N_2F_4 \rightleftharpoons 2NF_2$$

The structure of $NF_2$ (N-F = 1.36 Å; ∠FNF = 103°) is closely related to that of $NF_3$. The $NF_2$ radical has fundamental stretching frequencies at 1074 and 935 $cm^{-1}$ in the infrared. In the ultraviolet, $NF_2$ absorbs at 260 mμ to give an excited radical, $NF_2$*, which decomposes to NF and F·, but may undergo unique reactions. The reactions of $NF_2$ are discussed in the section on $N_2F_4$.

Nitrogen trifluoride is commercially available and its properties are well known. It has an ammonia-like structure with N-F = 1.37 Å and ∠FNF = 103°. Only 57 kcal/mol are required to dissociate a F· atom from $NF_3$, but an average of 71 kcal/mol are required for each of the remaining two N-F bonds of the stable $NF_2$ radical. $NF_3$ is relatively unreactive at mild temperatures, but functions as a fluorinating agent at elevated temperature. The most interesting reaction of $NF_3$ to be reported recently is that with fluorine and Lewis acids to give stable salts of the $NF_4^+$ ion.

$$NF_3 + F_2 + AsF_5 \xrightarrow[-80^\circ]{\text{elect. disc.}} NF_4^+AsF_6^-$$

$$NF_3 + F_2 + SbF_6 \xrightarrow[3000\ psi]{300^\circ} NF_4^+SbF_6^-$$

Difluorodiazine is now well established to exist in the cis and trans isomeric forms and the properties and structures of each are known.

TABLE II

NITROGEN FLUORIDES AND DERIVATIVES

| Compound | MP, °C | BP, °C | $^{19}F$ NMR | IR |
|---|---|---|---|---|
| $NF_2$ | -- | -- | -- | 1070, 931 |
| $NF_3$ | -208.5 | -129 | -142 | 1031, 1010, 907, 642 |
| $N_2F_2$ (cis) | -195 | -105.7 | -129 | 1524db, 952tr, 896db, 737tr |
| (trans) | -172 | -111.4 | -88 | 989 (1996m, 1581m, 1434m) |
| $N_2F_4$ | -164.5 | -73 | -58 | 1010, 998, 959, 946 |
| $N_3F$ | -154 | -82 | -- | -- |
| $NFO$ | -132.5 | -59.9 | -479 | 1844, 766, 521 |
| $NFO_2$ | -166 | -72.5 | -393 | 1793, 1312, 822, 742, 570 |
| $NF_3O$ | -160 | -85 | -363 | 1687, 887, 743, 528 |
| $NF_2NO$ | -- | dec. | -65 | -- |
| $HNF_2$ | -116 ± 3 | <23.6 | 6 | 3193w, 1428db, 1280db, 978db |
| $ClNF_2$ | -183 | -67 | -141 | 920tr, 853db, 694tr |
| $Cl_2NF$ | -10 to 0 (est.) | | -- | -- |
| $N_2F^+$ | | | -103 | 1050 |
| $N_2F_3^+$ | | | -144 (db.) | 1521, 1304, 1128, 924, 518, |
| | | | -192 | 497 |
| $NF_4^+$ | | | -214.7 (tr.) | 1163, 611 |
| $NF_2O^+$ | | | -331 | 1857, 1162, 905 |

Other derivatives include compounds of the types: $MNF_2$ (M = $SF_5$-, $SF_5O$-, $CF_3SF_4$-, $FSO_2$-, $FSO_2O$-, $CF_3S$-); $R(NF_2)_X$ (R = $R_f$, alkyl, anthracene, etc.; X = 1-4); R-C(=NF)-R'; and R-N(O)=NF.

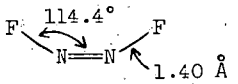


1.21 Å 0.17 D

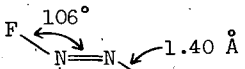


1.22 Å

The N-F bond is lengthened over that in $NF_3$ and the N=N bond is shortened compared to that (1.24 Å) in $N_2(CH_3)_2$. The N-F and N=N bond energies of the trans form is 68 and 109 kcal/mol, respectively. The trans $N_2F_2$ is conveniently prepared by reaction of $N_2F_4$ at low pressure with $AlCl_3$ at -80°. The trans form is converted to the cis form in over 90% yield at 75° in a well-passivated stainless steel cylinder. The $N_2F_2$ is obtained nearly quantitatively by the decomposition at 20° of the complex $KF \cdot HNF_2$ formed at -80°C. Difluorodiazine has also been offered commercially. The cis $N_2F_2$ is more reactive chemically than trans $N_2F_2$, but both can act as fluorinating agents. The so-called N=N double bond is unusually inert and does not undergo addition reactions. Detonations, especially with the cis isomer, have occurred upon application of high pressure. The fluorination of $N_2F_2$ to $N_2F_4$ has apparently not been reported. cis-$N_2F_2$ undergoes the fluoride abstraction with Lewis acids to give a stable salt of the $N_2F^+$ ion

$$N_2F_2 + AsF_5 \longrightarrow N_2F^+AsF_6^-$$

The trans isomer also gives this reaction with $SbF_5$.

Tetrafluorohydrazine has the structure in the gas phase on the left below (d and l isomers) but the symmetrical isomer on the right has also been observed in the liquid at low temperature.

| | |
|---|---|
| N-F | 1.39 Å |
| N-N | 1.53 Å |
| ∠ FNF | 104° |
| ∠ NNF | 102° |
| dihedral angle | 69° |
| $^{19}F$ NMR | -65.2, -53.2, -44.0, -31.9 ϕ |
| (in $NF_3$ at -155°) | |

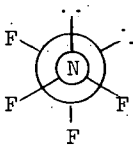


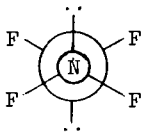


-60.4 ϕ

The abnormally long N-N bond (compared to 1.45 Å in $N_2H_4$) has a low dissociation energy (20 kcal/mol) and $N_2F_4$ exists in equilibrium with stable $NF_2$ radicals. Tetrafluorohydrazine has been available commercially since 1960 and its reactions have been studied intensively. It enters into at least five types of reactions: (1) normal $NF_2$ radical reactions including addition to olefins or a second radical, and abstraction reactions; (2) excited $NF_2$ reactions resulting from photolysis at about 260 mμ; (3) fluorination (oxidation) reactions; (4) reduction reactions; (5) fluoride abstraction reaction. Examples of each are illustrated in Figure 2.

Trifluoramine oxide, $NF_3O$, was reported in 1965. It can be prepared by electric discharge at -196° in mixtures of $NF_3$ and $O_2$ or $OF_2$, by the flame fluorination of NO with fast quench, or more conveniently at 25° by the fluorination of NO with $F_2$ photochemically or with certain metal hexafluorides such as $IrF_6$. The $NF_3O$ has a tetrahedral structure in which the N-F and N → O bonds are slightly

weaker than those in $NFO_2$. The $NF_3O$ has good thermal and hydrolytic stability, but undergoes the fluoride abstraction reaction with strong Lewis acids, to give salts such as $NF_2O^+AsF_6^-$, and adds to perfluoroolefins (under $BF_3$ catalysis) to give stable $R_fONF_2$ compounds. It apparently reacts slowly with NO to give NOF.

Difluoramine has an ammonia-like structure with the following parameters: N-H, 1.03-1.08; N-F, 1.38; FNF, 103°, HNF, 102°; dipole moment, 1.93 D. It is best prepared from difluorourea (which is obtained by aqueous fluorination of urea) by treatment with $H_2SO_4$ at 90° or by the reaction of $N_2F_4$ with $C_6H_5SH$ at 50°. The $HNF_2$ is stable and can be stored, but the usual procedure is to generate it as needed and pass it directly into a reaction vessel, since it has a tendency to explode when frozen. The reactions of $HNF_2$ are usually complex, but it undergoes three general types of reactions as follows: oxidation, for example with aqueous $Fe^{+3}$ solution to give $N_2F_4$ (perhaps the $NF_2^-$ ion is involved); reduction, as in the reaction with aqueous HI to give $NH_4F$ and HF; complex formation with ethers, Lewis acids, and metal fluorides.

Chlorodifluoramine $ClNF_2$ is well known, $Cl_2NF$ and $BrNF_2$ are known as unstable compounds, and the other halogen fluoramines appear to be very unstable. The $ClNF_2$ (or $BrNF_2$) can be prepared by the reaction of aqueous NaOCl (or NaOBr) with N,N-difluorourea or N,N-difluorosulfuryl amide. The $Cl_2NF$ is prepared by the reaction of ClF with $ClN_3$ at 25°C or with $NaN_3$ at 0°. The $ClNF_2$ is stable but dissociates readily to give Cl atoms and $NF_2$ radicals (which defines the reaction chemistry) while $Cl_2NF$ is explosively unstable in the liquid state.

A few remaining N-F compounds such as $NF_2NO$ and $N_3F$ are of limited interest, but a number of inorganic compounds and a host of organic compounds have been prepared in recent years in which $NF_2$ groups may be regarded as substituents, e.g., $SF_5NF_2$, $C(NF_2)_4$, $C(NF)(NF_2)_2$, $CF_3ONF_2$ and $CF_3N(O)=NF$.

A summary of the interconversions of the nitrogen fluorides is found in Figure 3.

## Chlorine Fluorides and Related Compounds

The halogen fluorides of prime interest as propellant oxidizers have been $ClF_3$, $ClF_5$, $ClO_3F$ and $BrF_5$, but a number of other halogen fluorides have been studied. Properties of halogen fluorides are summarized in Table III.

Chlorine monofluoride appears to have considerable ionic character as reflected in the $^{19}F$ NMR chemical shift of $\phi$ = +441 ppm (vs. $CFCl_3$). The Cl-F bond distance is 1.63 Å, the dipole moment, 0.88 D, the bond dissociation energy, 60.4 kcal/mol, and the heat of formation, -13.5 kcal/mol. The ClF is an energetic fluorinating agent. It reacts with fluorides such as CsF or NOF to give $Cs^+ClF_2^-$ and $NO^+ClF_2^-$, respectively, and has been reported to react with the Lewis acid $AsF_5$ to give $Cl^+AsF_6^-$ but substantiating evidence is lacking. The high volatility of ClF (b.p. -100°C) suggests that little or no association or self-ionization (to $Cl^+$ and $ClF_2^-$ ions or to $Cl_2F^+$ and $ClF_2^-$ ions) exists, but the electrical conductivity is higher than that of $ClF_3$. Chlorine monofluoride is prepared by reaction of $ClF_3$ and $Cl_2$.

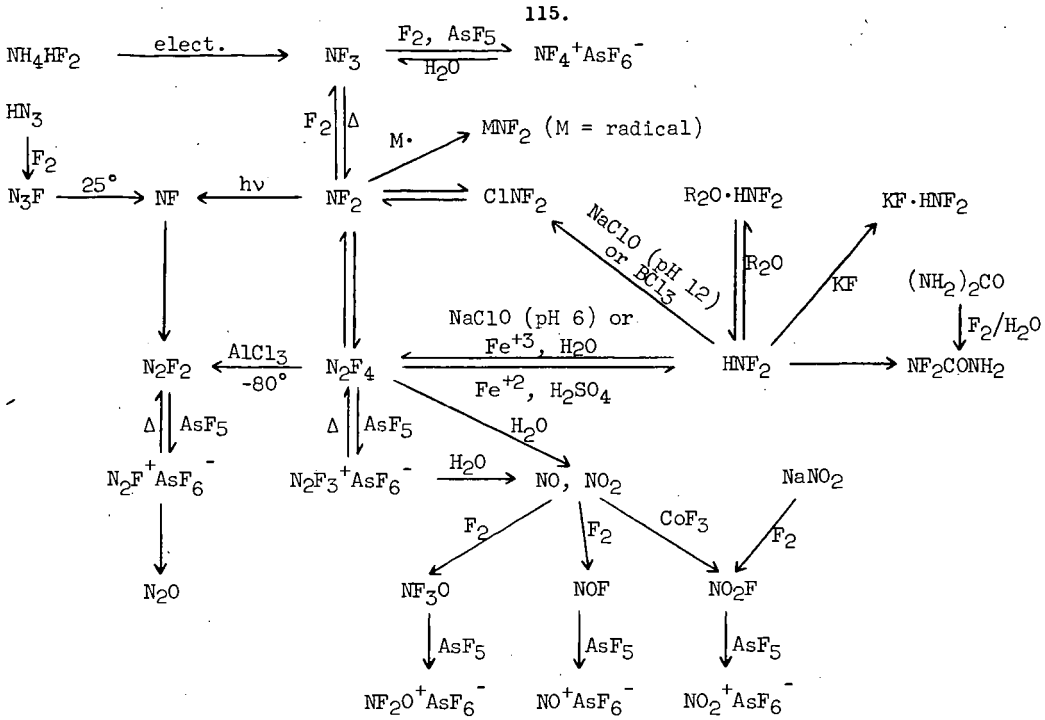


Figure 3 - Interconversion of Nitrogen Fluorides

TABLE III

PROPERTIES OF HALOGEN FLUORIDES AND DERIVATIVES

| Compound | MP, °C | BP, °C | NMR | IR |
|---|---|---|---|---|
| ClF | -154 ± 5 | -100.8 | 440 | 793, 785 |
| $ClF_3$ | -76.3 | 11.75 | -14(a), -123(e) | 761, 746, 713, 694 |
| $ClF_5$ | -103 ± 4 | -14 | -412(a), -247(e) | 786, 732, 541, 486 |
| $BrF_3$ | 8.8 | 127 | 39 | 674, 613, 384, 300 |
| $BrF_5$ | -60.5 | 40.8 | -132(e) | 683, 644, 587, 369 |
| $IF_5$ | 8.5 | 97.0 | -53(a), -4(e) | 710, 640, 318 |
| $IF_7$ | 4.8[a] | 4 (1 atm.) | -177 (-168) | 670, 547, 426, 368, 250 |
| $ClO_2F$ | above -115 | -6 | -329 (330) | 1270, 1259, 1104 (pqr) 632, 548 |
| $ClO_3F$ | -146 | -46.8 | -287 | 1315-1300, 725, 717, 714, 590 |
| $IF_5O$ | 4.5 | -- | -- | -- |

a Triple point 6.4.

Chlorine trifluoride is usually described as having a T-shape, but is better regarded as a trigonal bipyramid derivative. The two apical Cl-F bonds are elongated (1.70 Å) compared to the equatorial Cl-F bond (1.60 Å). The bond angles are 87.5° and 175°. The $^{19}F$ NMR of gaseous $ClF_3$ shows the apical fluorines to be further downfield (-145.6 ϕ) than the equatorial fluorine -19.7 ϕ. In liquid $ClF_3$ (with HF carefully removed) the resonances are -159.0 and -21.8 ϕ. The high dipole moment determined with the liquid (1.00-1.03 D) compared to that in the gas (~ 0.6 D) suggests considerable interaction and the relatively low volatility (b.p. 12°) confirms this, but the electrical conductivity shows that this interaction is essentially not in the form of self-ionization to $ClF_2^+$ and $ClF_4^-$ ions. Evidence for some dimerization in the gas has been suggested. However stable salts of both of these ions are known, e.g., $ClF_2^+SbF_6^-$ and $Cs^+ClF_4^-$. Chlorine trifluoride is commercially available in quantity, being prepared by fluorination of chlorine. It is an extremely vigorous fluorinating agent, but can in turn be fluorinated to $ClF_5$ under pressure. Moisture converts $ClF_3$ to $ClO_2F$ and $ClO_2$.

Chlorine pentafluoride is the newest member of the halogen fluoride family and has very recently become available commercially in laboratory quantities. It is prepared by the high pressure fluorination of $ClF_3$ or a salt such as $CsClF_4$ at 150° or above. It has also been prepared by the fluorination of $ClF_3$ under ultraviolet radiation or electric discharge at low temperatures and by platinum hexafluoride. The structure of $ClF_5$, a square pyramid, is an octahedral derivative with the apical Cl-F bond length of 1.62 Å and the equatorial bonds 1.72 Å. The $^{19}F$ chemical shifts are -412 ϕ (apical fluorine) and -247 ϕ (basal fluorines). The former is one of the most unshielded fluorine atoms known, being exceeded only by those in $F_2$, $O_2F_2$, and NOF. The dipole moment is probably 0.2-0.4 D. The boiling point indicates very little interaction exists in the liquid and self-ionization is not expected. The $ClF_4^+$ ion is an intense peak in the mass spectrum and the possibility of obtaining

stable salts such as $ClF_4^+SbF_6^-$ appears reasonably good. The addition of fluoride ion to $ClF_5$ to give $ClF_6^-$ does not appear likely (although $BrF_6^-$ salts have been reported) since the chlorine atom would be pseudo-heptacoordinate and this type of coordination is without precedence in elements of the second row of the Periodic Table.

The structures of $ClF_3$, $ClF_5$, and $ClO_3F$ have been determined and are shown below.

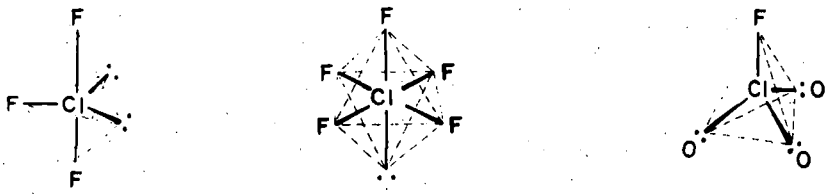


The commercially available higher halogen fluorides are $BrF_3$, $BrF_5$ and $IF_5$, with $IF_7$ available on special order. Bromine trifluoride is structurally and chemically very similar to $ClF_3$ except that self-ionization is extensive in liquid $BrF_3$:

$$2BrF_3 \rightleftharpoons BrF_2^+ + BrF_4^-$$

Bromine trifluoride has therefore an exceptionally high boiling point (126°) and electrical conductivity. It is an excellent solvent for many ionic materials. Stable salts of both the $BrF_2^+$ and $BrF_4^-$ ions are known, but in some instances with $BrF_2^+$ the complexes may be fluorine bridged rather than truly ionic. Bromine pentafluoride and iodine pentafluoride are also structurally similar to $ClF_5$. Self-ionization occurs to an appreciable extent in $IF_5$, but far less in $BrF_5$.

$$2IF_5 \rightleftharpoons IF_4^+ + IF_6^-$$

Stable salts have been reported for $BrF_4^+$ and $BrF_6^-$ as well as for $IF_4^+$ and $IF_6^-$, but structural studies are incomplete. Unlike $BrF_5$ or $ClF_5$, $IF_5$ undergoes fluorine exchange with HF. The $BrF_3$ and $BrF_5$ are quite energetic fluorinating agents. While $IF_5$ is a considerably milder fluorinating agent, it inflames or forms explosive mixtures with many organics. It can be dissolved in excess of such solvents as sulfolane, but forms crystalline complexes with certain oxygenated solvents such as dioxane.

Iodine heptafluoride is formed by the reaction of $IF_5$ with $F_2$ at about 100°. The dissociation of $IF_7$ to $IF_5$ and $F_2$ sets in at higher temperatures, ~300°, and $\Delta H_{dissoc}$ is 28.5 kcal/mol. The structure of $IF_7$ in the gas phase is the pentagonal bipyramid, but the structure in the solid is still uncertain. The $^{19}F$ NMR of the gas is a singlet ($\phi$ = -336 ppm) suggestiong intramolecular exchange. (The spectrum of the liquid is a doublet at lower temperatures, a singlet at higher temperatures because of quadrapole effects.) The symmetrical structure of $IF_7$ gives it an extremely short (~2°) liquid range (sublimes, 4.77°; triple point, 6.45°). The reaction of $IF_7$ as a fluorinating agent are much more vigorous than those of $IF_5$. With strong fluoride acceptors $IF_7$ forms salts such as $IF_6^+AsF_6^-$. No reaction to

form such salts as $Cs^+IF_8^-$ have been reported, but the fluorine exchange which occurs between HF and $IF_7$ in the gas phase may involve a $HIF_8$ or a $IF_6HF_2$ intermediate.

The halogen fluoride oxides of major interest are $ClO_2F$ and $ClO_3F$, but $BrO_2F$, $IO_2F$ and $IF_5O$ have been characterized. Only perchloryl fluoride, $ClO_3F$, is commercially available. Chloryl fluoride, $ClO_2F$, is readily prepared by allowing $ClF_3$ or $ClF_5$ to stand with excess of a chlorate or chlorite salt in a Monel cylinder:

$$2ClF_3 + 3NaClO_3 \xrightarrow{25°} 3ClO_2F + 3NaF + Cl_2 + 1.5O_2$$

$$ClF_5 + 3NaClO_2 \xrightarrow{25°} 2ClO_2F + 3NaF + Cl_2 + O_2$$

(The $O_2$ and $Cl_2$ are removed at -80°.) The $ClO_2F$ is also formed by the reaction of $ClF_3$ or $ClF_5$ with traces of moisture, but is in turn readily hydrolyzed with additional water. The $ClO_2F$ is isoelectronic with $PF_3$ and $SF_2O$ and should have approximately the same structure, i.e., a tetrahedral arrangement with an electron pair at one apex. The $^{19}F$ NMR shows the fluorine atom far downfield, $\phi$ = -332 ppm. This structure makes $ClO_2F$ an extremely reactive oxidizer. It is in turn fluorinated only with difficulty to $ClF_5$. The $ClO_2F$ undergoes the fluoride abstraction reaction to give stable salts such as $ClO_2^+AsF_6^-$, but efforts to form such salts as $Cs^+ClF_2O_2^-$ have not been successful. Pyrolysis of $ClO_2F$ at 300° and 0.5 atm. pressure gives ClF and $O_2$ apparently via an intermediate ClFO species.

Perchloryl fluoride has a closed tetrahedral structure with the approximate parameters: Cl-F, 1.55-1.60 Å; Cl→O, 1.40 Å, dipole moment 0.023 D. The $^{19}F$ NMR shows the fluorine at $\phi$ = -287 ppm. The structure of $ClO_3F$ gives it considerable kinetically derived stability and it is relatively unreactive at mild temperatures, e.g., it does not hydrolyze, or react with sodium. Above 150° $ClO_3F$ is a potent oxidizer for most organics and attacks many metals in the presence of moisture. Attempts to react $ClO_3F$ with fluoride acceptors such as $AsF_5$ have not led to stable salts, but the $AlCl_3$-catalyzed reaction of $ClO_3F$ with aromatics (to give $ArClO_3$ compounds) likely involves an intermediate $ClO_3^+$ ion. No reaction between CsF and $ClO_3F$ has been effected and $ClO_3F$ is quite resistant to fluorination. With $NH_3$, $ClO_3F$ is converted to $NH_4^+NHClO_3^-$, from which metal salts such as $KNHClO_3$ and $K_2NClO_3$ can be prepared. All of these salts are shock sensitive. Perchloryl fluoride is generally quite soluble without reaction with other oxidizers and has a small (0.5-5 g/liter) solubility in organic solvents and water.

Bromyl fluoride $BrO_2F$ (formed by the reaction $KBrO_3$ or $BrO_2$ and $BrF_5$ at -50°) is thermodynamically unstable and has been studied very little. Of the reported iodine fluoride oxides, only $IF_5O$ appears to be unequivocally established as a molecular entity. It is readily formed by reaction of $IF_7$ with traces of moisture or with glass and has a relatively low reactivity because of the nearly octahedral structure. The remaining iodine fluoride oxides, $IF_3O$, $IO_2F$ and $IO_3F$ are all white crystalline solids and may not be molecular entities. The "$IF_3O$" and "$IO_2F$" can be prepared by reacting $I_2O_5$ respectively with $IF_5$ and $F_2$. The pyrolysis of $IF_3O$ gives $IO_2F$ and $IF_5$ and the observed reversibility of this reaction suggested the ionic structure $IO_2^+IF_6^-$ for $IF_3O$. The $IO_2F$ may exist in a bridged form or possibly in the ionic form, $IO_2^+IF_2O_2^-$, since stable salts of both of these ions are formed. The $IO_3F$ (formed by fluorination of periodic acid in HF) is reported to undergo hydrolysis slowly and thus may in fact be structurally analogous to $ClO_3F$.

Suggestions for Additional Reading

1. Streng, A. G., Chem. Revs., 63, 607-24 (1963), "The Oxygen Fluorides."

2. Hoffman, C. J., Chem. Revs., 64, 91-8 (1964), "Organic and Inorganic Hypofluorites."

3. Schmeisser, M., and K. Brandle, in Advances in Inorganic Chemistry and Radiochemistry, Edited by A. J. Emeleus and A. G. Sharpe, Vol. 5, Academic Press, New York, 1963, pp. 42-84, "Halogen Oxides."

4. Colburn, C. B., in Advances in Fluorine Chemistry, ed., M. Stacey, J. C. Tatlow and A. G. Sharpe, Vol. III, Butterworths, 1962, "Nitrogen Fluorides."

5. Hoffman, C. J., and R. G. Neville, Chem. Revs., 62, 1-18 (1962), "Nitrogen Fluorides."

6. Pankratov, A. V., Russian Chemical Reviews, 32, 157 (1963), English, "Chemistry of Some Inorganic Nitrogen Fluorides."

7. George, J. W., Progress in Inorganic Chemistry, Vol. 2, pp. 33-107, Interscience, 1960, "Halides and Oxyhalides of the Elements of Groups Vb and VIb."

8. Musgrave, W. K. R., in Advances in Fluorine Chemistry, Vol. 2, Butterworths, 1960, pp. 1-28. Preparation and uses of halogen fluorides.

9. Wiebenga, E. H., E. E. Havinga and K. H. Boswijk, in Advances in Inorganic and Radiochemistry, Academic Press, 1961, pp. 133-70. Review on structure of interhalogen and polyhalide ions.

10. Clark, H. C., Chem. Revs., 869-94 (1958). Chemical and physical properties of halogen fluorides.

11. Woolf, C., in Advances in Fluorine Chemistry, ed. 5, Butterworths, 1965, "Oxyfluorides of Nitrogen."

12. Kemmett, R. D., and D.W.A. Sharp in Advances in Fluorine Chemistry, Vol. 4, Butterworths, 1965, "Fluorides of the Main Group Elements."

13. Stein, L., in Halogen Chemistry, edited by V. Gutmann, Vol. 1, Academic Press, 1967, "Physical and Chemical Properties of Halogen Fluorides."

# DETONABILITY TESTING AT NONAMBIENT TEMPERATURES AND PRESSURES

A. B. Amster, J. Neff, D. B. Moore, and R. W. McLeod

Stanford Research Institute, Menlo Park, California

## ABSTRACT

The generally adopted method for measuring the susceptibility of sensitive liquids to shock is described by the Chemical Propellant Information Agency in the publication "Liquid Propellant Test Methods."[1] The recommended test is limited to use under ambient conditions of temperature and pressure and relies only upon the damage to a witness plate as the criterion for detonability. This report discusses modifications to the test procedure which retain sample size and geometry but permit studies over the ranges of 77°K to 373°K at 1 atm to 10 atm. This broader applicability reduces the value of witness plates--always somewhat dubious. Therefore two other methods have been evaluated, both of which measure detonation velocity: one is electronic, and the other utilizes an explosive witness. The revised test satisfies the requirements for an extended range sensitivity test for use with high energy liquids.

## I. INTRODUCTION

High energy liquids are often exposed to conditions, such as extremes of temperature and pressure, which may change their susceptibility to shock initiation. Moreover, many high energy materials are condensed only under such extreme conditions. There exists a need for a detonation sensitivity test applicable to these situations. This report describes equipment and outlines procedures to adapt the current JANAF test[1] for use under the following conditions:

$$77^{\circ}K < T < 373^{\circ}K$$

$$1 \text{ atm} < P < 10 \text{ atm}$$

The two methods used measure detonation velocity, in contrast to the JANAF method which utilizes only damage to a witness plate to determine whether detonation occurred. The first (and perhaps the simpler) technique is an adaptation of D'Autriche's method.[2] In this method, shown schematically in Fig. 1, the detonation velocity of the unknown sample in the test cup is compared with that of an explosive sheet of

known detonation velocity on the witness plate. The tetryl booster initiates the mild detonating fuze (MDF) which in turn initiates the explosive sheet at the "start" position. This detonation propagates farther along each finger of the explosive sheet. The other end of each finger of the explosive sheet is initiated via the detonation probes by the strong wave traveling through the test cup. The detonation waves that collide within the fingers of the sheet explosive create dents in the witness plate that are deeper than those left by a unidirectional wave. The result of a typical shot is shown in Fig. 2. From the position of the dents and the properties of the system, the wave velocity within the sample can be calculated (see Appendix A). Although a strong wave from the tetryl booster traveling through the liquid or the cup may initiate the probes, detonation is detected by a constant velocity.

The second method utilizes a resistance wire in the detonation cup and a constant current power supply to provide a continuous detonation velocity record on an oscilloscope. This method is considerably more precise. It requires a modest amount of electronic equipment and considerable skill on the part of the user. The equipment and operating procedures are adequately described elsewhere[3] for solid explosives; modifications for adaptation to liquid testing under the conditions described above are included in this report.

Details of either method will vary with the properties (e.g., toxicity, vapor pressure, etc.) of the compound tested. In the following paragraphs, procedures employed with two compounds ($N_2F_4$ at low temperatures and $C_2H_5ONO_2$ at elevated temperatures) are described; other materials may require changes in design and in operational procedures.

Before attempting to determine the detonability of high energy materials it is important that persons who lack experience with explosives be thoroughly educated in the safe handling of explosives. Reference 1 lists many of the standard references for explosive handling. It is imperative that heated or cryogenic pressurized systems be considered as less predictable than systems at ambient conditions until detonation parameters are firmly established. Remote handling should be the rule because, even though the test liquid may not be extremely sensitive, sensitization of the booster and explosive train may occur. High energy oxidizers may also ignite the explosive train and cause premature detonations.

## II. TEST EQUIPMENT

### A. Cup

The liquid under test is held in a cylindrical metal cup closed at one end with a metal diaphragm soldered in place; the other end (the

top) is closed with caps which contain instrument probes. The cup is fabricated as follows: Each end of a section of 1" Schedule 40 extruded steel pipe (or other metal compatible with the test liquid) is faced on a lathe to an overall length of 6.0".

For the modified D'Autriche method, the cup is prepared as shown in Fig. 3. A 2.0-mil-thick stainless steel diaphragm 2" in diameter is centered and silver-soldered on the bottom of the cup. If the cup is to contain a cryogenic, toxic material or a substance which is not compatible with the atmosphere, the top must be sealed and special transfer lines must be installed.

For materials that are transferred in vacuum lines, the cups are threaded with 1" standard taper pipe threads. Two holes are drilled 3/8" below the last thread to accommodate 1/4" o.d. tubing. Two 1' pieces of 1/4" o.d. tubing are soldered in the holes so that the soldered ends are flush with the inner wall of the cup.

B. Caps

The caps, prepared from 1" pipe caps, support the necessary instrument probes for temperature measurement, liquid level sensors[4] and the continuous wire probes. The simplest test, using the modified D'Autriche method with a liquid such as ethyl nitrate which can be poured into the cup, requires only a pipe cap and no probes. For materials to be tested at nonambient conditions and to be transferred in a vacuum line (cryogenic materials and toxic materials) or for tests utilizing the continuous wire, instrument probes are installed in the cap.

For installing thermowells, a 1/8" hole is drilled into the cap and a length of 1/8" tubing extended through the cap. This tubing is cut and positioned to extend no farther into the cup than 2" above the bottom diaphragm when assembled and soldered to the cap. The bottom of the thermowell is closed and sealed with solder. The end outside the cup is left open for inserting thermocouples; a series of couples at different levels may serve as liquid level sensors. For caps that require resistance wire leads or thermistor leads, holes are drilled in the cap to accommodate insulated metal-to-ceramic electrical leadthroughs. These seals are soldered in place, preferably with a lower melting solder than that used for the thermowell. Two such seals, or a double seal, can accommodate a thermistor.

For the resistance wire and supporting bow, two holes are drilled in the cap. One, in the center of the cap, is drilled to contain an insulated electrical leadthrough. Approximately 1/4" from the center of the cap, another hole is drilled to hold the resistance wire support. This support is fabricated from a 1/16" rod long enough to extend through the cap into an assembled cup to a distance of less than 1" from the diaphragm. Both the rod and the electrical leadthrough are soldered in place. At a distance of 1/2" from the end, the rod is bent 90° toward the center of the cap. From the end of this rod to the electrical lead

on the cap, a length of 1-mil resistance wire is strung and the wire is anchored well at both positions to give good electrical contact. An assembled cup showing modifications for both the D'Autriche method and the continuous wire method is shown in Fig. 3. It is not necessary that all parts shown be used in every test.

C. Temperature Control of Cup

Under nonambient conditions it is advisable to use liquid baths around the test cups to control temperature along the entire cup. A convenient way to attach a leakproof metal container around the cup is to cut a 1-1/2" hole in the bottom of a high 6" diameter metal can and to solder the overlapping diaphragm of the detonator cup into the hole as shown in Fig. 3. Commercial 3-lb coffee cans have been satisfactory.

Above ambient temperatures, the bath is heated with heating tapes or inexpensive immersion heaters. For cryogenic materials, the cup is filled with the appropriate coolant--dry ice, liquid nitrogen, liquid argon, liquid oxygen, etc. Insulating materials may be used around the bath.

D. Bath Materials

It is extremely important to give careful consideration to the bath materials because they must be inert to all materials used in the shot. Oil baths are likely to contribute to fire hazard; spilled solvents or vapors may react with or sensitize the explosive train materials, and mixtures of solvents may be detonable.

E. Detonator and Booster

An explosive wire detonator is followed by 18" of Primachord. The Primacord in turn is followed by a small RDX pellet and the booster. The booster charges used for the temperature range from -196 to 100°C consist of two 1" x 1-5/8" diameter tetryl pellets, density about 1.56. For the higher temperature (100° to 150°C), higher melting HMX pellets may be substituted (m.p. 270° to 280°C).

F. Detection Equipment

1. Resistance Wire Method

The procedure for determining detonation velocity is fully described in Reference 3.

2. D'Autriche Probe Assembly

For each shot a test cup is prepared as shown in Fig. 3 and aluminum witness plates are prepared as shown in Fig. 4a. Using a razor blade,

five pieces of MDF, each 20.00" long, are cut on a piece of wood or Micarta. Five 1/2"-wide strips of sheet explosive are also cut, one about 4" long and the others 8.00". Using precise scales and squares, the short strip is cemented parallel to the short edge of the plate with one end over the single hole. The long strips are cemented parallel to each other, one end over each of the remaining four holes and the other end over and in contact with the short strip (see Figs. 4b and 5).

The test cup and booster are assembled as shown in Figs. 1 and 5 and the witness plate is secured nearby. One end of each of the 20" lengths of MDF is inserted through a hole in the plate until it contacts the explosive sheet (Fig. 4b). The other ends are put in place on the charge (no auxiliary booster is used) as shown in Figs. 1 and 5, four or more along the cup wall and one to the initiator. All ends are cemented securely in place.

G. Support Stand for Detonator, Charge, and Cup

A suitable frame is constructed to support the assembled charge. The detonator, booster, and cup are aligned and held in place with adhesive tape. The assembled shot and cup are later placed on the support stand and tied into place with adhesive tape. At elevated temperatures a noncombustible tape should be used.

H. Vacuum Transfer Equipment

For remote handling of volatile, toxic, or cryogenic materials which cannot be conveniently transfered in a simpler manner, a vacuum system is constructed (see Fig. 6). This system, which is suitable for fluorine oxidizers, was used for testing the detonability of $N_2F_4$. A fluorine tank is used for passivation of the system before testing high energy fluorine oxidizers. The system is designed to permit isolation of the supply tank from the detonator test cup to prevent possible detonation through the lines to the main supply tank. The lines are flushed with an inert gas after the transfer is completed. The system also contains a measuring bottle of sufficient volume, when filled with test material at a predetermined pressure, to exactly fill the cup with condensed liquid.

To prepare the system, the valves and other parts (components are described below) are completely disassembled and each is cleaned. Defective gaskets and parts are replaced. If the valves are to be soldered or welded to the transfer lines, the gaskets are left out of the valves until this operation is complete. To remove borax-type fluxes it may be necessary to steam-clean the soldered joints. Valves 1 through 6 (Fig. 6) and the solenoid operators are assembled and mounted on a small portable metal panel; enough tubing (1 to 2 feet) is attached to valves that lead to other components, tanks, pumps, and gauges so that connecting lines can later be installed on these ends without interrupting the

valve-panel system. This section should be leak tested before final assembly at the test site.

1. Vacuum Equipment Components

Valves 7 and 10 (Fig. 6) are Chlorine Institute valves available from Superior Valve Company, Pittsburgh, Pennsylvania (Fluorine Cylinder Valve Cat. No. 1214F). Valves 8 and 9 are conventional as supplied by the vendor. All other valves are Hoke Cat. No. 30206-6, with No. 80065-1 solenoid operators. These ball valves operate smoothly and thus may be less likely to initiate an explosion than would a solenoid-operated needle valve which operates more abruptly. The vacuum pump is a conventional, low-capacity, laboratory model filled with fluorocarbon oil but powered with a 1 h.p. motor for easy starting. All transfer lines are copper tubing, silver soldered to valves and fittings. The test cup assembly is 1" Schedule 40 pipe, surrounded by a can cooled with dry ice.

2. Operating Procedure

For remote transfer of a test sample from the supply tank, the following procedure is used: With valves 1, 7, 8, and 9 closed and all others opened, evacuate system. Close all valves. Open valve 10. Open valve 7. Open valve 2. Fill measuring bottle to desired pressure as indicated on gauge. Close valve 2. Close valve 7. Open, in order, valves 1, 3, and 7; this flushes this section with helium and serves to isolate the supply tank from the measuring bottle. Open valve 4. Essentially all of the $N_2F_4$ or other test material in the measuring bottle should condense in the test cup. Completeness of condensation is judged with the thermistor and thermocouple liquid level detector or by an appropriate pressure drop in the system. In this operation the test cup acts as a trap. Should any noncondensables interfere, they may be removed through the pump by briefly opening and pumping through valve 5. The preset needle valve prevents surging or splashing of liquid. Close valve 4 and the cup is ready for the test.

I. Auxiliary Breathing Air Supply

To test toxic materials and protect operating personnel from dangerous fumes, protection equipment and an auxiliary air supply should be available. Portable self-contained air or oxygen breathing equipment is suggested.

## III. FINAL ASSEMBLY

The prepared cups and caps containing the desired instrument probes, transfer lines, vacuum components, gauges, and instruments are assembled and checked at the test site. The test cup and shot assembly are positioned in the firing chamber to minimize damage to the lead lines and

auxiliary equipment. For convenience in repeating shots, the cups are attached to the transfer lines with quick-disconnect fittings.

It is advisable to schedule a preliminary test with an inert material of very nearly the same physical properties as the test material, to check the reliability of the equipment and gain experience in operating the system. Also, materials of known detonation characteristics should be tested for comparison.

When the assembled equipment has been checked, the test material supply tank is attached to the vacuum line and the transfer lines are evacuated up to the supply tank valve. Since most of the transfer lines are extremely small, several minutes may be required to pump the transfer system down to a desirable pressure (10 to 50 microns). This time can be employed to assemble the detonation train and D'Autriche witness plates (if used).

The first explosive attached to the equipment is the D'Autriche witness plate and assembly, if used. The MDF probes leading from the cup must be carefully positioned and firmly held to obtain maximum separation, thus preventing "shorting" of the shock train between probes. With the witness plate and probe assembly firmly secured to the test stand, the booster, detonator, and Primacord are assembled and the booster is placed flat against the diaphragm on the cup. The entire assembly is held together on the stand with adhesive tape. If the shot is to be heated, noncombustible tapes should be used. The electrical leads to the instrument panels are installed and checked.

If it is possible to pour the test liquid into the detonation cup (i.e., if the material is nontoxic and the shot is to be done above ambient conditions), no vacuum transfer equipment is used. This is the procedure with ethyl nitrate tested above ambient conditions. In this case one of the two side-arm tubes on the cups is closed with a quick-disconnect plug after the cup is filled. The liquid should not be allowed to wet the plug and quick-disconnect fittings when they are being closed, since this may cause premature detonation. The second tube arm of the cup serves as a lead to determine pressure in the system.

With the shot assembled and the transfer system evacuated, the remote control valves are closed. Next, the coolant or bath liquid is placed around the cup. This should be done remotely, if possible. The valve on the sample tank is opened to allow the gas to flow to the remote control valves only. The remainder of the transfer operation is completed as outlined previously. When this is complete, as judged by one or all of the methods used to determine the liquid level in the cup, the supply tank is isolated from the shot by inert gas in the transfer lines and the shot is fired.

## IV. DETERMINATION OF THE DETONATION VELOCITY

### A. D'Autriche Method

A failing (i.e., nonpropagating) detonation wave is detected by a decelerating wave velocity rather than by failure of the MDF. The strong shock from the tetryl booster usually initiates the MDF when the cup contains a nondetonating liquid. Positive results are reported when a constant velocity wave front is established. The method does not readily detect transient changes in detonation phenomena but has the advantage that a record is obtained on the plate even when nondetonating material is tested in the cups.

Appendix A outlines the procedure for determining detonation velocity from data obtained with plates. Reliability in calculating detonation velocity is believed to be approximately ±10%

### B. Continuous Wire Method

This method, developed for solid cast explosives, is adequately described in the literature.[3] The cup and booster charge described replace the solid explosive. This method has the advantage of producing a continuous record of shock disturbances in the test liquid but does not produce a record when the material does not detonate.

## V. TEST RESULTS

The procedure presented in this paper should yield results both reliably and safely. Each component and step has been evaluated by the authors in frequent tests with $N_2F_4$, $O_3F_2$, or $C_2H_5ONO_2$. The procedure was then used to determine the detonability of these three compounds as liquids. The results for $O_3F_2$, published elsewhere,[5] established the nondetonability of this liquid which is stable only below $\sim 100^\circ$K. $N_2F_4$, b.p. $200^\circ$K, was tested from $195^\circ$K to $213^\circ$K ($\sim 10^3$ torr). Several tests were run with the continuous wire method; all gave typical negative results. The one test run with the explosive witness showed the shock velocity decaying from an initial value of $\sim 2.8$ mm/μsec to a final value of $\sim 1.5$ mm/μsec. Again, this is characteristic of a nonpropagating shock. To evaluate the test at the other environmental extremes a hot liquid, ethyl nitrate ($C_2H_5ONO_2$), was used at high pressure. Although some difficulty was encountered because of the tendency of the liquid to detonate spontaneously above its boiling point, four successful continuous wire tests were conducted from $97^\circ$ to $114^\circ$C and up to 175 psig. Each indicated, again with typical records, that the liquid is detonable.

Although these were the only shots conducted with the exact procedure defined by this paper, many were run under conditions only slightly different; generally these affected safety and simplicity rather than

reliability. Details of most of these are available to the reader of the project reports (q.v.).[6] Important conclusions are that the tests, as described, reliably detect detonation and, equally reliably, non-detonation. Low velocity detonations are probably included in the latter. The results have been proven to be independent of either temperature or pressure. For example, incidental tests demonstrated that MDF detonates with a velocity invariant with temperature.

In summary, the authors present the procedure described in this report with confidence that, if used as described, it will serve as a useful, worthy supplement to the Liquid Propellant Test Method No. 1.

## VI. ACKNOWLEDGEMENT

The test procedure described in this report was developed as a part of research generously sponsored by the Office of Naval Research.

## REFERENCES

1. "Liquid Propellant Test Methods," JANAF Panel on Liquid Propellant Test Methods, The Liquid Propellant Information Agency, Applied Physics Laboratory, Johns Hopkins University, Silver Spring, Maryland,

2. H. D'Autriche, "The Velocity of Detonation in Explosives," Compt. Rend. 143, 641-44 (1906); Chem. Abstr. 1, 357-8 (1907).

3. A. B. Amster et al., "Continuous Oscillographic Method for Measuring the Velocity and Conductivity of Stable and Transient Shocks in Solid Cast Propellants," Rev. Sci. Instr. 31, 2, 188-92 (1960).

4. D. B. Moore, "A Thermistor As a Combustion Liquid Level and Temperature Sensor," Rev. Sci. Instr. 37, 1089(1966).

5. A. B. Amster, J. A. Neff, R. W. McLeod, and D. S. Randall, "Detonability of Cryogenic Oxidizers: Trioxygen Difluoride, $O_3F_2$," Explosivstoffe, No. 2, 33(1966).

6. A. B. Amster et al., reports prepared for Stanford Research Institute Project 4051, Contract Nonr 3760(00), September 1962 et seq.

## Appendix A

## ADAPTATION OF THE JANAF BOOSTER TEST: DATA REDUCTION

The equation for reducing the data from the witness plates is derived as follows. Assume the following:

1. There is a small, finite, but reproducible time for a detonation to propagate across explosive interfaces. This is frequently referred to as an "induction time."

2. The time required for two detonations originating at a common point and meeting at a point x is the same for two corresponding paths.

3. The detonation velocity of explosives is a reproducible function of environment.

The nomenclature used in the equation is as follows:

$P$ = lengths of MDF; the subscript denotes the particular branch

$P_b$ = length of MDF from tetryl booster than initiates the explosive on witness plate

$V$ = detonation velocity of any P with corresponding subscript

$V_s$ = wave velocity within sample

$V_w$ = detonation velocity of standard explosive used

$L$ = distance between opposing points of initiation for each sheet explosive finger

$x$ = point at which detonations meet; measured from MDF

$ds'$ = distances between MDF on sample cup

$dw'$ = distances between corresponding strips of explosive on witness plate

$ds$ = distance from tetryl pellet for first MDF

$dw$ = distance from the start to strip 1 on witness plate

$\mu, \eta$ = small, unknown, but reproducible delay or induction times in transition from cup to MDF and MDF to EL-506-D

The time required for the detonation to travel from the tetryl through the sample cup, the first "finger" of MDF and to point $x_1$ in the sheet explosive is:

$$t_1 = \frac{ds}{V_s} + \mu + \frac{P_1}{V_1} + \eta + \frac{x_1}{V_w} \qquad \text{(A-1)}$$

The time required for the detonation to travel from the tetryl through the "start" branch of the MDF and to $x_1$ through the sheet explosive from the opposite direction is:

$$t_1' = \frac{P_0}{V_0} + \eta + \frac{dw}{V_w} + \frac{L - x_1}{V_w} \qquad \text{(A-2)}$$

Equating (A-1) and (A-2) and rearranging terms:

$$\frac{ds}{V_s} = \frac{P_0}{V_0} - \frac{P_1}{V_1} + \frac{dw}{V_w} + \frac{L - 2x}{V_w} - \mu \qquad \text{(A-3)}$$

Similarly, by equating the times of travel from the tetryl to point $x_2$ in the second finger of sheet explosive:

$$\frac{ds + ds'}{V_s} = \frac{P_0}{V_0} - \frac{P_2}{V_2} + \frac{dw + dw'}{V_w} + \frac{L - 2x_2}{V_w} - \mu \qquad \text{(A-4)}$$

Subtracting (A-3) from (A-4) and noting that $P_1 = P_2$ and $V_1 = V_2$:

$$\frac{V_s}{V_w} = \frac{ds'}{dw' + 2(x_1 - x_2)} \qquad \text{(A-5)}$$

$V_s$, ds', and dw' are conditions of the experiment; $x_1$ and $x_2$ are measured; therefore $V_s$ can be calculated.

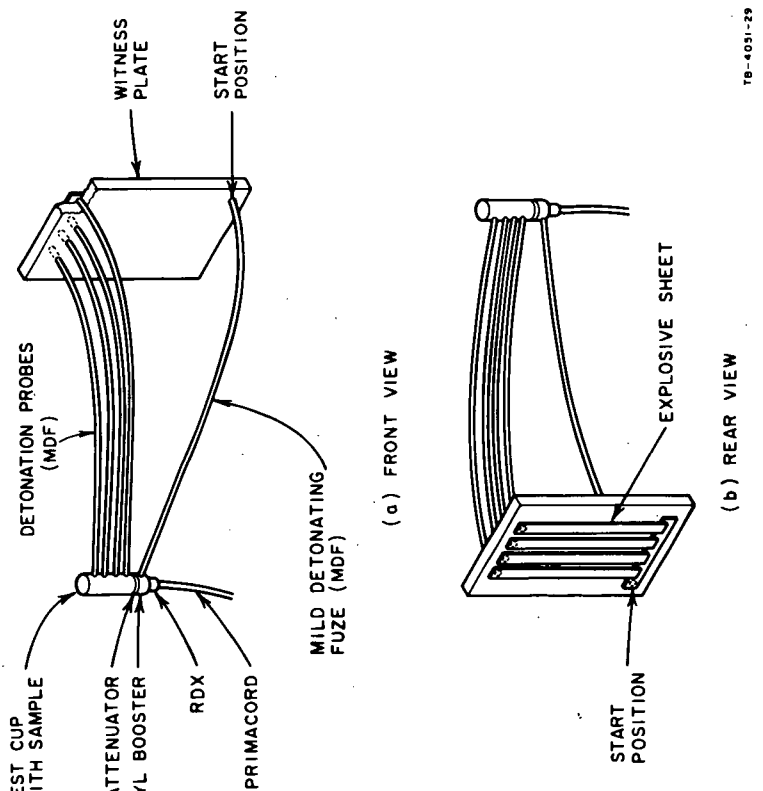


Fig. 1 Modified D'Autriche Assembly

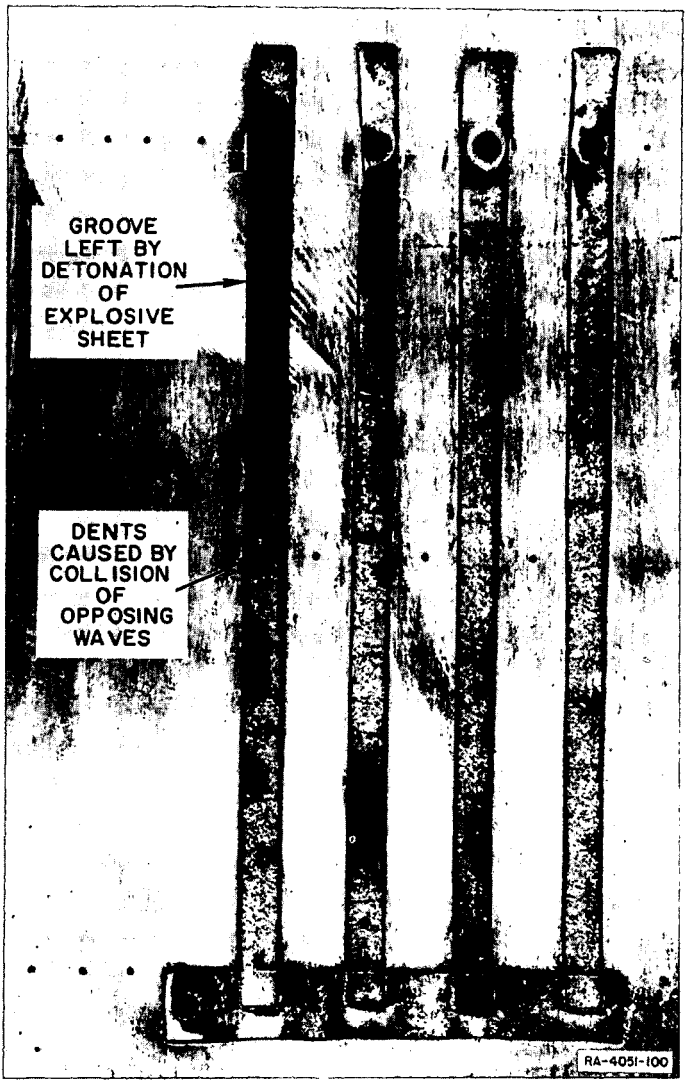


Fig. 2 Typical Witness Plate

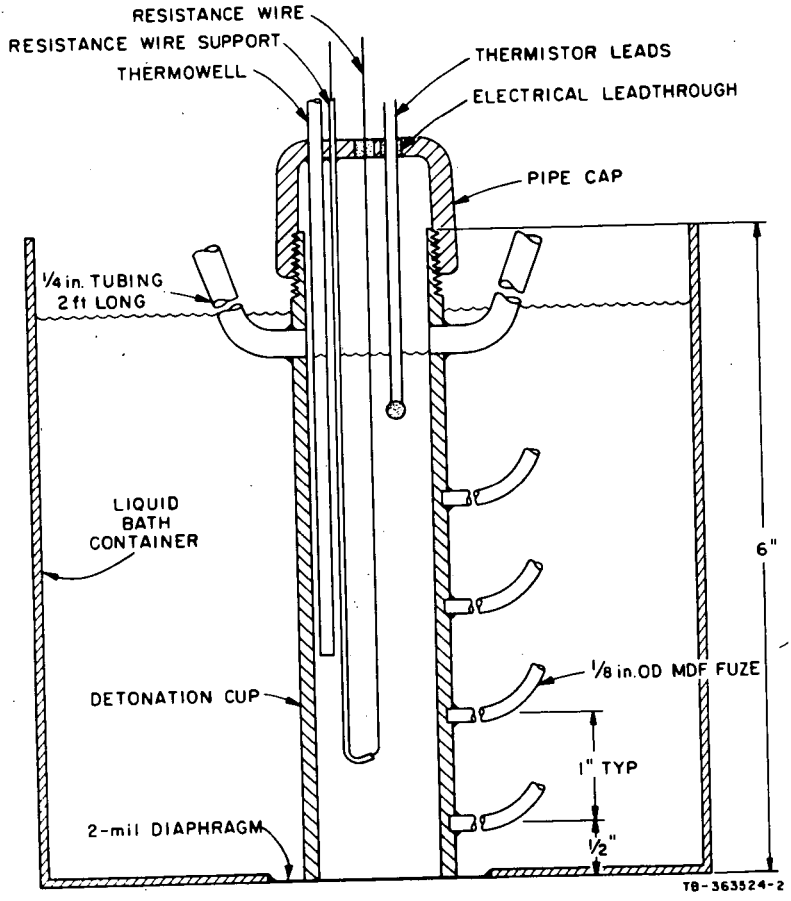


Fig. 3 Detonation Cup

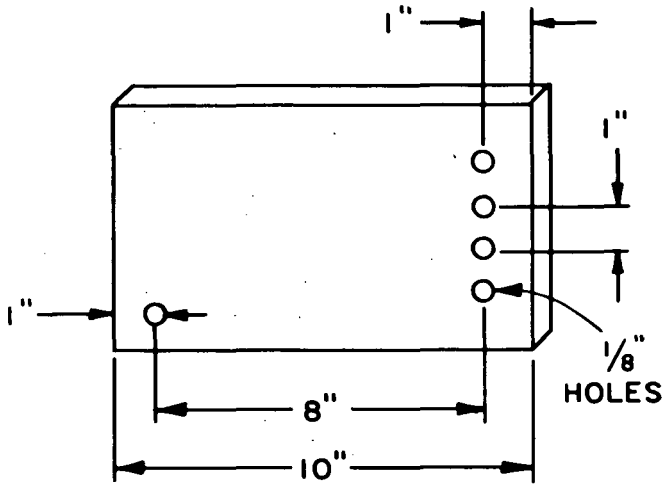


(a) ALUMINUM WITNESS PLATE

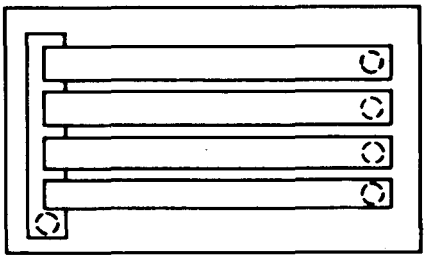

(b) SHEET EXPLOSIVE ON WITNESS PLATE

TA-363524-1

Fig. 4 Witness Plate Details

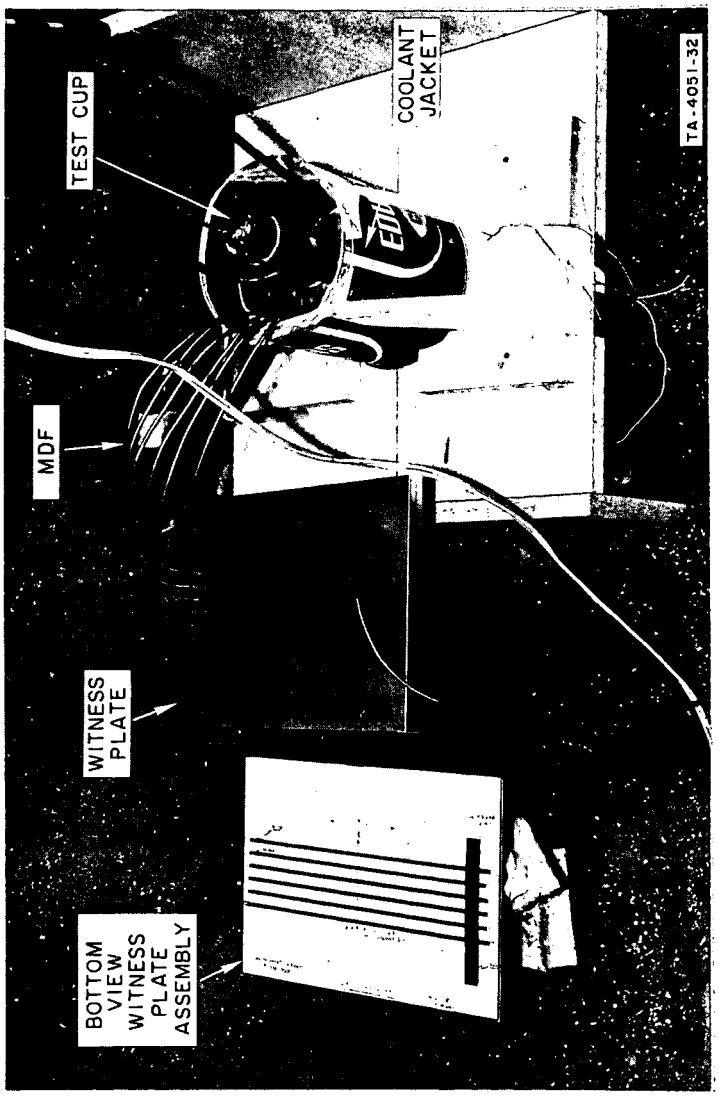


Fig. 5 Assembled Detonability Equipment

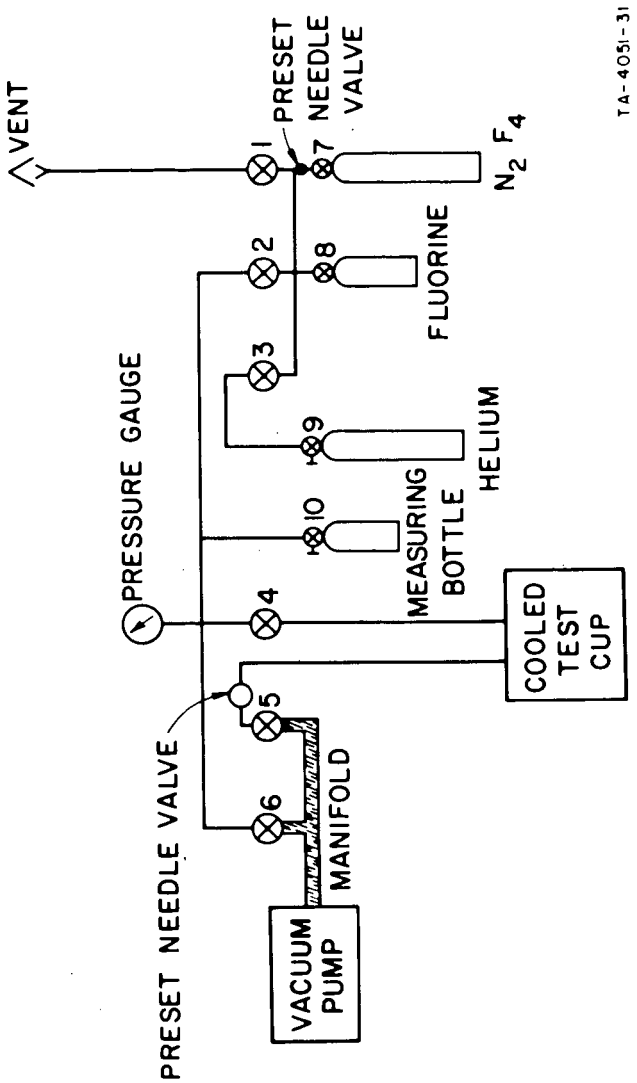


Fig. 6 Vacuum Transfer Line